INSTRUMENTATION FOR THE STUDY OF RAPID BIOLOGICAL OXIDATION-REDUCTIO
BALLOU, DAVID PENFIELD
ProQuest Dissertations and Theses; 1971; ProQuest Dissertations & Theses Global

72-14,796

BALLOU, David Penfield, 1942-

INSTRUMENTATION FOR THE STUDY OF RAPID BIOLOGICAL OXIDATION-REDUCTION REACTIONS BY EPR AND OPTICAL SPECTROSCOPY.

The University of Michigan, Ph.D., 1971
Biochemistry

University Microfilms, A XEROX Company, Ann Arbor, Michigan

THIS DISSERTATION HAS BEEN MICROFILMED EXACTLY AS RECEIVED

Reproduced with permission of the copyright owner. Further reproduction prohibited without permission.

INSTRUMENTATION FOR THE STUDY OF RAPID BIOLOGICAL OXIDATION-REDUCTION REACTIONS BY EPR AND OPTICAL SPECTROSCOPY

by

David Penfield Ballou

A dissertation submitted in partial fulfillment
of the requirements for the degree of
Doctor of Philosophy
(Biological Chemistry)
in The University of Michigan
1971

Doctoral Committee:

Associate Professor Graham Palmer, Chairman
Associate Professor Donald E. Hultquist
Associate Professor Hiroshi Ikuma
Professor Vincent Massey

Reproduced with permission of the copyright owner. Further reproduction prohibited without permission.

PLEASE NOTE:

Some pages have indistinct print. Filmed as received.

University Microfilms, A Xerox Education Company

Reproduced with permission of the copyright owner. Further reproduction prohibited without permission.

To the fond memory of

GORDON P. FOUST

who as a friend shared with me
an inspiring and privileged spirit of research
for which I am grateful.

Reproduced with permission of the copyright owner. Further reproduction prohibited without permission.

ACKNOWLEDGEMENTS

I wish to express my appreciation to Dr. Graham Palmer for his encouragement and patience, and especially for his timely and critical evaluations of the various phases of this work. I am most appreciative to Dr. Vincent Massey who originally encouraged me to study here and who has been a collaborator and a source of ideas throughout my studies. I would like to thank Mr. Rudy Wolff for training me in machining skills and Mr. Paul Holloway and his staff in the Physics Instrument Shop for collaboration in the construction of much of the instrumentation. It has been very rewarding to work with Mr. Gordon Foust and Dr. Bruce Burleigh in the design of the stopped-flow instrument. I would like to thank Dr. Robert Keller of the Mechnical Engineering Department for his initial suggestions in the basic power mechanism for the rapid freezing apparatus. My thanks also go to Mr. James Becvar for his stimulating discussions and suggestions. I am grateful to Mr. Gordon Ford for his much needed assistance with electronics problems and to Mr. Glenn Edict for the design of Figure 58a. Dr. Peter Knowles helped in the design of the cryogenic bath and Mr. David Sun wrote the computer program for the treatment of kinetic data. The studies on flavodoxin were done in collaboration with Dr. Stephen Mayhew. I am indebted to the National Science Foundation and the United States Public Health Service for the financial support which made this work possible. I would like to thank the Department of Biological Chemistry

Reproduced with permission of the copyright owner. Further reproduction prohibited without permission.

for my training and the Biophysics Research Division for providing me with space and equipment for these studies. I would like to thank Dr. Thomas Rebane for help in developing ideas about the mechanics of rapid freezing. It has been a pleasure to work with all the members of Dr. Palmer's and Dr. Massey's laboratories in the course of these studies.

I would like to thank Judy and Alison for persisting with me during the most trying periods. Finally, I want to express special thanks to Mrs. Peggy Rogers who has typed all of this thesis and has been most helpful in its organization.

Reproduced with permission of the copyright owner. Further reproduction prohibited without permission.

TABLE OF CONTENTS

	Page
ACKNOWLEDGEMENTS	iii
TABLE OF CONTENTS	v
LIST OF FIGURES	vii
LIST OF TABLES	xi
ABBREVIATIONS	xii
CHAPTER 1. INTRODUCTION	1
Part I. Continuous Flow, Stopped-Flow and Accelerated Flow Instrumentation	1
Part II. Rapid Freezing Technique	10
CHAPTER 2. DESIGN OF THE RAPID FREEZING APPARATUS	21
A. General Layout and Principle of Operation	21
B. Linear Velocity Mechanism - Details	21
C. Flow System - Details	36
D. Cryogenic Quenching Apparatus - Details	53
CHAPTER 3. EVALUATION OF THE RAPID FREEZING APPARATUS	67
Part I. Variables Associated with Measurement of Reaction Times	67
A. Reaction Tubes	67
B. Fluid Velocity	[illegible]
C. Uniformity of Driving Velocity	73
D. Mixing	81
E. Homogeneity of Flow	104
F. Quenching Studies	115

Reproduced with permission of the copyright owner. Further reproduction prohibited without permission.

TABLE OF CONTENTS (Cont.)

	Page
Part II. Variables Associated with Measurement of EPR Signals	136
A. Packing Factor	137
B. Measuring the Signal	144
Part III. Discussion	149
A. Instrument Improvements	149
B. Precautions and Unmeasured Parameters	155
C. Possible Applications of the Flow System	157
CHAPTER 4. AN ABSOLUTE ABSORBANCE STOPPED-FLOW SPECTROPHOTOMETER	165
Part I. Details of Construction	166
A. General Layout and Principle of Operation	166
B. Driving Unit - Details	169
C. Mixing and Observation Module - Details	173
D. Stopping Syringe Assembly - Details	180
Part II. Performance and Evaluation	183
CHAPTER 5. THE USE OF COMBINED STOPPED-FLOW AND RAPID FREEZING INSTRUMENTATION IN THE STUDY OF THE MECHANISM OF THE OXIDATION OF FLAVINS AND FLAVOPROTEINS BY OXYGEN	194
REFERENCES	214
Appendix 1. Treatment of Kinetic Data	224
Appendix 2. Tables for Operating Rapid Freezing Apparatus	235
Appendix 3. List of Manufacturers	240

Reproduced with permission of the copyright owner. Further reproduction prohibited without permission.

LIST OF FIGURES

Figure		Page
1	Schematic of Hartridge-Roughton Apparatus	3
2	Schematic of Bray Rapid Freezing Apparatus	15
3	Rapid Freezing Apparatus	22
4	Driveshaft Assembly	22
5	Gearbox-Cam Assembly	24
6	Linear Motion Cam for Rapid Freezing Apparatus	26
7	Push-Push Linear Motion Cam	27
8	Cam Follower	29
9	Cam Follower Support	29
10	Syringe Ram	30
11	Carriage Support for Syringe Driver	32
12	Adaptor for Carriage Assembly	32
13	Calibration Curve for AC Tachometer	35
14	Aluminum Water Bath	37, 38
15	Modified Syringe Plungers for Hamilton Syringes	40
16	Syringe Mounts	40
17	Polyethylene Tubing Connectors	43
18	Palmer-Beinert Mixer	46
19	Gibson-Milnes Mixer	46
20	Ballou Mixer	49
21	Mixer Mounts	49
22	Exit Nozzles	52

Reproduced with permission of the copyright owner. Further reproduction prohibited without permission.

LIST OF FIGURES (Cont.)

Figure		Page
23	Cryogenic Quenching Apparatus	54
24	Brass Container for Isopentane	55
25	Isopentane Bath Cover	57
26	Rapid Freezing EPR Tubes	60
27	Demountable EPR Tubes	60
28	Rapid Freezing Tube Holders	63
29	Sample Packer	63
30	Rapid Freeze EPR Tube Stabilizer	66
31	Uncertainty in C/C_o versus Percent Reaction Remaining	70
32	Position and Velocity Signals from Syringe Ram	74
33	Velocity of Syringe Ram at 800 RPM	76
34	Velocity of Syringe Ram at 1440 RPM	77
35	Velocity of Syringe Ram at 2400 RPM	78
36	Velocity Tests on Push-Push Mechanism	82
37	Apparatus for Mixer Evaluation	86
38	Mixing Tests on Ballou T-Mixer	89
39	Mixing Tests on Ballou 4-Jet Mixer	90
40	Mixing Tests on Gibson-Milnes Micromixer	91
41	Mixing Tests on Ballou 4-Jet Mixer at High Viscosity	92
42	Apparent Reaction Progress Curves with Imperfect Mixing	101
43	Logarithm of Apparent Reaction Progress Curves with Imperfect Mixing	101

Reproduced with permission of the copyright owner. Further reproduction prohibited without permission.

Figure		Page
44	Effect of Flow Dispersion on Apparent Reaction Progress (Theoretical)	111
45	Effect of Flow Dispersion on Apparent Reaction Progress (Experimental)	114
46	Arrhenius Plot for the Reaction of Metmyoglobin and Azide	120
47	Quenching Time Determination - Method	126
48	Quenching Time versus Nozzle Velocity	128
49	Schematic of Jet Dispersion	131
50	Alternative for Syringe Ram and Cam Follower	153
51	Three Syringe Continuous Flow Method	164
52	Absolute Absorbance Stopped-Flow Spectrophotometer	167, 168
53	Driving Module - Water Bath	170
54	Driving Module - Solenoid Valve and Hydraulic Cylinder	171
55	Solenoid Valve Activator	172
56	Stopped-Flow Observation Assembly	174, 175
57	Kel-F Observation and Mixing Block	177
58	Circuits for Conditioning Optical Density Signal for Stopped-Flow	179
59	Stopping Syringe Assembly	181, 182
60	Reproducibility and Signal-to-Noise of Stopped-Flow	184
61	Determination of Dead Time of Stopped-Flow - PMT Electronics	188
62	Determination of Dead Time of Stopped-Flow - Gilford Electronics	188

Reproduced with permission of the copyright owner. Further reproduction prohibited without permission.

LIST OF FIGURES (Cont.)

Figure		Page
63	Demonstration of Mixing and Flow Characteristics of Stopped-Flow	190
64	Reaction Scheme for Reduced Flavin with Oxygen	195
65	Reaction Scheme for Breakdown of Reduced Flavin-Oxygen Complex	195
66	EPR Spectrum of O_2^-	199
67	Production of Superoxide in the Reaction of $TARFH_2$ with Molecular Oxygen	201
68	Reaction of O_2^- with Erythrocuprein and Cytochrome c	203
69	Stopped-Flow Studies of the Reaction of $TARFH_2$ with O_2	205
70	Reaction of Reduced Flavodoxin with Oxygen	212
71	Reaction of Reduced Flavodoxin with Oxygen in the Presence of Superoxide Dismutase	212

Reproduced with permission of the copyright owner. Further reproduction prohibited without permission.

LIST OF TABLES

Table		Page
1	Apparent Mixing Rate Constants	102
2	Maximum Rate Constants with 4-Jet Mixer for K of 0.2 and 0.02	103
3	Dispersion of Material During Flow in Reaction Tube	106
4	Experimental Packing Factors	140
5	Minimum Concentrations Necessary for Effective Rapid Freezing Studies	146

Reproduced with permission of the copyright owner. Further reproduction prohibited without permission.

ABBREVIATIONS

A_i	Area of ith annulus
a	Radius of reaction tube
BSA	Bovine serum albumin
d	Diameter of reaction tube
EDTA	(Ethylenedinitrilo) tetraacetic acid
EPR	Electron paramagnetic resonance spectrometry
F, FH·, FH_2	Oxidized, semiquinoid, and reduced forms of flavins and flavoproteins
FAD, FADH·, $FADH_2$	Oxidized, semiquinoid, and reduced forms of flavin adenine dinucleotide
FMN, FMNH·, $FMNH_2$	Oxidized, semiquinoid, and reduced forms of flavin mononucleotide
k	Rate constant
k_m	Mixing rate constant
k_r	Reaction rate constant
r_i	Distance from center of reaction tube to i^{th} annulus
R.N.	Reynolds number
SD	Superoxide dismutase, erythrocuprein
t	Time after initiation of reaction
T	Temperature in ^oK
$t_{1/2}$	Half-time of reaction
TARF, TARFH·, $TARFH_2$	Oxidized, semiquinoid, and reduced forms of tetraacetyl riboflavin
U	Linear flow velocity ($m \cdot sec^{-1}$)

Reproduced with permission of the copyright owner. Further reproduction prohibited without permission.

V	Volume from mixer to observation point
dV/dt	Volume flow rate ($ml \cdot sec^{-1}$)
α	A/A_o
β	B/A_o
γ	C/A_o
ΔP	Pressure drop
η	Measured viscosity
$[\eta]_x$	Intrinsic viscosity of x
η_{sp}	Specific viscosity
κ	k_r/k_m
σ	Density
τ	$k_m t$

Reproduced with permission of the copyright owner. Further reproduction prohibited without permission.

CHAPTER 1

INTRODUCTION

Part I. Continuous Flow, Stopped-Flow and Accelerated Flow Instrumentation

A major advance in chemistry in the last 50 years has been the development of techniques which permit isolation and characterization of intermediates of chemical reactions. Many reaction mechanisms are thought to involve a series of intermediates which are consistent with the major products of the reaction. However, a good understanding of a mechanism can only be gained by direct experimental evidence of such intermediates.

At room temperature in the absence of catalysts, most biochemical reactions proceed very slowly. Yet in the presence of enzymes these reactions proceed very rapidly and with remarkable specificity. To understand why enzymes are such efficient catalysts it is necessary to characterize the enzyme-substrate (ES) and enzyme-product (EP) intermediates which must exist for catalysis to take place. Since pure biochemical compounds are usually valuable and in short supply, and since their reactions are rapid, the mechanistic study of biochemical reactions has provided the impetus for the development of rapid and sensitive methods for the observation of reaction intermediates.

One approach in learning about intermediates of reactions is the use of a physical technique which makes possible the observation

Reproduced with permission of the copyright owner. Further reproduction prohibited without permission.

of certain characteristics of the intermediates and which thereby can be used to determine the kinetics of the intermediates during the course of the reaction. If a suitable technique is available, it then becomes necessary to devise some means of defining the time of observation with respect to the time the reaction was initiated.

Before 1923 there were no methods for determining kinetics of reactions with half-lives shorter than several seconds. In that year Hartridge and Roughton (1) developed the continuous flow technique to study the kinetics of the combination of hemoglobin with oxygen. The time resolution of this method was about four orders of magnitude better than that of previous methods (i.e. they could now resolve one msec). The primary requirement in determining the kinetics of a rapid reaction is that the time between the initiation and observation of the reaction be short compared with the reaction. Hartridge and Roughton met this requirement (Fig. 1) by employing gas pressure to drive reactants at a high velocity from storage vessels, SV_1 and SV_2, into a mixing device, M, from which the mixed solution passed into an observation tube, OT. They observed the course of the reaction visually with a reversion spectroscope (2), RS, at various points along the observation tube. If flow were constant, the observation points could be translated into times after mixing by equation 1.

Reproduced with permission of the copyright owner. Further reproduction prohibited without permission.

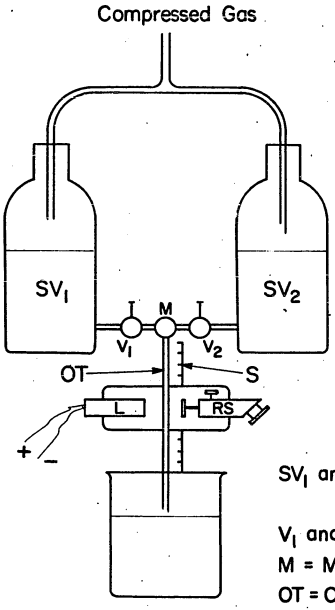

Figure 1. Schematic of Hartridge-Roughton Apparatus

Reproduced with permission of the copyright owner. Further reproduction prohibited without permission.

1. $$t = \frac{V}{dV/dt}$$

where, V = volume from mixer to observation point (ml), and dV/dt = volume flow rate (ml/sec).

In their early studies Hartridge and Roughton (1, 3) had shown that the continuous flow method could be adapted to photoelectric, thermal and electrical measurement, and chemical analysis. They had shown that the age of the mixture could be varied by either changing the volume between the mixer and the point of observation (or quenching), or by changing the flow velocity, or both. Hartridge and Roughton (4) have discussed most of the experimental problems associated with making rapid reaction measurements in continuous flow devices and have suggested practical solutions to these problems. In particular, they had studied the mechanics of thoroughly mixing two reactants in a short period of time, a condition necessary for obtaining accurate measurements on fast reactions, and had designed fluid mixers which were capable of complete mixing within one msec. They had also studied the character of flow in observation tubes under various conditions to insure that the average age of the reaction mixture at the point of observation corresponded to the times as calculated from equation 1.

The principles introduced by Hartridge and Roughton form the basis of all of the flow systems used today. In spite of the fact that many ingenious devices have been made since then, very little

Reproduced with permission of the copyright owner. Further reproduction prohibited without permission.

improvement in the time resolution has resulted. However, a major disadvantage of their apparatus was that due to the insensitivity and slow response of their detection systems, three to twenty liters of reactants were required for the determination of a single kinetic curve, an amount which was impractical for most biological studies. The application of the photoelectric cell by Roughton and his colleagues (5-7) decreased the response time of the measuring system and made possible a corresponding reduction in the volume required per kinetic determination (ca. one liter per curve or 200 ml per observation). Millikan (8) further reduced this amount with an apparatus he devised in 1936 which can be called the first pulsed-flow instrument. This instrument employed: (a) a more sensitive photoelectric device which consisted of a two-filter colorimeter plus photoelectric cell, (b) a narrow observation tube (ca. 1 mm) with a correspondingly small mixing chamber, (c) an electrical measuring system with a response time of "only 2 sec", and (d) a rapid starting fluid drive employing motor driven syringes. The volume required with this instrument was about 20 to 100 ml per kinetic curve which is still too much for many applications in biochemistry.

Chance (9) in 1940 applied his electrical engineering training to the problem and improved the detection time constant from about 2 sec in the Millikan system to about 10 msec by replacing the galvonometer with a cathode ray oscilloscope. Regulated lamp supplies and auxillary equipment which he designed improved the accuracy and

Reproduced with permission of the copyright owner. Further reproduction prohibited without permission.

sensitivity of his measurements. Since the stable continuous flow necessary for accurate kinetic measurements was difficult to achieve in such a short time (10 to 50 msec), he replaced the motor-driven system with a driving system which was accelerated with a sharp manual push (hence the name accelerated-flow), and concomitant with the optical observations, he measured the flow velocity with a variable potentiometer and differentiation circuit. Applying equation 1. he could calculate the reaction time corresponding to a given observation. This is called the accelerated flow method. At the end of the push, flow was stopped suddenly and the reaction could be followed for an indefinite period of time, a feature which is the basis of the stopped-flow technique.

Gibson (10, 11) markedly improved the stopped-flow technique by adding a third syringe which stopped the fluid flow within a period of one msec when its plunger came to rest at a stopping block. The use of a rapid responding photomultiplier tube for detection of the light rather than a photoelectric cell, made it possible to easily resolve times of one msec. With the stopped-flow technique an entire kinetic curve can be determined with one "shot" of only a few tenths of a ml of each reactant from the driving syringes.

The stopped-flow, continuous-flow, and accelerated-flow methods have been adapted to many physical measuring techniques including absorption and fluorescence spectroscopy, electron paramagnetic resonance spectrometry (EPR), magnetic susceptibility

Reproduced with permission of the copyright owner. Further reproduction prohibited without permission.

measurement, thermal measurement, electrometric measurement and chemical quenching. These are discussed in detail (with many references given) in the following sources:

1. Caldin's book (12) is very readable and is probably the best introduction to rapid reaction techniques. 2. The article by Roughton and Chance (13) is an extensive coverage of the methods available up to 1962 and it describes many of the problems, methods for calibration of instruments, and also a history of the development of rapid flow techniques. 3. Gibson's article (14) in Annual Review of Biochemistry discusses the usefulness of rapid reaction techniques in studying biological oxidations and describes many examples of such studies. 4. Gibson (15) also has a very practical article in Methods in Enzymology, Vol. 16, about the stopped-flow method which would be of use to anyone using this technique. 5. Gutfreund (16) has an excellent article in the same volume which would similarly be of value to anyone using continuous flow methods. 6. The account of the International Symposium on Rapid Mixing and Sampling Techniques (17) contains many practical designs for rapid reaction study, and, in addition, has valuable discussions about the problems which various workers have encountered.

The study of oxidation and reduction reactions is an area in which flow methods are especially helpful (17). Oxidation-reduction reactions involve the transfer of electrons and are therefore most often associated with transition metals and highly conjugated organic

Reproduced with permission of the copyright owner. Further reproduction prohibited without permission.

molecules. It is not surprising to find that enzymes which catalyze biological oxidations frequently contain metals (e. g. hemoproteins) or highly conjugated ring systems (e. g. flavoproteins). The electronic properties of these molecules not only make them suitable for electron transfer but also give rise to absorption and fluorescence in the visible and ultraviolet ranges of the electromagnetic spectrum and often to electron paramagnetism in one or more of the valence states of the components of the reaction. The ability to show whether or not a species which has an unpaired electron as determined by EPR, has the same kinetics as a species which has a particular optical spectrum, can be a powerful contribution to the understanding of oxidation-reduction reactions. Kinetic studies of the optical spectra of these reactions can be performed conveniently with the stopped-flow technique of Gibson, while rapid kinetic studies of the paramagnetism of a reaction can, in principle, be performed with the rapid freezing method of Bray (18). This method, described in Part II of the Introduction, is fraught with numerous difficulties, few of which have been examined carefully. A large part of this thesis is devoted to examining and correcting these problems.

The Gibson-type stopped-flow instruments are becoming quite common and there are several commercially available, such as Durrum, Aminco (4 models), Atom-Mech Machine Co., and Yanagimoto Manufacturing, Ltd. (see list of Manufacturers).

Reproduced with permission of the copyright owner. Further reproduction prohibited without permission.

However, there are certain disadvantages to all of these devices. (a) In no instrument available is there provision for a reference cell so that the absolute absorbance can be displayed directly. (b) Biological molecules are often highly sensitive to trace amounts of metals and in the available apparatus either the solutions come into contact with metal parts or the temperature control and range is traded off to avoid metal contact. (c) In some of the instruments, volumes in excess of 0.1 ml per determination are required. This can be a substantial amount when measuring the numerous shots required to obtain spectra of intermediates. (d) Studies under anaerobic conditions do not appear to be realistic in any practical sense in many of these instruments. (e) The cost of these instruments is quite high (between $5,000 and $15,000).

The possibility of using the Gilford logarithmic converter and amplifier as a means of simplifying data acquisition, led to consideration of designs for stopped-flow which had provision for a reference chamber in the observation assembly, and which overcame many of the deficiencies mentioned above. An instrument of this type is described in Chapter 4.

The rapid freezing technique is much less common than other types of flow methods and therefore Part II of this Introduction is devoted to the history and the peculiar requirements of this technique.

Reproduced with permission of the copyright owner. Further reproduction prohibited without permission.

Part II. Rapid Freezing Technique

The rapid freezing technique was conceived in 1959 by Bray (18-20) to study the rapid kinetics of the xanthine oxidase reaction by electron paramagnetic resonance spectrometry (EPR). This reaction has numerous intermediates with half-lives ranging from 5 msec to several seconds, times which suggested the use of continuous flow methods. However, the EPR signals present in many biological species are difficult to observe at temperatures above $0^{\circ}C$ (xanthine oxidase included), mainly due to three temperature dependent effects, all of which are minimized at low temperatures. (a) The most important of these effects is the relaxation time. The relaxation time becomes shorter with increasing temperature according to complicated relationships which often include temperature terms of high orders. As the temperature increases the net effect is a broadening of the spectrum and hence a decrease in the spectral intensity. This is known as uncertainty broadening. (b) The Boltzman distribution of molecules dictates that the probability of absorption, and therefore the intensity of a signal, will be related to T^{-1}. (c) The filling factor, a technological parameter which is related to the sensitivity of the EPR method, is greater for frozen samples than for liquid samples. This often makes it necessary to perform EPR measurements below $-150^{\circ}C$ ($123^{\circ}K$) which, of course, obviates the usual kinds of flow studies in aqueous solution.

Reproduced with permission of the copyright owner. Further reproduction prohibited without permission.

Since chemical reaction rates are temperature dependent, a mechanism which could quickly cool and freeze reaction mixtures at known short times after mixing would also effectively stop the reaction and leave the sample in a frozen state suitable for EPR measurement. In principle this could be accomplished with a Roughton-type (1) continuous flow system with a rapid quenching device replacing the observation mechanism. Rapid freezing and chemical quenching both have the desirable feature that the analysis of the reaction intermediates can be done more or less at one's leisure. With rapid freezing it is possible to enhance the signal-to-noise ratio and to study more carefully any possible details in the spectra. An advantage over the chemical quenching method is that in rapid freezing actual intermediates of the reaction can often be observed rather than chemical products of the quenching procedure. In contrast to the chemical quenching method which presumably requires specific quenching reagents for each reaction being studied, the freezing method would be the same for all reactions. Gutfreund (16) has found, however, that moderately strong acids are effective quenchers for several enzyme-catalyzed reactions.

If the quenching method is to be useful, it is important that the time required for quenching be short compared with the reaction half-time. A reaction with a low activation energy and therefore a small temperature dependence can not be quenched as quickly as a

Reproduced with permission of the copyright owner. Further reproduction prohibited without permission.

reaction with a large activation energy. This may be a double jeopardy when studying fast reactions since although fast reactions have to be quenched more quickly than slow reactions in order to obtain meaningful results, they also tend to have lower activation energies than slow reactions. This can be seen from equation 2. which is the general form of the Arrhenius equation (12).

2. $k = (A)\exp(-E_a/RT)$

where, k = rate constant, A = about $10^{11} M^{-1} sec^{-1}$, R = gas constant, and T = temperature; E_a = activation energy.

A practical method of obtaining rapidly frozen material is not obvious. Although there are available very cold liquids such as nitrogen and oxygen, these are gases at room temperature. As soon as a warm reaction mixture enters one of these cryogenic liquids, an insulating layer of gas produced by boiling the coolant forms around the droplets of the reaction mixture and the heat transfer, and thus the quenching process is not efficient. A painful example illustrating the insulating properties of such a gaseous layer is the comparison of inserting one's hand for a fraction of a second into liquid nitrogen ($-196^{\circ}C$) and then similarly into isopentane maintained at $-140^{\circ}C$. The liquid nitrogen barely feels cool whereas the isopentane feels unbearably cold. For this reason any good quenching liquid must remain a liquid at room temperature as well as at cold temperatures. A second property necessary for the quenching material is that of inertness towards the chemical reaction being studied. Furthermore,

Reproduced with permission of the copyright owner. Further reproduction prohibited without permission.

it is important to be able to conveniently extract the sample from the quenching liquid for analysis without warming the sample. These required properties suggest a low molecular weight hydrocarbon.

Bray (18) found that a suitable method for rapid freezing was to squirt the reaction mixture as a fine stream into a relatively large volume of isopentane which was maintained at about -140°C, pack the frozen particles into the bottom of an EPR tube for subsequent measurement, and then pour off the bulk of the isopentane leaving only the packed frozen particles in the bottom of the tube. (Isopentane boils at 28°C and freezes at about -160°C depending upon its purity.) Because of their higher density the frozen aqueous particles readily settle and can be packed tightly into a measuring tube. It is presumed that the isopentane is inert to most biological reactions, especially at -140°C.

A result of EPR being a relatively insensitive spectroscopic measuring technique is that high concentrations of reactants are necessary for acceptable signal-to-noise ratios. Since high concentrations of biological reactants are usually very hard to obtain in large quantities, it is necessary to use only minimum volumes. In principle this can be accomplished with the continuous flow method by instantly attaining the desired flow velocity, maintaining it long enough to fill the volume of the reaction tube appropriate to the time as calculated from equation 1. plus the volume needed for measurement, and then stopping the flow immediately. To this end Bray

Reproduced with permission of the copyright owner. Further reproduction prohibited without permission.

used a hydraulically driven syringe system powered by pressurized gas.

The Bray (18) apparatus is shown schematically in Figure 2. The reaction begins at the mixer, M, of a conventional continuous flow system, progresses in the polyethylene reaction tube, V, and is quenched after squirting through the polyethylene nozzle, N, into the cold isopentane contained in the EPR tube modified as shown. By collecting several of these samples, employing reaction tubes of different volumes corresponding to times as calculated from equation 1., and then measuring the intensity of the EPR signals, a kinetic curve is obtained.

The primary objection to the rapid freezing technique is that it has not been thoroughly evaluated. The uncertainties of the method certainly have been considered and a great deal of thought has been put to the vital question of how to measure the quenching time, but no acceptable solutions have been found. In one attempt Bray (18) had estimated the quenching time to be 30 ± 30 msec by using the well known carbonic acid decomposition (21) (equation 2.) and visually observing the appearance of bromphenol blue in frozen samples quenched at known times after mixing. As the carbonic acid decom-

$$\underline{3}. \qquad HCl + NaHCO_3 \xrightarrow{\text{v. fast}} H_2CO_3 \xrightarrow{t_{1/2} \simeq 100 \text{ msec}} H_2O + CO_2$$

poses, the pH rises and in the presence of bromphenol blue the reaction can be monitored by the appearance of the basic blue form of the

Reproduced with permission of the copyright owner. Further reproduction prohibited without permission.

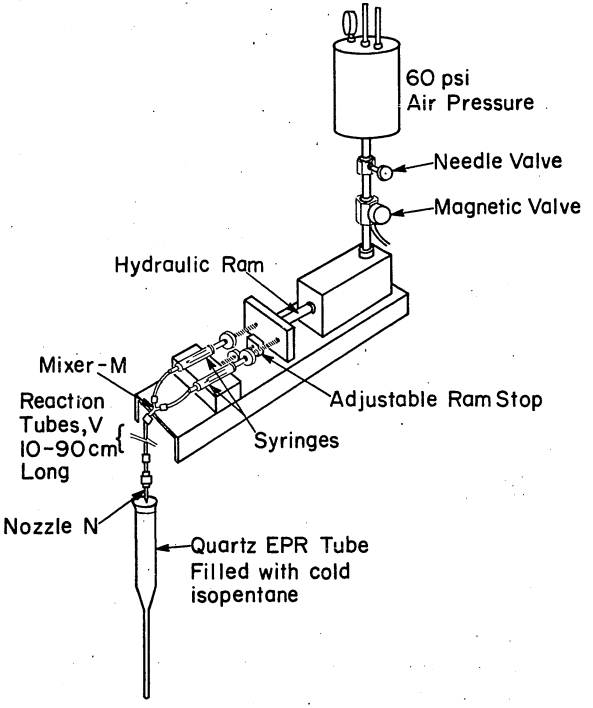

Figure 2. Schematic of Bray Rapid Freezing Apparatus

Reproduced with permission of the copyright owner. Further reproduction prohibited without permission.

indicator. Bray had also broached the subject of flow velocity by measuring the average ram speed, but his conclusion, "the ram velocity was fairly uniform and reproducible and relatively independent of the presence of the syringes", was not quantitative. As shown by Palmer and Beinert (25), there was an additional uncertainty of 5-10 msec in the reaction time due to incomplete mixing by the simple y-junction mixers which Bray employed. Nevertheless, it is to Bray's credit (22,23,24) that the method was extremely useful in studying the order of appearance of the paramagnetic intermediates of xanthine oxidase.

During 1964 in Madison, Wisconsin, a collaboration of Palmer, Bray, and Beinert (20,25) resulted in a substantial technical refinement of the rapid freezing instrument and the first quantitative evaluation of the quenching process. The refinements were: (a) replacement of the y-junction mixer with a more efficient 4-jet tangential mixer, (b) replacement of the polyethylene nozzle with Lucite nozzles which could not expand under pressure and therefore would give identical fine sprays for all experiments, and (c) replacement of the thin-walled polyethylene reaction tubes with reaction tubes of a considerably more substantial polyethylene which was not as likely to expand during the course of flow.

The major contribution of the above collaboration, however, was a more detailed study of the quenching time. The requirement for this type of study was a reaction which could be kinetically

Reproduced with permission of the copyright owner. Further reproduction prohibited without permission.

followed independently by optical spectroscopy (or other means) as well as by EPR and which had a rate which enabled the resolution of quenching times shorter than 20 msec. An independent measuring technique not only obviates the necessity for the reaction to have simple kinetics (although the results are more conveniently interpreted in this case), but it also gives more weight to the results obtained if the two methods agree. Since they were unable to find a reaction which could be followed by a changing EPR signal, they chose a reaction which could be followed by optical means and used reflectance spectroscopy to measure the extent of the reaction in the frozen solutions and compared the kinetics obtained in this manner to those obtained by stopped-flow methods. From studies of the reduction of cytochrome c by ascorbate they (25) concluded that the quenching time was of the order of 10 msec. They (24) substantiated this conclusion with experiments performed on xanthine oxidase.

Although reflectance spectroscopy is useful for many studies, its quantitative interpretation is usually difficult at best (26) and since rapid freezing was developed primarily for EPR studies, an EPR evaluation of the quenching process would be more relevant.

The reaction between ferrimyoglobin hydrate, $[Mb(Fe^{3+}) \cdot H_2O]$, and sodium azide was considered suitable for studying the quenching process. This reaction can be followed spectrophotometrically at numerous wavelengths and with EPR by following the disappearance of the high-spin ferrimyoglobin hydrate as it is converted to the

Reproduced with permission of the copyright owner. Further reproduction prohibited without permission.

low-spin ferrimyoglobin azide complex, $[Mb(Fe^{3+})\cdot N_3^-]$ (27,28). Previous studies (29,30) indicated that a suitable reaction velocity could be obtained by carefully choosing the pH at which the reaction took place. It was decided that if this reaction were indeed suitable for quenching studies, it would be well to examine how the quenching rate was affected by: (a) the flow velocity at the nozzles, (b) the temperature of the quenching bath, and (c) the temperature at which the reaction was occurring.

It might be pointed out that the cytochrome c reduction by ascorbate which Palmer and Beinert (25) used for quenching studies can also be monitored with EPR by measuring the disappearance of the oxidized cytochrome c signal. However, measurement of this signal can only be made at temperatures significantly below $77^{\circ}K$ (31) and therefore requires specialized cryogenic equipment. (Even if Palmer and Beinert had this equipment, the cytochrome c signal was not known until after they had completed their studies.) In any event, the expense of liquid helium is prohibitive to extensive studies on the quenching process by using the cytochrome c-ascorbate reaction.

Since it was conceivable that a detailed study of the quenching process would show that the quenching time was short (perhaps as short as 2 msec), it was necessary to demonstrate that the mixing process and the constancy of flow were sufficient to resolve 2 msec. A constant mean flow only assures that the volume passing through

Reproduced with permission of the copyright owner. Further reproduction prohibited without permission.

the flow system in a given period of time remains constant. However, examination of cross-sections of flow tubes reveals that the microscopic flow rates vary from near zero at the wall of the tube to a maximum at the center of the tube. The ideal case of plug flow never exists in flow systems. Therefore the problems of flow can be divided into two parts: (a) that of maintaining the constant mean flow rate necessary for accurate flow studies and (b) that of minimizing the deviations from bulk or plug flow, a condition which would exist only if the fluid moved as a solid body.

Constant mean flow can be achieved by driving the syringes at a fixed velocity, having attained and terminated this velocity in times very short compared with the period of flow. Hansen and Beinert (32) described a ram system which is fully capable of driving syringes with this kind of motion. This ram employs a one horsepower d. c. servo-motor as a source of mechanical power and translates the rotary motion of the motor into linear motion by a drive screw and rider mechanism. There is a fairly complicated trigger which disengages the drive mechanism at the appropriate time. Thorough evaluation of this ram showed that even under conditions which demolished the syringes, the ram maintained a constant velocity. Although this was certainly sufficient for doing rapid freezing, the cost of such an apparatus prohibited its duplication for use by this author. It was suggested that the use of a 1/2 hp motor to turn a flywheel at a high velocity, would be an alternative method

Reproduced with permission of the copyright owner. Further reproduction prohibited without permission.

of producing power comparable to that of the machine developed in Madison. The presumption is that the energy to drive the syringes is an insignificant fraction of the energy which can be "stored" in a spinning flywheel. This flywheel angular velocity could be transformed into linear displacement via a gear reduction box, a linear motion cam and a cam follower. Chapter 2 describes the design of such a ram and Chapter 3 evaluates its performance.

Several people (Roughton and Millikan (7), Dalziel (21), and others) have examined the problem of minimizing deviations from plug flow. They have all concluded that these deviations can be kept at a minimum if turbulent flow rather than laminar flow occurs in the reaction tubes. It was felt that these calculations were not completely valid when applied to the rapid freezing technique and therefore Chapter 3 of the thesis discusses more fully and provides some experimental evaluation of this problem. Chapter 5 describes some studies which have been done and which have used rapid freezing and stopped-flow techniques.

Reproduced with permission of the copyright owner. Further reproduction prohibited without permission.

CHAPTER 2

DESIGN OF THE RAPID FREEZING APPARATUS

A. General Layout and Principle of Operation

The rapid freezing instrument is shown in Figure 3. An electric motor (M) which operates between 800 and 2000 rpm is the source of motive power and is used to accelerate the flywheel (FW) to the same speed. The flywheel is mounted on a driveshaft (DS) directly coupled to a reducing gearbox (GB) which can engage a spiral cam (C). The cam converts the rotary motion from the output of the gearbox into linear displacement and thus via the syringe ram (R) drives the syringe plungers (SP). The linear motion of the syringe plungers forces the reactants to flow at a constant rate through plastic flow tubes and into the mixer (X). From there the mixture passes along a plastic reaction tube (RT) into the nozzle (N), and then is ejected as a fine stream into the cold isopentane (the quenching liquid) contained in the special sampling EPR tube (ST). The cold bath (CB) maintains the sampling tubes at cryogenic temperatures. The entire flow system, consisting of syringes, connecting hoses, mixer, reaction tube, and nozzle, is submerged in an aluminum water bath (WB) to maintain a constant temperature for the reaction.

B. Linear Velocity Mechanism - Details

The motor (M) is a Sears and Roebuck Craftsman 1/2 hp silicon-controlled-rectifier (SCR) controlled D. C. motor (Cat. No.

Reproduced with permission of the copyright owner. Further reproduction prohibited without permission.

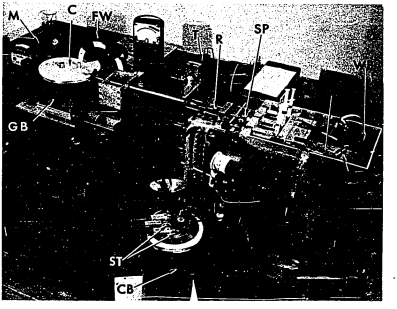

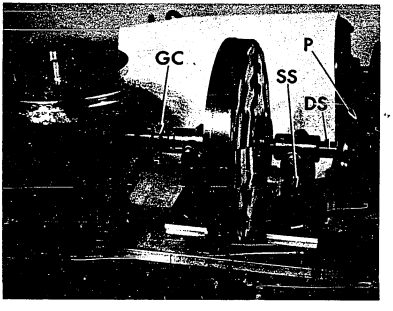

Figure 3 (Top). Rapid Freezing Apparatus
Figure 4 (Bottom). Driveshaft Assembly
(M) electric motor (1/2 hp), (FW) flywheel, (DS) driveshaft, (GB) 100:1 gearbox, (C) linear motion cam, (R) syringe ram, (SP) syringe plungers, (X) mixer, (RT) reaction tubes, (N) nozzles,* (ST) EPR sampling tubes, (CB) cold bath, (WB) aluminum water bath, (P) V-belt pulleys, (SS) shaft supports and bearings, (GC) gear couplings, and (T) tachometer.

* Nozzles (hidden) eject from the base of the water bath.

Reproduced with permission of the copyright owner. Further reproduction prohibited without permission.

99H2344K) with speed continuously adjustable from 500 to 5000 rpm. The SCR speed control eliminates the need for an expensive variable speed transmission and also allows the motor to operate with relatively constant output torque over the entire speed range (33). The motor is coupled via two 3 inch V-belt pulleys (P) and a 10 inch diameter V-belt to the driveshaft (DS) (Fig. 4) which is a 3/4 inch steel shaft turned down from two inch round stock. The flywheel was obtained from a discarded Volkswagen motor (for safety reasons the gear teeth were removed) and is bolted onto the mounting flange of the driveshaft. This driveshaft-flywheel assembly is supported by two adjustable self-aligning shaft supports equipped with bronze bearings (Boston Gear SAP 122). A pair of Boston 3-jaw gear couplings (GC) (FCBB 15), one accepting the 3/4 inch driveshaft, and the other accepting the 1/2 inch input shaft of the gearbox, couple the driveshaft to the gearbox. The gearbox is a Boston LW9 100:1 double reduction worm gear reducer.

The output of the gearbox is a seven inch diameter turntable mounted on a 1/2 inch shaft (Fig. 5). A 1/4 inch thick brass ring with a major diameter of 6-1/2 inches and a minor diameter of 2-1/2 inches supports the cam on the table and serves as a bearing for the cam. To prevent wear, the brass ring-bearing is well oiled. A 3/4 inch shaft, which is bolted to the center of the turntable, centers the cam (or cams, vide infra). The cam can be held motionless while the turntable rotates beneath it and the surface

Reproduced with permission of the copyright owner. Further reproduction prohibited without permission.

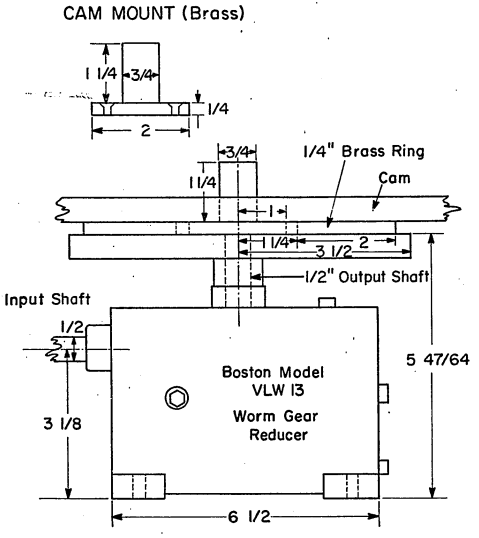

Figure 5. GEARBOX-CAM ASSEMBLY

Reproduced with permission of the copyright owner. Further reproduction prohibited without permission.

tension of the bearing-oil-cam interfaces holds the cam flat to the table.

The heart of the driving mechanism is the linear motion cam. There are two types of cams in use; one (Fig. 6) is for a single push motion and another (Fig. 7) is for a "push-push" motion. The cams were constructed from 1/2 inch aluminum (20-24, a hard grade) and they were milled with a pitch of 5.473 inches per 360° using a vertical milling machine with an indexing head appropriately geared to the feed table. Since 6 cm (2.362 inches) of travel are required to deliver the total capacity of Hamilton Gas Tight syringes (which are used exclusively in flow systems described in this thesis), the total linear motion projected by the spiral of the single push cam is 2.362 inches or about 180°. This corresponds to 0.25 ml in the smallest syringes and 5.0 ml in the largest syringes which will fit in the apparatus. Of course, any fraction of these amounts can be shot in a single experiment. The push-push device (Fig. 7) is composed of two cam sections. The first, the injector, displaces the follower 0.426 inches (which corresponds to 0.09 ml of a one ml syringe). This section mounts on the turntable in the same way as does the single-push cam (Fig. 5). The second section, the ejector, mounts on top of the first and its spiral is a continuation of the injector spiral. The ejector labeled A pushes 0.426 inches (0.09 ml on a one ml syringe) and the ejector labeled B pushes 0.332 inches (0.07 ml on a one ml syringe). These volumes are useful

Reproduced with permission of the copyright owner. Further reproduction prohibited without permission.

Reproduced with permission of the copyright owner. Further reproduction prohibited without permission.

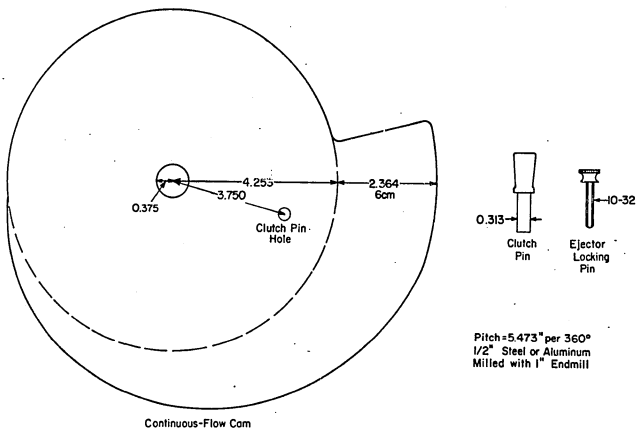

Figure 6
LINEAR MOTION CAM
FOR RAPID-FREEZING
APPARATUS

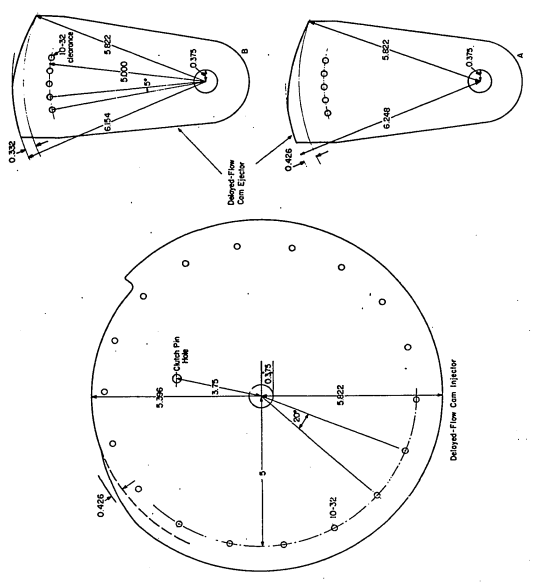

Figure 7. Push-Push Linear Motion Cam

Reproduced with permission of the copyright owner. Further reproduction prohibited without permission.

amounts for most situations encountered in rapid freezing. There are eighteen threaded holes (10-32) equally spaced at 20° on the injector and five 10-32 clearance holes equally spaced at 5° on the ejectors; all of the holes are on a radius of 5 inches. By aligning the holes and screwing the two sections together, when the cam turns a push-push motion is obtained with a delay between the two pushes which depends upon the rotational velocity of the cam and the number of degrees the second cam is offset from the first. The 5° spacing of the holes allows one to offset the ejector sequentially from the injector with increments of 5°. Therefore delay times can be increased with increments corresponding to the time required to turn the cams through 5°.

The cam follower consists of two 1-1/8 inch O. D. Nice 1616 DS ball bearings (obtained from Boston Gear) mounted on a one inch diameter steel shaft (Fig. 8), and a support (Fig. 9) which slides on the ways of a lathe bed (Sears and Roebuck L9-1X Bed, Legs, and Rack Assembly) to transmit the linear motion to the syringe ram. The cam follower support has an adjustable gib so that it can offer resistance to the cam before striking the syringes. This resistance is necessary to take up any backlash in the system before the syringe plungers are struck, and is useful for overcoming the problems resulting from a small amount of flexibility inherent in the 1/2 inch output shaft of the gearbox. This latter point will be discussed in some detail in Chapter 3. The syringe ram is shown in Fig. 10.

Reproduced with permission of the copyright owner. Further reproduction prohibited without permission.

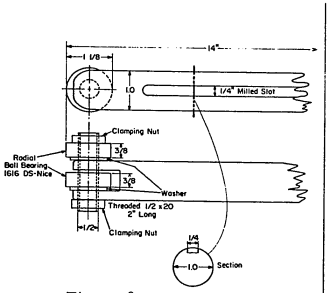

Figure 8. CAM FOLLOWER

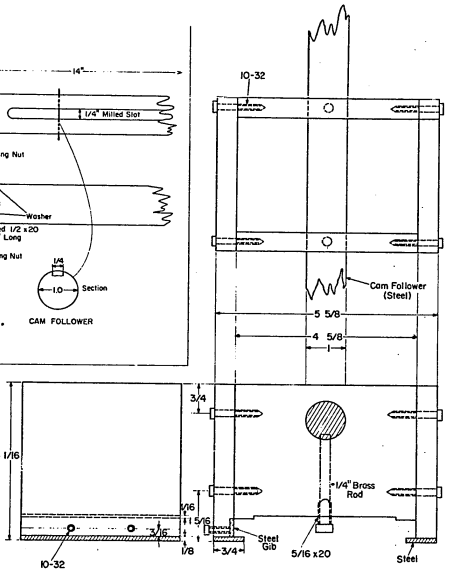

Figure 9. CAM FOLLOWER SUPPORT

1/2" Aluminum Plate Used Throughout Except Where Specified

Reproduced with permission of the copyright owner. Further reproduction prohibited without permission.

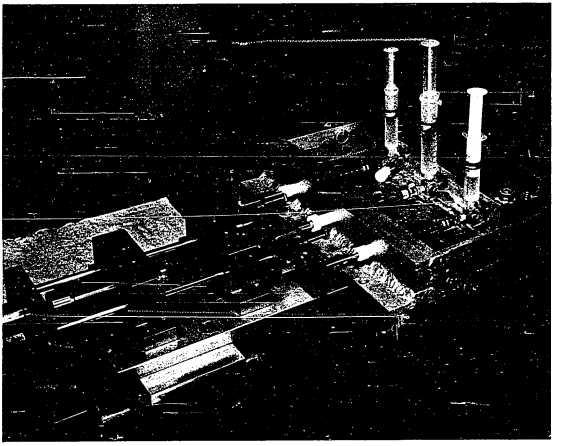

Figure 10. Syringe Ram

Reproduced with permission of the copyright owner. Further reproduction prohibited without permission.

The base plate is fixed in place on the lathe bed with two adaptors. One adaptor mounts directly on the ways (Fig. 11) and can be locked to the ways by tightening the three screws which apply pressure to the gib. The other adaptor (Fig. 12) clamps onto the lathe bed carriage assembly (Sears and Roebuck M6-9X Carriage Assembly less Compound Rest and Threading Dial) with a dovetail fitting. Pressure applied to the gib clamps the adaptor. This carriage assembly is very convenient for accurately moving the transmitting device and the water bath to desired positions with respect to the cam. (It might be noted that although it costs less than one hundred dollars, this lathe bed and carriage assembly is very accurate and sturdy and is quite adaptable to many laboratory situations which require the ability to accurately position components with one variable dimension, e.g. optical components.)

The linear motion from the cam follower is transmitted to the plungers of the syringes by the slide of the syringe ram (Fig. 10). The slide is made from two 1/4 inch stainless rods held together by two end plates which move in circular teflon bearings press-fit into the stainless blocks A and B. The blocks A and B are fastened to a base plate which also holds the water bath. An adjustable stopping screw (SS) is threaded into block A. This screw is adjusted so that it stops the motion of the slide at the exact time the cam reaches the end of its spiral and thus it provides a positive stop for the motion of the syringe ram and also prevents destruction of the syringes in the

Reproduced with permission of the copyright owner. Further reproduction prohibited without permission.

Figure 11. Carriage Support for Syringe Driver

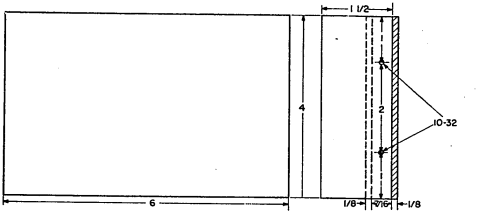

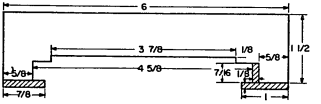

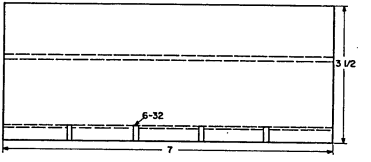

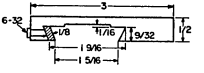

Compound Rest Substitute for Mounting Syringe Driver

Figure 12. ADAPTOR FOR CARRIAGE ASSEMBLY

Reproduced with permission of the copyright owner. Further reproduction prohibited without permission.

event that the positioning of the various components on the lathe bed is not correct.

There are three ways in which the velocity of the linear motion can be monitored on this machine. The method routinely used is to measure the velocity of the flywheel with a simple stroboscope. With fluorescent overhead lighting, a spinning ring consisting of evenly spaced black spots of the same size will "strobe" or appear to stand still when the frequency of the spots passing a single point is 7200 per minute (the frequency of the fluorescent lights). Thus, when the spots appear to be standing still, the velocity of a spinning ring is given by equation 4.

$$4. \qquad \text{rpm} = \frac{7200}{\text{No. of spots on ring}}$$

There is glued onto the flywheel a paper which bears seven concentric rings, each of which consists of uniform-sized, equidistant black spots. The innermost ring has three spots, the outermost ring has nine spots, and the others have intermediate numbers of spots. The speeds at which the various rings isolate are listed in Table 4 of the Appendix. Since the line frequency is usually constant to better than 0.1%, the method can be quite accurate. An example of this accuracy follows: suppose one is observing 1440 rpm (5 spots). If the apparent motion of the isolated spots is three rpm, a condition commonly achieved, the velocity of the flywheel is only three rpm away from 1440 rpm, or about 0.2%.

Reproduced with permission of the copyright owner. Further reproduction prohibited without permission.

In the rare instances that there is need for velocities intermediate between any two of the speeds which can be isolated by the above method, a second tachometer is employed (T in Fig. 3). This tachometer is an AC generator whose output is proportional to the velocity of the driveshaft. Fig. 13 is the calibration curve for the tachometer (Edmund Scientific, about ten dollars). This tachometer was supplied originally with a readout meter, but the meter was defective and is currently replaced by a common VOM. The calibration is easy to perform since the seven strobed points determined by the above method can be used for reference velocities.

Another method is to measure the linear displacement of the syringes directly using a linear displacement potentiometer (CIC, Type 113, 2KΩ, 4 inch). The body of the potentiometer is mounted on the blocks A and B of the syringe ram (Fig. 10), and the wiper is attached to and moves with the slide, and therefore with the syringes. When a small voltage is applied across the ends of the resistor, the output of the wiper is a voltage directly related to the position of the syringes. Alternatively, the output at the wiper is electronically differentiated with respect to time and the linear velocity of the syringes is measured directly. Both of these methods have been used and are documented in Chapter 3. This method is somewhat cumbersome for routine work, so having shown that the velocity is linear under all experimental situations and that it is also proportional to

Reproduced with permission of the copyright owner. Further reproduction prohibited without permission.

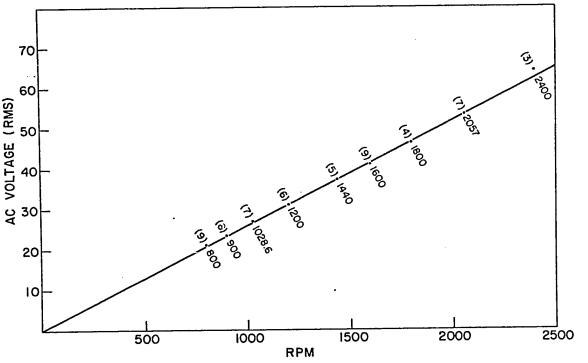

Figure 13. Calibration Curve for AC Tachometer

The numbers in parentheses correspond to the numbers of spots on the rings which isolate at the rotational velocities indicated on the figure.

Reproduced with permission of the copyright owner. Further reproduction prohibited without permission.

the flywheel velocity (vide infra), the driving speed of the ram is now routinely monitored by the stroboscopic or tachometer methods.

C. Flow System - Details

Water Bath: The entire flow system is submerged in a welded aluminum water bath (Fig. 14) which is mounted directly on the base plate of the transmitting device. The shape and size of this bath make it possible to: (a) accomodate three syringes while leaving ample space for manipulation of auxillary equipment such as tonometers and supports for same, (b) submerge the entire flow system to maintain good control of the reaction temperature, (c) allow room for future adaptations of the flow system to equipment which can measure such parameters as pH, potential, or temperature, (d) maintain rather stable temperatures, (e) change syringes without completely emptying the water bath (the water level need only be lowered by about one inch for syringe changes), and (f) conveniently mount the bath on the syringe ram.

Syringes: The syringes are Hamilton Gas Tight barrels (No. 1001, 1002) with specially designed plungers (Fig. 15). It has been found that although commercially available Hamilton Gas Tight syringes resist leakage quite well when operated at room temperatures, they leak considerably at lower temperatures. This is due to the fact that the temperature coefficient of expansion for the Teflon plungers is greater than that of the glass barrels. To circumvent this problem, a plunger tip which has an O-ring seal was designed.

Reproduced with permission of the copyright owner. Further reproduction prohibited without permission.

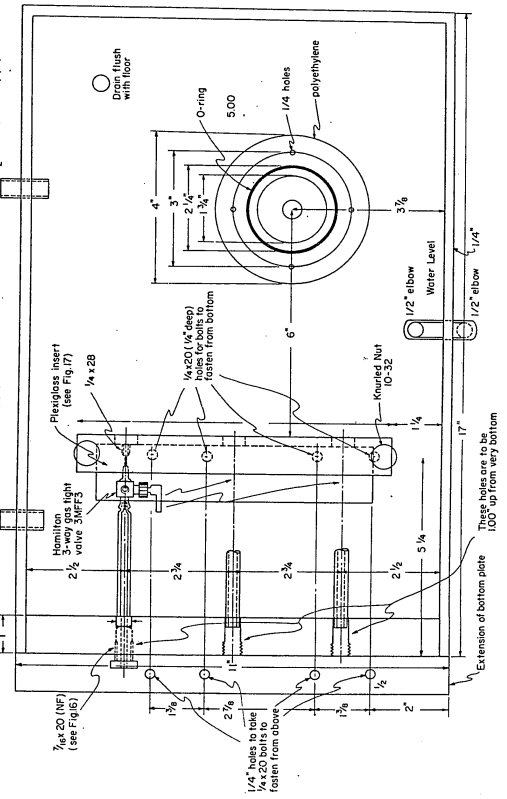

Figure 14 A

Reproduced with permission of the copyright owner. Further reproduction prohibited without permission.

Figure 14 B

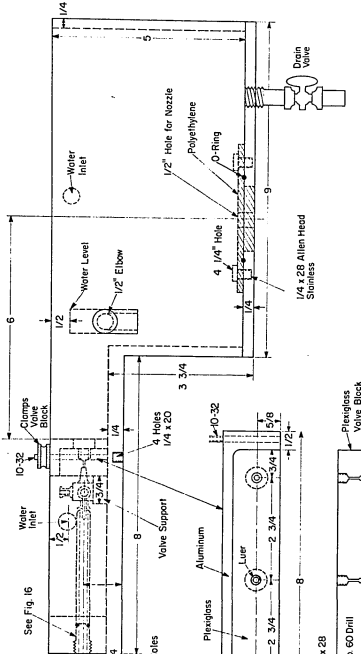

Figure 14. Aluminum Water Bath

A. Top view of aluminum water bath for rapid freezing instrument. All parts are of aluminum unless otherwise specified. The walls and bottom of the bath are welded together to insure permanent water-tightness.
B. Side view of aluminum water bath for rapid freezing instrument.

Reproduced with permission of the copyright owner. Further reproduction prohibited without permission.

Legend to Figures 15 and 16

The plunger is made from stainless steel and is fitted with a Teflon tip with a leak-tight Viton O-ring seal (Roger Zatkoff Co.). The dimensions appropriate for the different sized syringe barrels are:

Syringe (ml)	x	y	y'	z	z'	O-ring
0.25	0.309	0.091	0.85	0.060	0.045	---
0.50	0.309	0.128	0.123	0.085	0.064	001
1.00	0.355	0.181	0.176	0.121	0.091	003
2.50	0.375	0.286	0.281	0.191	0.143	006

The Teflon tip should be made to fit smoothly in the syringe barrel and the O-ring should just barely protrude.

The part marked (*) is used with the brass tip as an aid in putting on the O-ring. This is usually sliced off with a razor blade after the O-ring is on.

Reproduced with permission of the copyright owner. Further reproduction prohibited without permission.

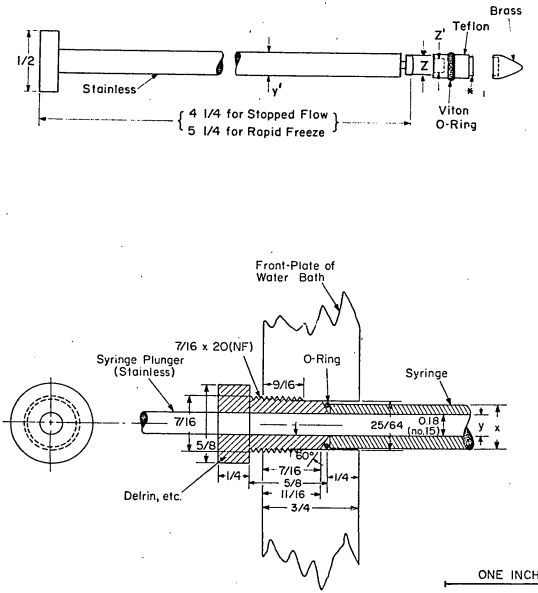

Figure 16. Syringe Mounts

Reproduced with permission of the copyright owner. Further reproduction prohibited without permission.

The Teflon tip which is similar to the Hamilton tip is made to be a good fit at room temperature. The O-ring (Viton O-rings, Roger Zatkoff Co.), which is considerably compressed at this temperature (but not so much that the plunger cannot be withdrawn and inserted easily), maintains the seal even though the Teflon tip and glass barrel do not contract identically. It has been found that when the O-rings are in good shape there is no leakage behind the plungers even when encountering the large flow resistances in rapid freezing and at the stopping of flow in the stopped-flow method.

Syringe Mounts and Three-way Valves: The syringes are mounted into the water bath with an O-ring seal (Fig. 16). A Delrin screw fitting with a tapered tip presses the barrel into the Hamilton 3-way valve (2MFF3) and presses the valve into the Lucite block (Fig. 14) while at the same time compressing the O-ring to make a leak-tight seal between the syringe barrel and the water bath. This Delrin screw fitting also helps to prevent the plunger rods from sagging when they are withdrawn to fill the syringes. The Hamilton 3-way valves allow no metal to contact the solution (only Teflon and Kel-F contact the solutions) and are extremely convenient for introducing solutions into the driving syringes. Although there is some differential contraction between the Teflon and the Kel-F when the valves are cooled, the adjustment cap can be tightened to maintain the liquid seal. The Lucite block (Fig. 14) serves as part of a connector from the valves to the polyethylene tubes which lead to the mixer.

Reproduced with permission of the copyright owner. Further reproduction prohibited without permission.

Connecting Tubing: The polyethylene tubing connector design is shown in Fig. 17A and is a slight modification of the design by Bray (18). The connectors can be made of stainless steel, brass or aluminum. Since no solution ever contacts the metal connectors (they merely serve to press the polyethylene tubing into the screw holes), the nature of the metal only matters in that it should resist corrosion in the water bath. Heavy-walled polyethylene tubing with an O. D. of 0.114 inches and an I. D. of either 0.022 or 0.042 inches was obtained from Bel Arts Plastics (Cat. No. F-21852). Leak-tight flanges can be made on the ends of the tubes with the flange making device (Fig. 17B). The procedure is as follows: the polyethylene tubing is inserted through a connector so that the end protrudes about 3/16 inch. A piece of tape is wrapped around the tube next to the connector to serve as a marker. The brass rod mounted on a ring stand, is moistened with water and the connector is screwed into the rod until the tubing just touches the bottom of the hole. (The tape marker will indicate when this happens.) Since the deformation point of polyethylene is about 100°C, water is a convenient temperature indicator. The brass device is heated gently with a propane torch until the water ceases to boil, then for an additional two seconds and immediately the connector is screwed in snugly while at the same time the tubing is pressed towards the brass rod to facilitate the molding of the tip. Then the flange-making device, tubing, and connector are quickly doused in cold water to prevent

Reproduced with permission of the copyright owner. Further reproduction prohibited without permission.

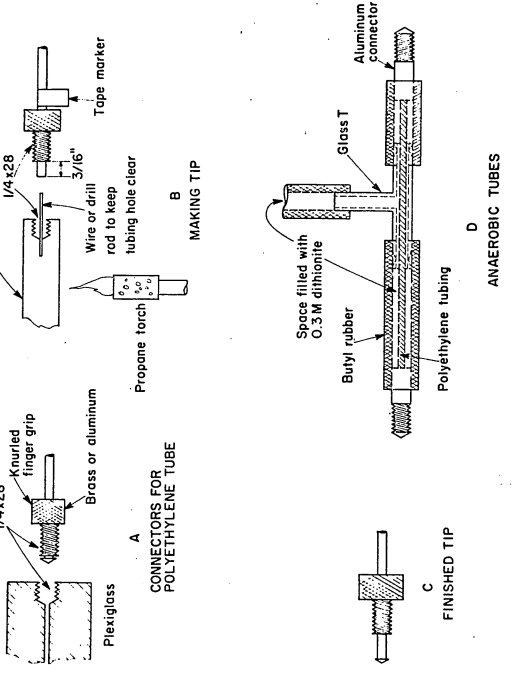

Figure 17. Polyethylene Tubing Connectors

Reproduced with permission of the copyright owner. Further reproduction prohibited without permission.

excessive heat deformation of the plastic. (After trimming the excess polyethylene from the tip, it should appear as in Fig. 17C.)

The thick-walled polyethylene tubing is very convenient since it is flexible and translucent, and it resists expansion under pressure. However, the permeability of polyethylene to gases makes it quite unsuitable for anaerobic work. Therefore, when anaerobiosis is required, the tubing shown in Figure 17D is used. The same types of tips and connectors are used (with the exception of the finger grip on the connector), but butyl rubber tubing (which has a low gas permeability) encases the plastic tubing. The space between the rubber and plastic is rendered oxygen-free by filling it through the glass T-joints with a solution approximately 0.3 M in sodium dithionite and 0.5 M in phosphate at pH 8-9. The phosphate buffer stabilizes the dithionite (34). Flavin or indigo disulfonate is added in small amounts to scavenge oxygen and to serve as an indicator which can be observed through the glass T-joints. This tubing, although used only recently for rapid freezing, has proven successful also with the stopped-flow instrument (vide infra). Since the stopped-flow method is more sensitive than the rapid freezing method, smaller concentrations of reagents are used, and therefore the requirement for anaerobiosis in stopped-flow studies is more stringent than for the rapid freezing technique. The butyl rubber covered tubing, although not as flexible as the polyethylene tubing alone, is flexible enough that work can be done with minimal inconvenience.

Reproduced with permission of the copyright owner. Further reproduction prohibited without permission.

An earlier attempt at achieving anaerobic conditions involved inserting the polyethylene hoses into tightly fitting stainless steel tubing. It was thought that the stainless steel would prevent oxygen from diffusing to the sample; yet the sample, being totally confined in the polyethylene tubing, would avoid contact with the metal. It was found, however, that although it was somewhat more anaerobic than the polyethylene tubing alone, the tubing was not sufficiently anaerobic for rapid freezing studies. Furthermore, the stainless steel prevented visual checks on the anaerobiosis, and being rather inflexible, it was more difficult to manipulate. However, if the tubes are thoroughly flushed with pure nitrogen gas just prior to use, they are useful as reaction tubes. In this application the fluid passes through the tubes very quickly; this coupled with the fact that there is very little oxygen present in the tubes (due to the nitrogen flushing) leads to only insignificant oxygen effects on the reaction.

Mixers: Several types of fluid mixers have been employed in the rapid freezing apparatus and extensive tests of these mixers are described in Chapter 3. One of the mixers employed is the Palmer and Beinert mixer (25) which has one set of four tangentially opposed jets (Fig. 18). The design is slightly modified from that in reference 25 for ease of machining and assembling. This mixer is constructed in the following way (Figure 18): In a lucite rod one inch in diameter and one inch long is milled a 5/8 inch hole 1/4 inch in diameter. From the opposite end a hole is drilled with a number 3 drill to a

Reproduced with permission of the copyright owner. Further reproduction prohibited without permission.

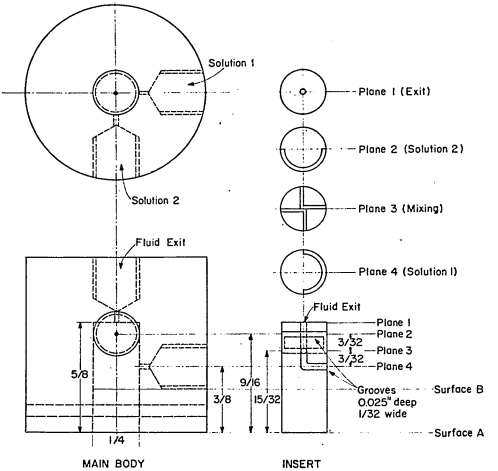

Figure 18. PALMER-BEINERT MIXER
All Tapped Holes 1/4-28.
All Small Holes no.75 Drill
Lucite

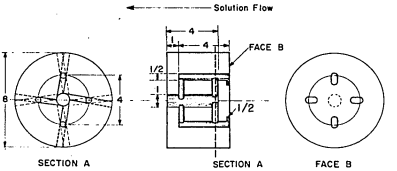

Figure 19. GIBSON-MILNES MIXER

Reproduced with permission of the copyright owner. Further reproduction prohibited without permission.

depth of 5/16 inch and this is tapped to 1/4-28 to become the exit hole for the mixer. Then a hole is drilled clear through with a number 75 drill (0.21 inch). Two holes 5/16 inch deep are drilled with a number 3 drill at right angles to each other at distances from surface A of 3/8 inch and 9/16 inch respectively. These are also tapped to 1/4-28. A 1/4 inch diameter rod 5/8 inch long has two semicircular grooves milled into it as shown, each with a width of 0.032 inch and depth of 0.025 inch. From each of the grooves, two channels 3/32 inch long are milled (same depth and width as the semicircular grooves). The channels from a single groove are opposite each other and the channels from different grooves are at right angles to each other. (Improvements to this design will be discussed in Part 3 of Chapter 3, Discussion.) Then holes are drilled to the center of the rod from the ends of the channels slightly off-axis so that the intersection of the four holes is a 4-jet tangential mixer. A hole drilled to the mixer with a number 75 drill allows the mixed fluids to exit. From plane B to the bottom of the rod, the diameter is 0.248 rather than 0.250 inch. The wider end of the rod press-fits into the main body of the mixer, while the narrower end is glued to make a leak-tight seal. Attempts to glue around the channels failed because the glue tended to fill up the channels. Press-fitting the portion around the channels and only glueing the end eliminated this problem. A 1/16 inch hole was then drilled clear through the two

Reproduced with permission of the copyright owner. Further reproduction prohibited without permission.

assembled units (see figure) and a brass rod was glued into place to supply added strength to the mixer seal.

A second type of mixer which has been used is the well known Gibson-Milnes mixer (11). This mixer consists of 2 sets of 4 tangential jets; the first swirls the fluid one way, and the second swirls the fluid in the opposite sense (Fig. 19). These Gibson-Milnes mixers (which were made by L. Milnes) differ from the usual type in that the diameters of all of the holes have been reduced by a factor of two. This decreases the dead space by a factor of four and increases the linear flow velocity (m/sec) for any given volume flow velocity (ml/sec) by a factor of four from the standard mixer.

Mixing studies (see Chapter 3, Part 3) showed that the Gibson-Milnes mixer was unsuitable for use at the small flow velocities employed in rapid freezing (1 ml/sec as compared with more than 10 ml/sec in stopped-flow). Therefore, two other types of mixers (Ballou mixers) were designed (Fig. 20). These have the same outer dimensions as the Gibson mixers, but they are considerably easier to construct. They can be made out of inert materials (e.g. Kel-F or Teflon) and most importantly, they work well at the low flow velocities employed. These mixers are constructed in the following way: a Kel-F rod 5/16 inch in diameter is cut and faced so that it is about 3/16 inch long. The "button" so obtained is mounted on a milling machine (preferably on an indexing head) and four equidistant holes are drilled on a 1/16 radius with a number 68

Reproduced with permission of the copyright owner. Further reproduction prohibited without permission.

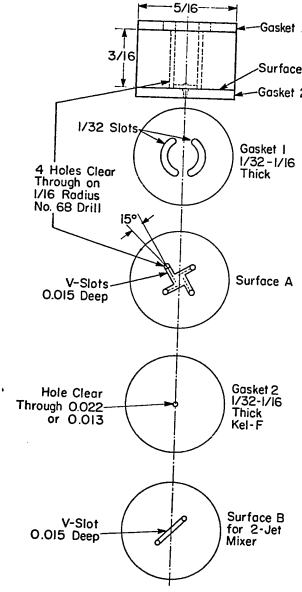

Figure 20. BALLOU MIXER
Kel-F

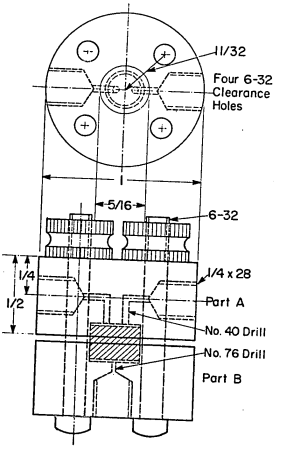

Figure 21. MIXER MOUNTS
Lucite

Reproduced with permission of the copyright owner. Further reproduction prohibited without permission.

drill (0.031 inch, 0.75 mm). The milling machine spindle is tilted to 45° from the vertical and a 1/16 inch end mill is mounted in the spindle. (A smaller mill can be used, but this size works well and is not likely to be broken.) The mixer is turned so that a line intersecting two opposite holes, forms an angle of about 15° with the direction in which the table is fed. A hole is lined up with the corner of the end mill and a V-shaped groove with a depth of 0.015 inch is scribed from the hole to the center of the mixer. This is repeated for the three remaining holes. A 4-jet tangential mixing surface results. A thin slice (about 1/32 to 1/16 inch thick) is cut off a 5/16 inch diameter Kel-F rod, into which has been center drilled either a 0.021 or 0.013 inch diameter hole. The disc is pressed against the 4-jet mixing surface to form the mixing chamber. This disc is an integral part of the mixing chamber design and is necessary to produce good mixing at low flow velocities (see mixing studies). A 2-jet mixer is produced in exactly the same way, except that only two holes are drilled rather than four. In the two-jet mixers manufactured, the V-grooves are not offset by 15°, but are simply channels between the two holes. Thus they are really T-mixers.

This type of mixer undoubtedly causes optical artifacts (cavitation) at high flow velocities, but with rapid freezing and other flow techniques which do not rely on optical measurements made simultaneously with flow, these artifacts are of little or no importance. The simplicity of design and the possibility of achieving very small

Reproduced with permission of the copyright owner. Further reproduction prohibited without permission.

dead spaces (of the order of 0.25 microliter) make this type of mixer very desirable.

The Gibson-Milnes and the Ballou mixers are connected to the flow system identically (Fig. 21). Two pieces of one inch diameter Lucite rod (or any other suitable material) are drilled as shown, and are used to clamp the mixer and the two discs together. One disc is part of the mixing chamber as mentioned above and is inserted between part B and the mixer and the other disc has two C-slots cut into it and goes between part A and the mixer. The exact size and shape of these is not critical since these slots merely serve to direct the reactants from the two capillary entrance holes to the appropriate holes in the mixer and to make leak-tight seals. Note that no mixing occurs until the solutions are brought together at the 4-jet intersection. The parts A and B are bolted together with four brass 6-32 bolts and knurled nuts.

Nozzles: The Lucite nozzles were constructed (Fig. 22) nearly identically to those described by Palmer and Beinert (25) with the only change being that the exit holes were 0.008 inch (#92 drill) rather than 0.006 inch in diameter. This dimension was used because it was found that with the 0.006 inch nozzles, the frozen particles produced were too fine to pack into the EPR tubes. It is probable that the finer nozzles Bray used (18-20), which were made of thin-walled polyethylene tubing, expanded under the hydraulic pressure and were, in fact, nearer to 0.008 inch in diameter than

Reproduced with permission of the copyright owner. Further reproduction prohibited without permission.

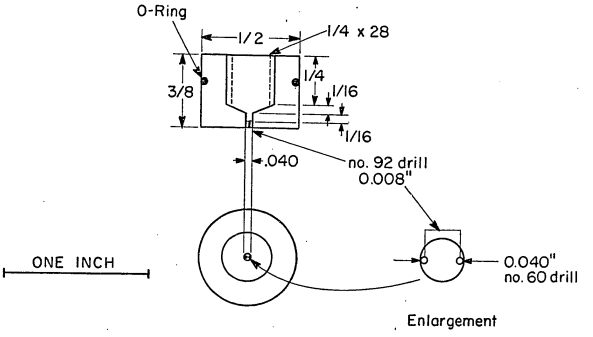

Figure 22. EXIT NOZZLE - (Lucite)

Reproduced with permission of the copyright owner. Further reproduction prohibited without permission.

to the 0.006 inch diameter which they were during the absence of the hydraulic pressure.

When performing experiments requiring long reaction times, in order to conserve reactants (see equation 1.), the flow rate is halved and a nozzle which has only one exit jet is used. Thus the flow velocity at the nozzle, and hence the quenching conditions, are the same as for the two-jet nozzle at twice the velocity. Since the times in these experiments are long, effects from inefficient mixing due to lower flow velocities (see Chapter 3) are negligible.

D. Cryogenic Quenching Apparatus - Details

The cryogenic quenching apparatus (Fig. 23-25) consists of: (a) a stainless steel dewar which holds liquid nitrogen, (b) a brass container which is filled with isopentane and is cooled by contact with the liquid nitrogen in the dewar, (c) the temperature controller, (d) a plexiglass top (Figure 25) which holds in the isopentane bath, the stirrer (S), the sampling EPR tubes, the tube holders (TH), the heater (H), the temperature sensor (T), the packers and the packer holder (P).

The dewar is a stainless steel 5-1/2 [illegible] dewar obtained from Supairco Co. Although stainless steel dewars are not as efficient as glass dewars, they are preferred in this application because of their superior ruggedness. The brass container is shown in Figure 24. It is made from 1/4 inch brass and is coated to within about one inch from the bottom with a layer (about 1/8 to 3/16 inch

Reproduced with permission of the copyright owner. Further reproduction prohibited without permission.

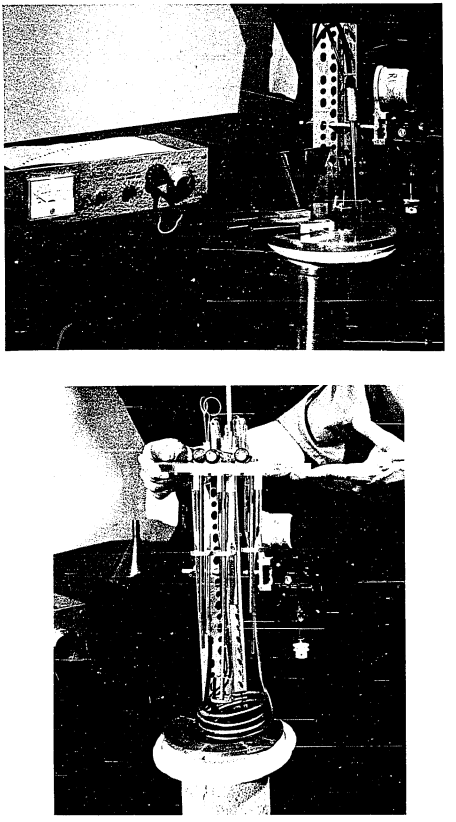

Figure 23. Cryogenic Quenching Apparatus

Reproduced with permission of the copyright owner. Further reproduction prohibited without permission.

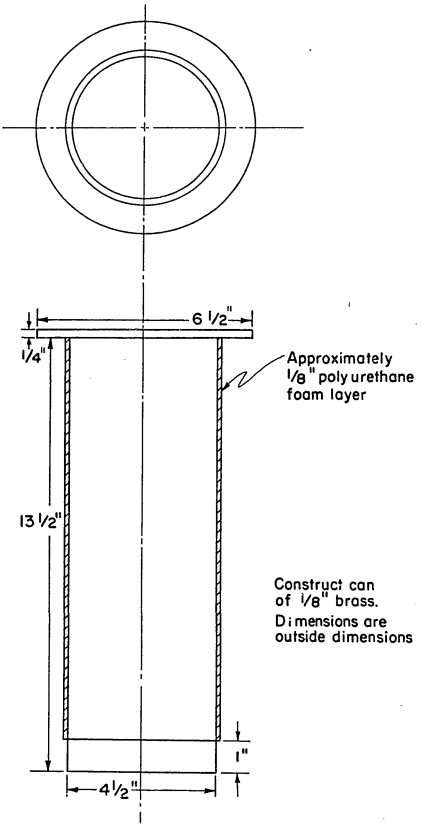

Figure 24. Brass Container for Isopentane

Reproduced with permission of the copyright owner. Further reproduction prohibited without permission.

Legend for Figure 25

(OR O-ring drive belt for stirrer, (H) heater, (T) temperature sensor, (PS) plexiglass shield, (P) packer holder, (S) stainless steel stirrer, (DP) delrin pulley, (TH) EPR tube holes, (B) bearings.

Reproduced with permission of the copyright owner. Further reproduction prohibited without permission.

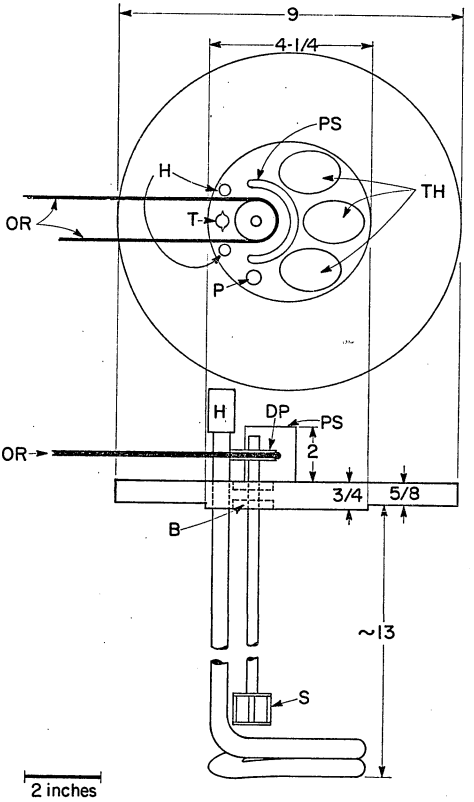

Figure 25. Isopentane Bath Cover

Reproduced with permission of the copyright owner. Further reproduction prohibited without permission.

thick) of polyurethane foam, the purpose of which is to insulate most of the brass cannister from the liquid nitrogen so that the thermal contact between the isopentane and the liquid nitrogen is mainly through the one inch uncoated section of the brass container. Thus, the rate of heat transfer from the isopentane is not affected very much by the level of liquid nitrogen in the dewar.

Polyurethane foams can be purchased from Dow Chemical Co. or Wyandotte Chemical Co. The recommended form of polyurethane is the base/catalyst type which is mixed just before using.

To avoid frost formation, the top of the cooling apparatus (Fig. 25) is constructed from 3/4 inch Plexiglass, a poor conductor of heat. This is to minimize the possibility of frost dropping into the sampling tubes and then being packed with the sample. The stainless steel stirrer (Bel Art Products Cat. No. 887) which is necessary to prevent severe temperature gradients from forming in the isopentane bath, rotates on two small ball bearings mounted on the Plexiglass top. To prevent the bearings from freezing, they are coated with a few drops of a graphite lubricant (Dixon Graphited Lock Fluid, Lock Ease). A two inch long half-section from a two inch diameter Lucite tube is glued onto the Plexiglass top to form a shield between the stirrer and the sample tubes so that any frost which forms on the stirrer will not drop into the sample tubes. The stirrer is powered by a common laboratory stirring motor (Talboys Instrument Corp.) via a 4 inch diameter O-ring drive belt and two

Reproduced with permission of the copyright owner. Further reproduction prohibited without permission.

Delrin one inch pulleys. This mechanism allows one to place the motor to the side of the quenching bath where it will not interfere with any manipulations of the sampling tubes. Another benefit of being at the side of the quenching bath is that the electric motor does not have to be as close to the flammable isopentane as it would if it were directly above the bath.

The temperature of the quenching bath is regulated to within about 2°C of the desired temperature (usually -142°C) by means of a solid state temperature controller (Bayley Instrument Co., Model 74-15). This controller is operable in the range -200°C to +100°C and provides proportional temperature control with a band width adjustable from 0.1°C to 2°C. (The latter is generally used for the rapid freezing application.) The sensor (T) and the heater (H) (Sargent, Model S-40825) are mounted on the Plexiglass top (Fig. 25). The heater is a 1000 watt copper sheathed nickel-chromium element and has been coiled as shown to insert into the brass container. This conformation allows room for the stirrer, the sensor, and the sample tubes and since most of the heating element is at the bottom of the container (where the major heat transfer occurs), the temperature regulation is very good.

EPR Sampling Tubes: The EPR sampling tubes are made from fused quartz (Thermal American Fused Quartz Co.) with a design (Fig. 26) which is very similar to that of Bray and Petersson (19). The measuring portions of the tubes are carefully selected to

Reproduced with permission of the copyright owner. Further reproduction prohibited without permission.

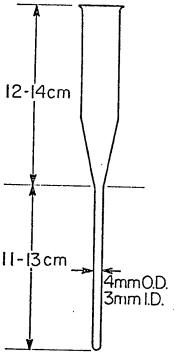

Figure 26. Rapid Freezing EPR Tubes

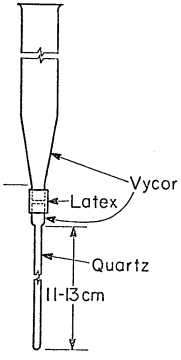

Figure 27. Demountable EPR Tubes

Reproduced with permission of the copyright owner. Further reproduction prohibited without permission.

be of constant bores to facilitate packing of the samples and to be of constant wall thickness so that retuning of the EPR spectrometer is not necessary in the course of making measurements. Besides being an inconvenience in the measuring of the samples, retuning can lead to inaccuracies in the quantification of the signals. The EPR tubes should have smooth walls as shown, since irregularities in the walls tend to hinder the packing procedure. The tubes used in this rapid freezing apparatus have been made by Mr. J. Babbit of the Quality Glass Apparatus Co.

This type of tube although convenient for rapid freezing, is very cumbersome to store at low temperatures. Therefore, when it is desired to save samples which have been rapidly frozen, a tube which has a demountable top (Fig. 27) is used. This type was developed in collaboration with Mr. L. Strong and was constructed by Mr. J. Babbit. The measuring part of the tube is made from the usual quartz tubing (4 mm O. D. and 3 mm I. D.), but pieces of an intermediate size (8-10 mm O. D.) are fused onto each section. Making sure that they are aligned properly, the two sections are fastened together with a short piece of latex rubber tubing. It has been found that it is easier to disassemble the tubes if a drop or two of glycerol is placed on the quartz pieces before fastening them together with the latex tubing. When the tubes are cooled in the isopentane bath, the latex becomes hard and contracts tightly around the quartz making a rigid EPR sampling tube. When the frozen

Reproduced with permission of the copyright owner. Further reproduction prohibited without permission.

sample has been prepared (vide infra), warming of the latex facilitates easy removal of the top.

The tube holders are shown in Figure 28. The aluminum rings A and B can be adjusted to accommodate either the regular sample tubes or the separable tubes. The packers which are shown in Figure 29 are somewhat simpler than the design of Bray and Peterson (19) although they appear to work just as well. The threaded stainless steel is screwed into a hole that runs clear through the Teflon packer cutting threads in the Teflon as it is screwed in. So that the sample is not melted during packing, these packers are precooled in a small pyrex vessel (Fig. 23) which is kept in the isopentane bath.

Preparing the Packed Sample: The method of preparing the frozen sample is essentially the same as that of Bray (20). The sampling tubes are filled with isopentane (about 40-50 ml) and cooled in the brass cannister to -142 ± 2°C. With this apparatus three tubes can be cooled at the same time. A tube is momentarily removed from the isopentane bath and held so that the surface of the isopentane in the tube is one cm or less below the nozzles which squirt the reaction mixture from the bottom of the water bath. The shot is made and the tube is immediately replaced in the isopentane bath. After a few seconds the frozen sample will settle into the taper and by carefully working the packer up and down, the sample can be packed into the bottom of the tube. It has been found that small organic molecules

Reproduced with permission of the copyright owner. Further reproduction prohibited without permission.

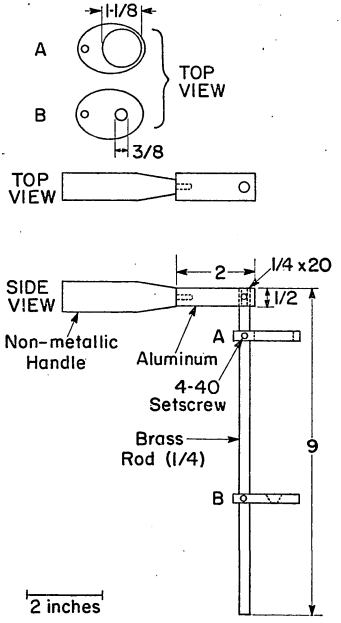

Figure 28.
Rapid Freezing Tube Holders

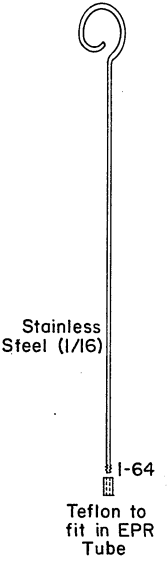

Figure 29.
Sample Packer

Reproduced with permission of the copyright owner. Further reproduction prohibited without permission.

(such as flavins) and inorganic molecules (such as dithionite) usually have to be packed by rapidly moving the packer to avoid the formation of plugs in the neck of the tube, whereas proteins often have to be packed with slow motions or else the crystals will simply float in the isopentane and make it impossible to pack the sample. Although the nature of the frozen particles is largely determined by the nozzle velocity, the variation in the ease of packing different chemical species squirted at the same nozzle velocity, indicates that good packing technique is really somewhat of an art and therefore must be learned through experience. One pointer in packing samples is that in order to prevent the formation of small spaces in the sample which could lead to irreproducible results, considerable downward force must be exerted on the packer. Once the sample has been packed, the tube is lifted out of the isopentane bath, wiped free of isopentane and that part of the tube containing the packed sample is immediately immersed in liquid nitrogen. The isopentane is poured off and, the sample still immersed in liquid nitrogen, the last bit of isopentane is removed with the aid of a small piece of polyethylene tubing connected to an aspirator. This last step is important because if not done, storage in liquid nitrogen may freeze a plug of the isopentane in the tube just above the sample. When manipulating the tube while making measurements, this plug may thaw unevenly and explode with a loud pop, the result being a ruined sample, or worse, a broken tube.

Reproduced with permission of the copyright owner. Further reproduction prohibited without permission.

Sample Measurement: The samples are measured on a Varian V4500-10A EPR spectrometer at X-band frequencies. Since EPR signals are very temperature dependent, quantitative work demands good temperature control ($\pm$ 0.5^{o}C or better). The low temperature system used on this spectrometer is similar to that of Hansen et al. (35) and is described fully therein. This is a gas flow system and when operated at low temperatures (e.g. below -190°C) the high flow rate required often causes small movements of the EPR tubes. To avoid problems which may derive from such instabilities, a Lucite stabilizer was constructed (Fig. 30) which inserts between the magnet coils.

Thawing of the Samples: In order to thaw samples frozen in EPR tubes the usual procedure is to immerse the tube quickly and completely in water at room temperature so that the sample thaws uniformly. However, when using the above procedure with samples prepared by the rapid freezing method, the isopentane thaws very rapidly, and because of frozen aqueous material, its ensuing expansion is often blocked so that when sufficient pressure builds there is a loud pop, as described earlier, with concomitant breaking of the tube. This can usually be avoided if the tube is warmed more slowly by reimmersing the tube into cold isopentane or by carefully warming the tube in air until the isopentane melts. Subsequently the tube can be completely immersed in a water bath to melt the frozen aqueous particles as is done for conventional tubes.

Reproduced with permission of the copyright owner. Further reproduction prohibited without permission.

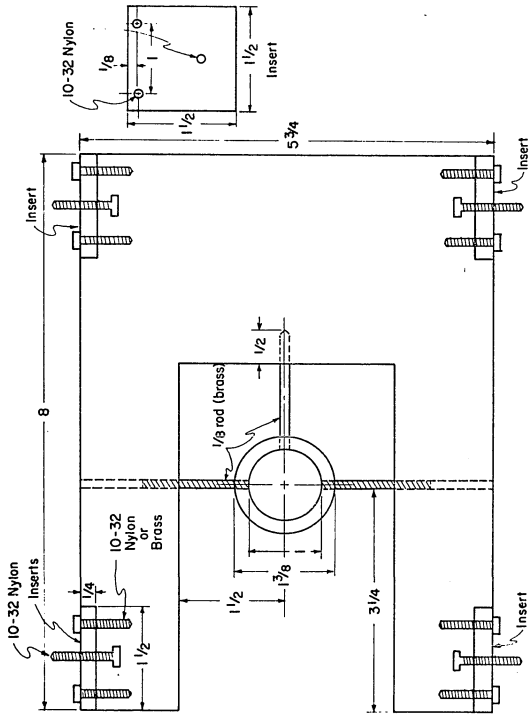

Figure 30. Rapid Freeze EPR Tube Stabilizer

Reproduced with permission of the copyright owner. Further reproduction prohibited without permission.

CHAPTER 3

EVALUATION OF THE RAPID FREEZING APPARATUS

The proper use of any analytical method requires a knowledge of the method's limitations: therefore, this chapter is devoted to an evaluation of the rapid freezing apparatus described in this thesis. For convenience, the uncertainties associated with the rapid freezing method will be divided into two categories: those which pertain to resolving reaction times, and those which pertain to measuring concentrations of chemical species.

Part I. Variables Associated with Measurement of Reaction Times

The measured reaction time will depend upon: (a) the volume of the reaction tubes, V, (b) the constancy of the fluid velocity, (c) the homogeneity of flow, (d) the efficiency of mixing, and (e) the quenching time. The first four parameters are characteristic of all continuous flow methods while the fifth is peculiar to quenching methods.

A. Reaction Tubes

The reaction tubes are made of either 0.022 or 0.042 inch bore polyethylene tubing - the former are used for times shorter than 70 msec and the latter for longer times. Since the bores are not accurately uniform, calibration of the reaction tubes was performed by two independent methods. The first involved filling the tubes with a concentrated solution of $K_3Fe(CN)_6$, emptying the $K_3Fe(CN)_6$ from the filled tubes into a cuvet which contained 2.00 ml of water, and

Reproduced with permission of the copyright owner. Further reproduction prohibited without permission.

then measuring the optical density of the mixture at 420 nm. From the optical density, the volume of the tubes could be calculated directly or determined from a standard curve. For each reaction tube the calibration procedure was performed at least three times and from the average deviations of the results, the uncertainty of the measured volume is estimated to be 1% or less. The second method involved connecting the tubes via suitable connectors to Hamilton syringes of appropriate sizes and measuring the volume necessary to just fill the tubes. It was found that the volumes determined in this way agreed with those determined by the optical method to within the uncertainty of the method - 1% for volumes greater than 200 ul and 2% for smaller volumes.

Knowing the uncertainty of the volumes of the reaction tubes, it is desirable to see what effect this uncertainty will have on the determination of reaction kinetics. The uncertainty in a function due to the uncertainty in time is given by equation 5.

5. $$\text{uncertainty}_{(t)} = \left|\frac{\partial (f)}{\partial t}\right| dt$$

where a reaction which follows unimolecular decay kinetics will have the form

6. $$f = (\frac{C}{C_o}) = \exp(-kt) \text{ , with } k = \text{rate constant}$$

therefore:

7. $$\left|\frac{\partial (\frac{C}{C_o})}{\partial t}\right| dt = k \exp(-kt)dt$$

Making the approximation that dt can be equated with the uncertainty

Reproduced with permission of the copyright owner. Further reproduction prohibited without permission.

in t, we have: $dt = t(\frac{\%\text{ uncertainty in t}}{100})$ which gives us

uncertainty in $f = kt(\frac{\%\text{ uncertainty in t}}{100})\exp(-kt)$ and since

$\exp(-kt) = (\frac{C}{C_o})$ and $+kt = \ln(\frac{C_o}{C})$

8. uncertainty in $f = (\frac{\%\text{ uncertainty in t}}{100})(\frac{C}{C_o})\ln(\frac{C_o}{C})$

From 8. the uncertainty in C/C_o as a function of C/C_o can be calculated and is shown in Fig. 31.

Although the absolute uncertainty in C/C_o decreases with increasing time, the value of C/C_o decreases at an even faster rate resulting in an overall increase in the % uncertainty in C/C_o as time increases. From this it is clear, however, that the 1 or 2% uncertainty in the reaction tube volume does not create a serious problem in the measurements of the reaction progress.

B. Fluid Velocity

The fluid velocity is determined by the driving speed of the syringe plungers and tests have been performed to evaluate the constancy of the velocity of the plungers. However, before describing these tests it is useful to discuss the power requirements of the flow system. Chance (9) has measured pressure drops for mixing chambers and observation tubes of various bores and the results from his work will be used in the following discussion. Let us calculate the hydraulic pressure in the system for a flow rate of 1.8 ml/sec (generally the maximum flow rate used in this apparatus).

Reproduced with permission of the copyright owner. Further reproduction prohibited without permission.

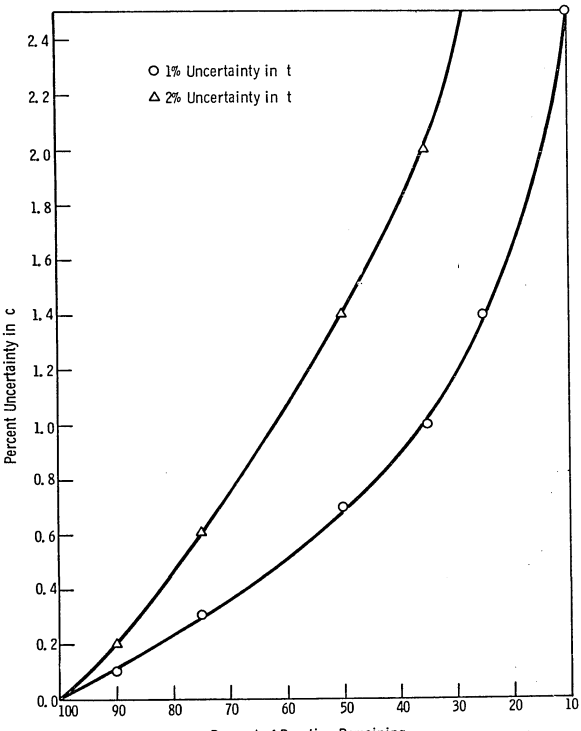

Figure 31. Uncertainty in C/C_o versus Percent Reaction Remaining

Reproduced with permission of the copyright owner. Further reproduction prohibited without permission.

The Prandtl-Karman equation (9) for pressure drop, Δp, in a tube of which the ratio length/diameter is less than forty is;

9. $$\Delta p = 1.4 \frac{\rho}{2} U^2$$

where ρ= fluid density (1 gm/ml = 0.036 lb/in^3), U = linear fluid velocity. Thus the pressure required to produce a flow rate of 30 m/sec (1200 in/sec) through the 0.008 in nozzles is:

$$\Delta p = 1.4\left(\frac{0.036 \text{ lb/in}^3}{2}\right)(1200 \text{ in/sec})^2\left(\frac{1}{3.84 \times 10^2 \text{ in/sec}^2}\right)$$

The quantity, 3.84×10^2 in/sec^2, is the gravitational constant. The pressure drop in the reaction tube will, of course, depend upon the length and the bore and Chance has demonstrated that a 31 cm tube of 0.617 mm bore (0.024 in) - a typical size for a reaction tube used in this apparatus - has a $\Delta p \approx 25$ lb/in^2 for a flow velocity of 1 ml/sec. According to theory, the pressure drop is proportional to the square of the velocity; with this assumption it can be calculated that the pressure drop at 1.8 ml/sec will be about 70 lb/in^2 for a 31 cm tube of 0.617 mm bore. Although this assumption is not totally valid for tubes of this length/diameter ratio, it is used for ease of calculation. Chance has found that for a 2-jet mixer with 0.32 mm jets, a condition similar to that often used in this apparatus, the pressure drop at 1.8 ml/sec is about 40 lb/in^2. If a 0.013 in mixing jet is employed (when using a Ballou mixer), an additional pressure of 26 lb/in^2 can be calculated from equation 9. The connecting tubes which are about 15 cm in length and of 0.6 mm bore, will have a pressure drop of

Reproduced with permission of the copyright owner. Further reproduction prohibited without permission.

approximately 16 lb/in^2. Thus the total hydraulic pressure is about 250 lb/in^2 at 1.8 ml/sec flow rate. When employing two Hamilton 1 ml syringes, the syringe cross-sectional area is 0.334 cm^2 or about 0.0517 in^2, so that the force on these syringe plungers during flow will be about 13 lb. Manual operation of the syringe driving system at this flow velocity indicated that this calculated force, although smaller than expected, is about correct. These values were calculated for solutions with a viscosity of 0.01 poise (e.g. water) and would be increased considerably for more viscous solutions.

The power needed to drive the syringes can be calculated from equation 10.

10. Power = (force)(distance)/time = (force)(velocity)

The velocity at 2400 rpm being 2.2 in/sec or about 0.18 ft/sec, the power is about 2.4 ft-lb/sec which is equal to 4.4 x 10^{-3} hp. This would indicate that the 1/2 hp motor used in this apparatus should be sufficient to drive the syringes. However, there are two factors which must be considered: (1) Most simple motors slow down considerably under loads, a condition which is obviously unsatisfactory for good continuous flow systems. (2) Although the calculated force required to maintain a flow of 1.8 ml/sec is only 13 lb, the force required to rapidly accelerate the fluids to this flow rate is undoubtedly much larger. It was these considerations which suggested the use of a flywheel as a simple means of increasing the

Reproduced with permission of the copyright owner. Further reproduction prohibited without permission.

effective power for the drive system. The expense of other possible systems (such as servo-motor drives) prohibited their use.

C. Uniformity of Driving Velocity

The uniformity of the driving velocity was measured by three methods: (1) The linear potentiometer mounted on the syringe ram (Figure 10) has a voltage impressed across it resulting in a voltage output at the wiper that can be related to the position of the syringe plungers. If during flow this output is recorded as a function of time, a measure of the flow rate is obtained (see Figure 32). (2) If the wiper output is differentiated electronically, a direct measure of the flow velocity as a function of time can be obtained (Figure 32). (3) The stopping syringe assembly of the stopped-flow device (see below) was connected directly to receive the fluid from the reaction tube so that the velocity transducer of this assembly yielded an output which was proportional to the flow velocity. Method (3) was only used to verify that the flow rate at the end of the flow system had the same profile as that at the syringes; this was to find out, if possible, whether expansion in the polyethylene hoses influenced the flow velocity.

The CIC linear potentiometer was factory calibrated to within 0.1% and therefore was not checked further and the output of the velocity transducer (method 2) was checked by comparison with the stroboscopic method. The results indicated a relationship between the velocity and the output voltage which was linear to within the

Reproduced with permission of the copyright owner. Further reproduction prohibited without permission.

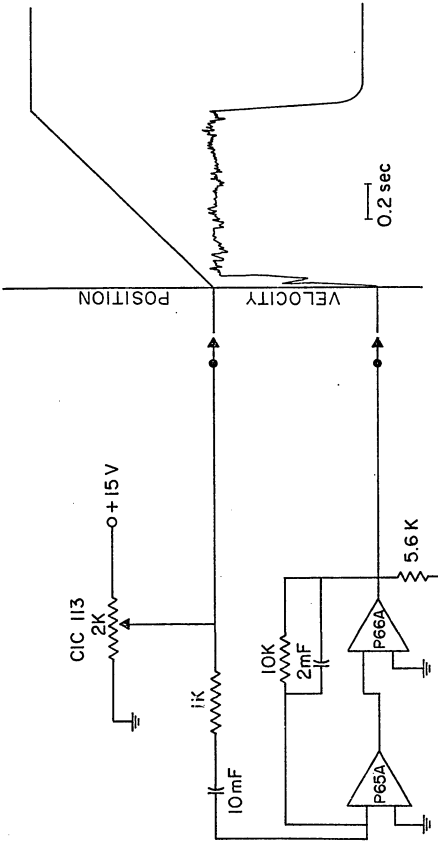

Figure 32. Position and Velocity Signals from Syringe Ram

Reproduced with permission of the copyright owner. Further reproduction prohibited without permission.

ability of measuring the trace (about 1%). It can be noticed from the traces of Figure 32, which were recorded simultaneously with a dual trace oscilloscope, that: (a) the velocity trace is more sensitive to small fluctuations in the flow rate than is the displacement trace, and (b) the time constant of the differentiation device is roughly 50 msec as judged by comparison with the potentiometer output. Because of its greater sensitivity to flow rate fluctuations, the differentiated output was used for most of the tests. However, the 50 msec response time of the differentiating circuit precluded its use for examination of the rapid acceleration and deceleration of the syringe plungers; consequently these parameters were deduced by observing the linear potentiometer output under several load conditions. In all cases the curves were very similar to the trace in Figure 32. The absence of any observable delay during acceleration or deceleration, leads to the conclusion that these times are considerably shorter than the response time of the differentiation circuit. Tests made using method 3 indicated that an upper limit to the acceleration and deceleration times is 10 msec, which is about 1% of the flow time under the following conditions: 1 ml/sec, 1 ml Hamilton syringes, 1 ml total flow (see Figure 36).

Results from tests of the single-push system under various conditions were obtained from the output of the differentiator and are shown in Figures 33-35. The entire flow system was used with a typical reaction tube. The three conditions of viscosity which were

Reproduced with permission of the copyright owner. Further reproduction prohibited without permission.

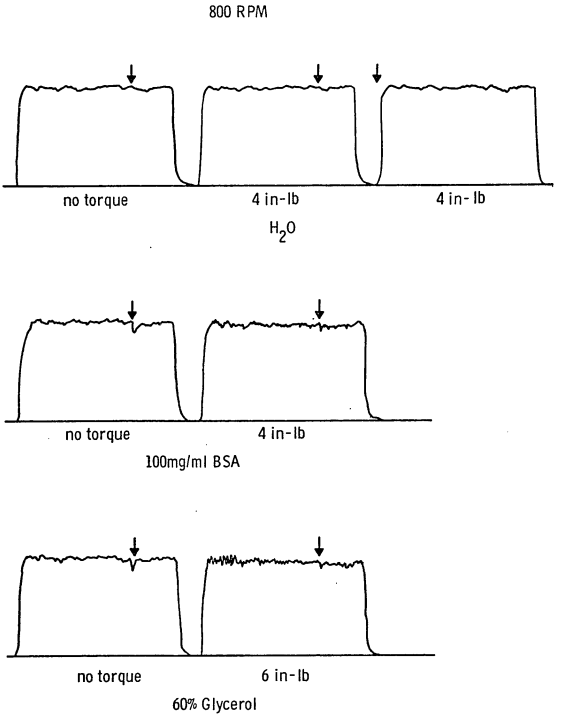

Figure 33. Velocity of Syringe Ram at 800 RPM

Reproduced with permission of the copyright owner. Further reproduction prohibited without permission.

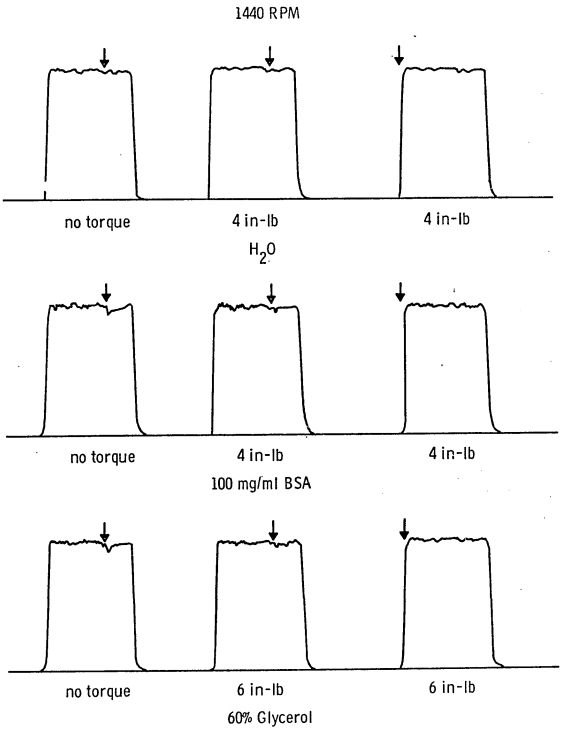

Figure 34. Velocity of Syringe Ram at 1440 RPM

Reproduced with permission of the copyright owner. Further reproduction prohibited without permission.

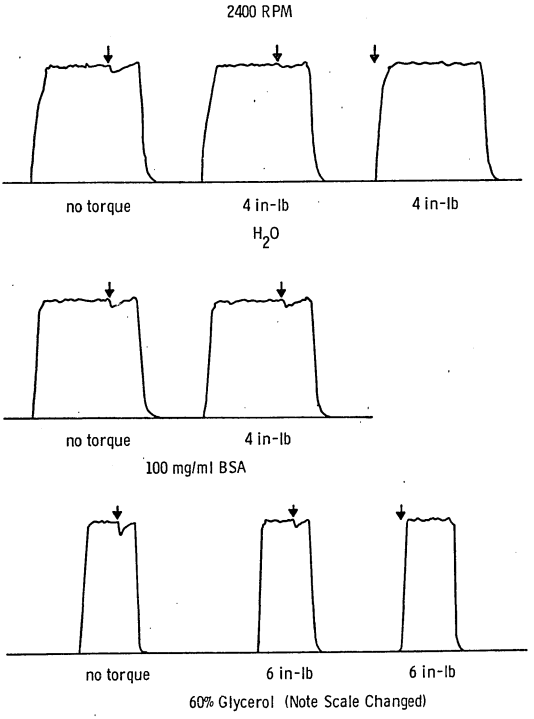

Figure 35. Velocity of Syringe Ram at 2400 RPM

Reproduced with permission of the copyright owner. Further reproduction prohibited without permission.

investigated were: (1) water to approximate the conditions encountered with dilute solutions, (2) 100 mg/ml of bovine serum albumin (BSA) to approximate the conditions encountered with concentrated solutions of proteins, (3) 60% glycerol, to approximate conditions which are probably more extreme than usually encountered in rapid freezing experiments (except possibly for pastelike mitochondrial preparations or similar materials). The viscosity of protein solutions can be calculated from equations 11. and 12. (37, p. 394).

11. $\eta_{sp} = [\eta]_{BSA} C + k_h [\eta]^2_{BSA} C^2$

12. $\eta = \eta_{sp} + 1$

where k_h = Huggins constant, η_{sp} = specific viscosity, $[\eta]_{BSA} \approx 4$, C = concentration in gm/cm^3, η = measured viscosity.

The viscosity of a 100 mg/ml solution of BSA is thus 1.72 centipoise. The viscosity of 60% glycerol at room temperature is about 10 centipoise (38, p. 1669). Using equations 11. and 12. it can be calculated that 10 centipoise is equivalent to about 500 mg/ml of BSA (if BSA behaves ideally at these high concentrations - which is unlikely).

It can be seen from Figures 33-35 that the flow perturbations are small in all cases. The small deflection in the velocity traces which occurs when the ram strikes the syringe plungers (as indicated by the arrows) is due to a small amount of bending of the 1/2 inch output shaft of the gearbox on which the cam is mounted. By tightening the gib clamp screws on the cam follower slide (Figure 9) with a torque

Reproduced with permission of the copyright owner. Further reproduction prohibited without permission.

wrench (Cleco Pneumatic TSK-30A) adjusted as indicated in the figures, a resistance is encountered by the cam before it drives the syringes. This preload tends to flex the shaft such that the force required to drive the syringes does not cause it to flex any further. When fluids of viscosity 1.72 centipoise or less (viscosity of 100 mg/ml BSA) are flowed through the apparatus at flow velocities of 1 ml/sec or less (1440 rpm) the perturbation can be almost completely removed by applying torque (Figures 33 and 34). At 10 centipoise viscosity and 2400 rpm, however, even 6 in-lb of torque does not completely remove the perturbation in the flow (Figure 35). The experiments in the third columns of Figures 33-35 show that the flow is not perturbed when the load is encountered at the beginning of the ram motion, and therefore the limitation is not due to the available power of the system, but is due to the weakness of the gearbox. In these cases the gearbox shaft is flexed during the rise time of the velocity curve and is therefore masked by the response time of the differentiation circuit.

In no case is the magnitude of these perturbations very large. Considering the worst case - 2400 rpm, 60% glycerol, no torque (Fig. 35) - the perturbation only amounts to a 2% error in the average ram velocity and therefore in the average delay time. If flow were longer than the approximately 0.17 sec of this trace, the fractional error would be even smaller. In most cases the error is

Reproduced with permission of the copyright owner. Further reproduction prohibited without permission.

considerably less than 1% and can be neglected in consideration of kinetic curves (see Figure 31).

Figure 36 shows some results of tests performed on the push-push system. Figure 36a shows traces simultaneously recorded by methods 2 and 3. The noise is inherent in the transducing systems when used at these amplifications and is not indicative of the velocity profile. The important point is that the flow velocity at the end of the hydraulic system shows motion which mimics the flow velocity at the syringe plungers. The impression that the flow in the stopping syringe precedes that in the driving syringe is due to the fact that the time constant of the stopping syringe transducer is smaller than that of the differentiation circuit.

D. Mixing

When a chemical reaction takes place, it is usually assumed that its kinetics can be described by equations which are characteristic of the reaction mechanism. If the reaction mixture is truly homogeneous the overall reaction rate will depend only on the concentrations of the reactants and the reaction rate constants. However, in nonhomogeneous solutions the local reaction rate may be greater than, equal to, or less than the rate which is characteristic of the reaction in homogeneous solutions. The rate of a reaction which follows first order kinetics will not be affected by nonhomogeneous conditions, but a reaction which follows second order or higher order kinetics will depend upon the local reactant concentrations. In

Reproduced with permission of the copyright owner. Further reproduction prohibited without permission.

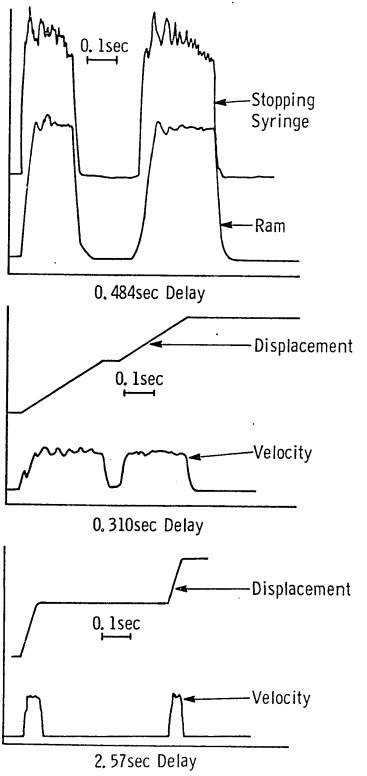

Figure 36. Velocity Tests on Push-Push Mechanism

Reproduced with permission of the copyright owner. Further reproduction prohibited without permission.

nonhomogeneous solutions the mean rate of a type I second order reaction, A + A $\longrightarrow$ Product, is greater than the homogeneous mean rate, while the mean rate of a type II second order reaction, A + B $\longrightarrow$ Product, is less than the homogeneous mean rate.

The reason for using rapid mixing devices is to produce homogeneous solutions of two or more reactants in as short a time as possible so that the homogeneous mean rate of rapid reactions of type II second order and higher order can be determined (note that pseudo first order reactions are of these types). In order to properly interpret the kinetics of chemical reactions measured with rapid reaction devices, it is necessary to know the mixing characteristics of the mixer. As will be discussed later, in the study of reactions which are slow compared to the rate of mixing, the effects of mixing can be ignored, while in the study of reactions which are very fast compared with the rate of mixing, it is the mixing rate which is, in fact, being studied. The study of reactions with rates comparable to the rate of mixing results in quite complicated situations, the interpretation of which, must be made with extreme care. Although many of the common types of mixers used in rapid flow studies have been examined by several workers (see reference 13), in general the studies were performed at flow velocities five to ten times higher than those used in the rapid freezing technique, at viscosities of about one centipoise, and in 1:1 volume ratios. Therefore it was necessary to examine the performance of

Reproduced with permission of the copyright owner. Further reproduction prohibited without permission.

the various mixers used under the various conditions encountered in the rapid freezing technique which included viscosities higher than one centipoise and volume ratios as high as 10:1. There are several methods which have been used to study the mixing process: (a) A study of diffusion-controlled reactions (reactions which have rates several orders of magnitude higher than the rate of mixing) will yield an apparent rate which is actually the rate of mixing (13). In order to measure mixing, studies of this type have been done using thermal (13, 39) and optical (9, 13, 40) methods of observation. (b) When two solutions of different refractive indices are brought together, the approach to optical homogeneity is a measure of the mixing. Mixing studies of this type have been done by Trowse (40) and Dubois (41). (c) For fast second order reactions, an adherence to second order behavior as one of the reactants is increased is a good test of efficient mixing (16). It was decided in this work to use method (a) using optical detection since the measuring technique causes no perturbation on the flow (as does the thermal method), and furthermore, the results could be easily obtained and analyzed with only minor modifications to existing equipment.

The reaction chosen for this study was the aqueous diffusion-controlled neutralization of sodium hydroxide by nearly equimolar hydrochloric acid using phenol red as an indicator and monitoring the reaction at 550 nm. The reaction observed is:

Reproduced with permission of the copyright owner. Further reproduction prohibited without permission.

13. $A^{-2} + H^{+} \underset{k_{-1}}{\overset{k_1}{\rightleftharpoons}} HA^{-}$

14. $HA^{-} + H^{+} \underset{k_{-2}}{\overset{k_2}{\rightleftharpoons}} H_2A$

where H_2A = protonated form of phenol red. The main color change at 550 nm is due to reaction 13. since only the doubly charged species has appreciable absorptivity at this wavelength. Since both the neutralization and the indicator reactions are diffusion-controlled (42) ($k_1 = 7.2 \times 10^{10}$ M^{-1} sec^{-1}), the observed rate of the reaction is treated as the rate of mixing.

The solutions were made up with glass distilled water from reagent grade chemicals. In all experiments the acid and base were about 0.12 N and the phenol red was 0.5 to 1.5 mM after mixing.

The simple photometer arrangement is shown as an exploded view in Figure 37. The light from a 30 watt tungsten lamp powered by a Sorenson QB6-15 D. C. supply passes through a 550 nm Bausch and Lomb narrow band-pass filter and is focused on the flow tube. A fiber optics light guide (Ealing Optical Corp.) directs the transmitted light to a photomultiplier tube (EMI 9592) equipped with a current to voltage converter which is integral with the PMT housing (43). The voltage output is measured by a Sanborn D. C. amplifier and 151 recorder. This recorder has a time constant of less than 50 msec and is therefore quite useful for those rapid flow studies which have flow times of 100-500 msec. The observation chamber

Reproduced with permission of the copyright owner. Further reproduction prohibited without permission.

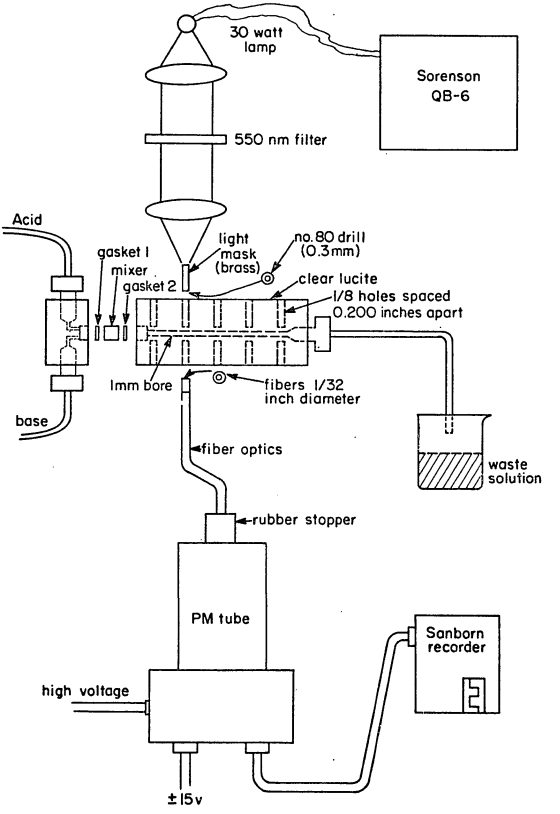

Figure 37. Apparatus for Mixer Evaluation

Reproduced with permission of the copyright owner. Further reproduction prohibited without permission.

is made of transparent Lucite which makes possible visual studies of mixing which are done parallel with the photometric measurements. When using the photomultiplier, the observation chamber is inserted into a brass tube which masks all of the chamber except for the observation ports. The light is further masked with a brass sleeve having a pinhole (#80 drill - 0.34 mm) through which the light impinges on the one mm bore flow tube, and by the light guide which is 1/32 inch in diameter. There are five sets of identical observation ports at various distances from the mixer, into which the light guide and the brass sleeve can be inserted to make measurements of the mixing. To improve the optical quality of the device, a drop or two of glycerol was routinely placed on the tip of the fiber optics. Calibration curves were made for each set of experiments by measuring the transmittance of standard solutions made by diluting the basic phenol red with base and flowed through the observation chamber. The optical density corresponding to completely mixed solution is determined from a reading obtained after flow has stopped, and since small fluctuations in the flow at the very end of the shot could cause large color changes when the acid and base are very closely titered, it is found that the experiments are easier to perform when the acid is 4-6% in excess. Vassilatos and Toor (44) have shown that in mixing studies of this type, a small excess of one reagent has only small effects on the relationship of percent mixed to percent reacted. It can be estimated

Reproduced with permission of the copyright owner. Further reproduction prohibited without permission.

from their data that a 6% excess of HCl will overestimate the mixing by no more than 2%.

The mixing tests performed on the mixers commonly used in this rapid freezing apparatus were designed to show the mixing characteristics at various flow velocities for 1:1 and 10:1 volume ratios under the conditions: viscosity of one centipoise and viscosity of ten centipoise. In addition, the effect of the mixing jet diameter (see Figure 20) on mixing was also studied. The flow velocity was determined from the flywheel speed as described in Chapter 2.

For 1:1 mixing two one ml syringes were used whereas for 10:1 mixing one 2.5 ml syringe and one 0.25 ml syringe were used. This implies that for a given ram velocity, the fluid velocity in 10:1 mixing is 2.75/2.00 higher than for 1:1 mixing.

The studies of mixing are summarized in Figures 38-41. There are several general points to notice. The most important is that under most conditions mixing is more than 95% complete within the first 5 msec which is sufficient for studying reactions with half-lives longer than 5 msec (7). One marked effect is that mixing efficiency is improved both by increasing the flow velocity and by decreasing the mixing jet diameter. (Table 3 of the Appendix gives the fluid velocities for various tube bores corresponding to the ram driving rates used in these studies.) Decreasing the mixing jet bore has the effect of increasing the linear flow velocity for a given volume velocity and of forcing the fluid through a smaller hole.

Reproduced with permission of the copyright owner. Further reproduction prohibited without permission.

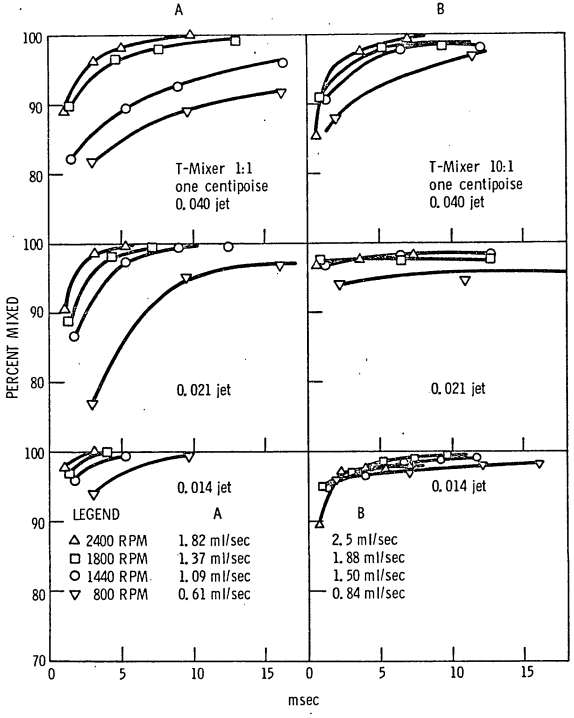

Figure 38. Mixing Tests on Ballou T-Mixer

Reproduced with permission of the copyright owner. Further reproduction prohibited without permission.

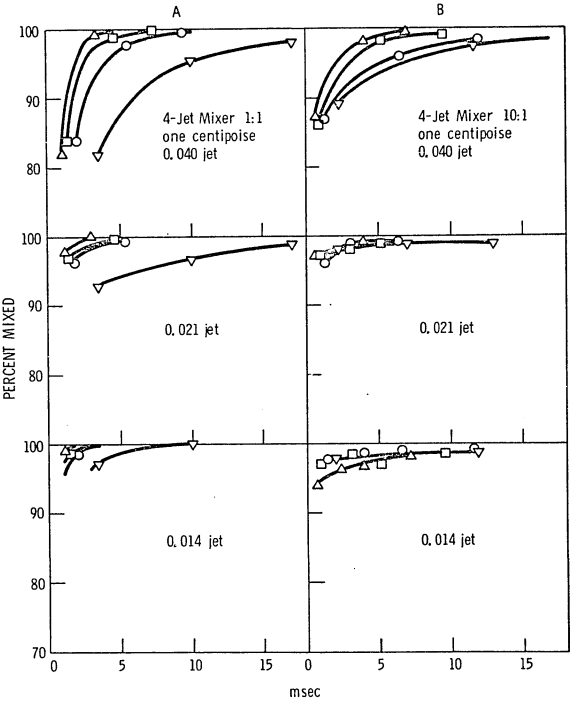

Figure 39. Mixing Tests on Ballou 4-Jet Mixer

Reproduced with permission of the copyright owner. Further reproduction prohibited without permission.

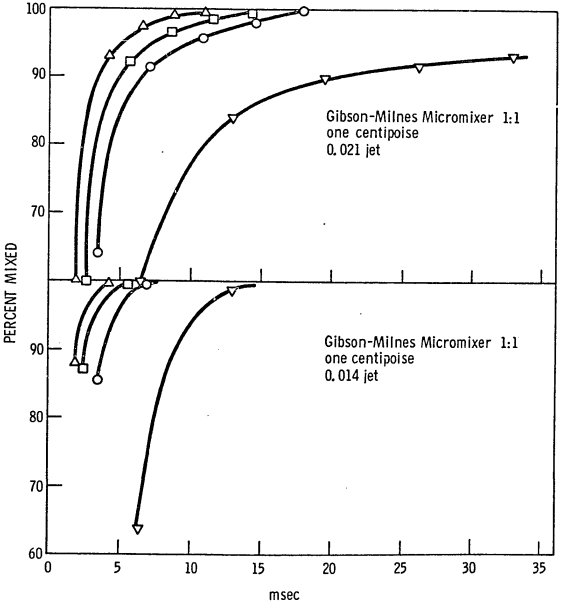

Figure 40. Mixing Tests on Gibson-Milnes Micromixer

Reproduced with permission of the copyright owner. Further reproduction prohibited without permission.

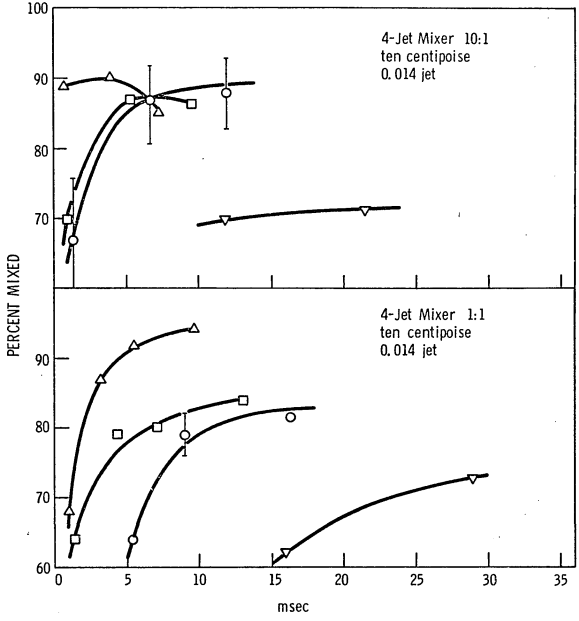

Figure 41. Mixing Tests on Ballou 4-Jet Mixer at High Viscosity

Reproduced with permission of the copyright owner. Further reproduction prohibited without permission.

These actions break up the normal flow patterns thereby promoting turbulence and hence mixing. The mixing jet can be envisioned as a device through which energy can be applied to the mixing process, since more energy is applied to the mixing process by virtue of the additional pressure drop it creates in the flow system.

Another result which is somewhat surprising, is that in most cases, mixing is at least as good for 10:1 volume ratios as it is for 1:1 volume ratios. (In a few cases 10:1 ratios actually give better mixing.) These mixers were not designed specifically for mixing uneven volumes - for this purpose the mixer would probably be more efficient if the diameters of the entrance jets were chosen so as to maintain a constant linear flow velocity for the two solutions. It is thought that the reason for their good mixing efficiency with 10:1 volume ratios is due to the flow rate for a given ram velocity being somewhat higher with a 10:1 mixing ratio than with a 1:1 ratio (2.75/2.00 higher).

An important point shown here is that at the flow velocities employed in these studies the simple T-jet and the 4-jet tangential mixers have nearly identical mixing efficiencies and are considerably more efficient than the more complex Gibson-Milnes mixer. The rationalization for this result is that the Gibson-Milnes mixer splits the flow into eight jets and thus the velocity of the individual jets at the point where the fluid jets collide is only a half or a quarter as great as for the simpler Ballou mixers. Thus the energy

Reproduced with permission of the copyright owner. Further reproduction prohibited without permission.

expended in the mixing process is less in the Gibson-Milnes mixer than in either of the Ballou Mixers. The Gibson-Milnes mixer used in this study was specially constructed so that its bore sizes were decreased by a factor of two from the usual Gibson-Milnes mixers (11). Visual observations on the latter indicated that it was even less efficient than the smaller bore mixer at similar flow velocities.

It should be mentioned that the Gibson-Milnes mixer was not designed for the rapid freezing technique, but was designed for the stopped-flow technique which has quite different requirements. In the stopped-flow technique a high flow rate is desired so that the solution which is to be observed (of the order of 0.1 ml) can be injected into an observation chamber and stopped in as short a time possible. The prevention of cavitation makes it necessary to maintain a constant linear flow velocity throughout the flow chamber; thus the bores of the mixing chamber are designed to be equal in area to the cross-sectional area of the observation tube. Since the flow velocity is usually quite high (about 10-20 ml/sec compared to about 1 ml/sec for the rapid freezing technique), mixing is much less of a problem and is achieved well within the time of transporting the solution to the observation chamber. In the rapid freezing technique, however, in order to conserve sample and still meet the conditions necessary for the quenching process (discussed later), the flow rate is much slower than in the stopped-flow method

Reproduced with permission of the copyright owner. Further reproduction prohibited without permission.

and hence good mixing is achieved by different means. Cavitation is of no concern and thus it is found that the use of small bores is quite an effective means of mixing. Although it might be expected that the transition from the mixing jet to the flow tube would cause cavitation, it was found in these mixing studies (which use optical detection) that cavitation was not a problem at any of the flow velocities employed, except possibly in the solutions of high viscosity. (Cavitation could be produced, however, by manually driving the syringe plungers at a rate much higher than normally used for rapid freezing.) It is possible that the reason no cavitation occurred was that the 1 mm bore observation tube and the exhaust tube produced sufficient back pressure to prevent the conditions which cause cavitation. Cavitation normally occurs when the pressure drop is greater than the vapor pressure of the fluid (45).

Figure 41 shows the results of mixing under the conditions of high viscosity (60% glycerol; 10 centipoise at room temperature (38)). These results show that mixing is not complete at any point in the observation tube. Although optical artifacts of unknown origin were observed, and the results have rather large uncertainties (as indicated), these cannot explain the apparent poorness of mixing, since parallel visual tests verified that mixing was never complete while the solution flowed through the observation tube at any of the flow velocities employed. The poorness of mixing as shown implies that rapid flow studies under these extreme conditions should be

Reproduced with permission of the copyright owner. Further reproduction prohibited without permission.

interpreted with caution. As a first approximation, the half-life of reactions should be longer than 20 msec if accurate results are to be obtained. As noted in the previous section, ten centipoise is equivalent to solutions containing several hundred mg of protein per ml and is probably beyond the limits usually encountered in flow studies; the exceptions might be experiments with mitochondrial (of similar) preparations.

From the above studies it is proposed that mixing in the devices tested in this work occurs in three stages. First, the collision of the two solutions causes them to break up into small interspersed blocks which in the chemical sense are mixed only at the block surfaces. The mixing jet forces these small blocks to move at high velocities producing turbulent eddies which cause random coalescing and redispersing of the fluid, and thus further mixing. Finally, the turbulence in the flow tube causes dispersion of the fluids until a homogeneous mixture is obtained. This model is in accord with that proposed by Trowse (40). Trowse considered the mixing process to take place in two stages. The first was a macroscopic process in the mixing chamber of mechanical mixing giving a uniform dispersion of minute blocks of the two solutions. The second was a microscopic process in the observation tube in which diffusion produced a homogeneous solution. Since all of the mixers were tested at the same flow velocities and with the same mixing jets, it would be assumed, according to either of these

Reproduced with permission of the copyright owner. Further reproduction prohibited without permission.

models, that the difference in the mixing efficiency was due to the average effective size of the blocks produced by the initial collisions of the fluids. The effective size of these blocks cannot simply be related to the fluid velocity when the fluid jets collide, however, since it can be seen from Figures 38 and 39 that the four-jet tangential mixer (which has a lower flow velocity) is somewhat more efficient than the two-jet mixer. This is probably due to the tangentially oriented jets, an arrangement which Hartridge and Roughton (1) found to be more efficient nearly 50 years ago.

Gutfreund (16) has stated that "Equal volumes of aqueous solutions of reactants with similar properties can be mixed efficiently on a 2-msec time scale by the simplest mixer, as long as the rate of flow is sufficient to maintain turbulence." The degree of turbulence in a flow system can be estimated by examination of the Reynolds numbers (46). The Reynolds numbers, R.N., can be calculated from equation 15.

15. $$\text{R.N.} = \frac{U\rho d}{\eta}$$

where U = velocity (cm/sec), ρ = density (gm/cm^3), d = diameter (cm), η = viscosity (poise).

It has been found that a fluid velocity which yields a Reynolds number of about 2000 is the transition velocity from laminar to turbulent flow in straight pipes (46). With sharp entrances and constrictions this number may be somewhat lower. In Table 3 of the Appendix are tabulated along with the flow velocities, corresponding

Reproduced with permission of the copyright owner. Further reproduction prohibited without permission.

Reynolds numbers for one centipoise solutions. It can be seen that under the conditions where efficient mixing is found (0.021 and 0.014 inch jets at 1 centipoise) nearly all of the Reynolds numbers are above 2000 and therefore it is likely that turbulent flow exists. However, for any given flow velocity, ten centipoise solutions have Reynolds numbers ten-fold smaller than those tabulated in Table 3 and thus a Reynolds number of 2000 is not reached under any of the flow conditions employed. The resulting laminar or quasi-laminar flow results in poor mixing. The only mechanisms for mixing in laminar flow are molecular diffusion and laminar convection (47) and these processes are slow on the time scales used for rapid kinetics (48).

It is desirable to find how the mixing rate affects the study of rapid reactions. For simplicity, let us consider a pseudo first order reaction. Examining the Figures 38-41, it is found that as a rough approximation, the extent of mixing versus time curves can be related to exponential progress curves; therefore mixing rate constants can be determined for each mixing condition. Since no chemical reaction can take place until mixing occurs, the observed reaction can be treated as a series first order reaction set as shown in equation 16.

16. $A \xrightarrow{k_m} B \xrightarrow{k_r} C$

where k_m = mixing rate constant, k_r = reaction rate constant (pseudo first order). A represents the unmixed reactants, B

Reproduced with permission of the copyright owner. Further reproduction prohibited without permission.

represents the mixed reactants, and C represents the product. Frost and Pearson (49) have treated this type of system and give the following results:

$$A = A_o \exp(-k_m t)$$

$$\underline{17}. \quad B = \frac{A_o k_m}{k_r - k_m} [\exp(-k_m t) - \exp(-k_r t)]$$

$$C = A_o \left[1 + \frac{1}{k_m - k_r} [k_r \exp(-k_m t) - k_m \exp(-k_r t)] \right]$$

Making the substitutions:

$$\alpha = A/A_o \qquad \tau = k_m t$$

$$\beta = B/A_o \qquad K = \frac{k_r}{k_m}$$

$$\gamma = C/A_o$$

equations 17. simplify to 18.

$$\alpha = \exp(-\tau)$$

$$\underline{18}. \quad \beta = \frac{1}{K-1} [\exp(-\tau) - \exp(-K\tau)]$$

$$\gamma = 1 + \frac{1}{1-K} [K\exp(-\tau) - \exp(-K\tau)]$$

Experimentally either the appearance of C or the disappearance of B is measured. In the latter case, the measurement will actually be of the sum of A plus B since the measuring technique does not distinguish between mixed and unmixed reactants. Since

$\frac{A + B}{A_o} = \frac{A_o - C}{A_o}$ this is seen to be

$$\underline{19}. \quad 1 - \gamma = \frac{1}{K-1} [\exp(-\tau) - \exp(-K\tau)]$$

Reproduced with permission of the copyright owner. Further reproduction prohibited without permission.

This function is plotted vs. time in direct form (Figure 42) and in logarithmic form (Figure 43) for $k_r = 300\ sec^{-1}$ and various values of K. When $K = 0.02$ the reaction curve is nearly indistinguishable from the "true reaction curve" (the "true reaction curve" is obtained when $K = 0$ i.e. when $k_m \longrightarrow \infty$). When $K = 0.1$ and 0.2, the progress curves differ considerably from the "true reaction curve", but when the logarithm of the value $1-\gamma$ is plotted versus time (Figure 43) one finds that to a first approximation, the curve is simply shifted to the right while, except for the first 20-30% of the reaction, the slope is essentially the same as for the "true reaction". When K is greater than 0.2 (e.g. 0.5 or 0.99), considerable curvature is evident which casts doubt on whether or not the reaction is first order. Although this result shows us that the rate constant can be determined quite accurately if K is smaller than 0.2, it is important to realize that when K is much greater than 0.02, quite serious errors will result in the actual concentration versus time curves (as shown in Figure 41). This could lead to misinterpretations of the data such as assigning the wrong order to a reaction or assigning a second step to a reaction which has only a single step. It is these kinds of errors which are most difficult to avoid when K is much larger than 0.02.

Table 1 shows k_m values for the three mixers under the various conditions. These constants were calculated from equation 20.

Reproduced with permission of the copyright owner. Further reproduction prohibited without permission.

Reproduced with permission of the copyright owner. Further reproduction prohibited without permission.

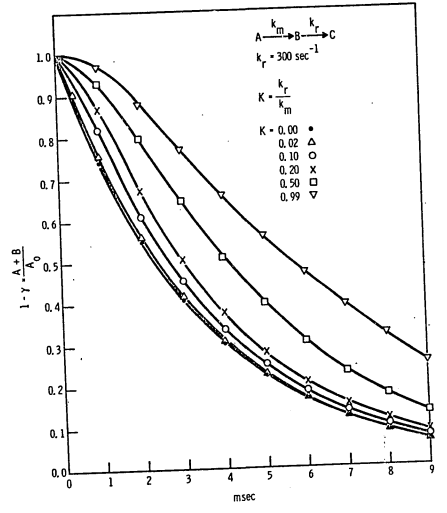

Figure 42. Apparent Reaction Progress Curves with Imperfect Mixing

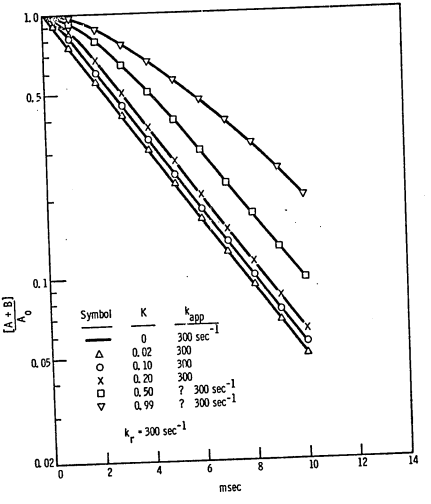

Figure 43. Logarithm of Apparent Reaction Progress Curves with Imperfect Mixing

Table 1

Apparent Mixing Rate Constants, k_m (sec^{-1})

RPM	Mixing Jet Size			Mixing Jet Size		
	0.040	0.021	0.014	0.040	0.021	0.014
	2-Jet Mixer			4-Jet Mixer		
800	300	310	800	370	690	1000
1440	520	700	1400	800	1400	2300
1800	900	1100	2300	1100	2300	4300
2400	1400	1800	3500	1600	4000	7000
	Gibson			4-Jet Tangential (10 centipoise)		
800	--	140	240	--	--	41
1440	--	350	560	--	--	170
1800	--	500	830	--	--	340
2400	--	750	1100	--	--	900

Note: 10:1 mixing volumes gave very similar values and are not recorded here.

Reproduced with permission of the copyright owner. Further reproduction prohibited without permission.

20. $$k_m = \frac{(0.693)(x)}{(\text{time to reach } x)}$$

where x = number of half-lives.

The Palmer-Beinert mixer is quite similar to the Ballou 4-jet mixer with a 0.021 inch mixing jet and thus the values for the latter mixer are probably quite representative of the Palmer-Beinert mixer.

Considering that rate constants can be determined accurately for reactions when $K \leq 0.2$, and the direct progress of the reaction can be measured quite acurately when $K \leq 0.02$, the following table shows k_r for $K = 0.02$ and for $K = 0.2$ for the 4-jet tangential mixer with a 0.014 inch mixing jet using two one ml syringes.

Table 2

Maximum Rate Constants with 4-Jet Mixer for K of 0.2 and 0.02

	RPM	800	1440	1800	2400
1 centi-poise	$k_m(sec^{-1})$	1000	2300	4300	7000
	$k_r(0.02)(sec^{-1})$	20(35)*	46(15)	86(8)	140(5)
	$k_r(0.2)(sec^{-1})$	200(3.5)	460(1.5)	860(0.8)	1400(0.5)
10 centi-poise	$k_m(sec^{-1})$	41	170	340	900
	$k_r(0.02)(sec^{-1})$	0.8(870)	3.4(200)	6.8(102)	18(38)
	$k_r(0.2)(sec^{-1})$	8(87)	34(20)	68(10.2)	180(3.8)

* Values in parentheses are $t_{1/2}$ in msec.

Reproduced with permission of the copyright owner. Further reproduction prohibited without permission.

The most common condition I use in rapid freezing is 1440 rpm with approximately one centipoise solutions. Therefore it is seen that the mixing effects are very small for the rapid freezing technique.

The assumption in making these calculations has been that the mixing process can be approximated by a simple exponential function. Careful examination of these curves will show that they more closely resemble inverse functions. Therefore a more correct model for the mixing effect would have been to use a second order reaction followed by a pseudo first order reaction. However, the first order model which makes the analysis much easier than the second order model, is useful for obtaining reasonable approximations for the effects of mixing.

E. Homogeneity of Flow

Ideally, in the continuous flow method, all volume elements of the reacting mixture should pass from the mixing chamber to the observation point in the same amount of time. This requires a constant flow velocity for the entire period of flow as described earlier, and moreover, requires that there is no intermixing of volume elements of fluid which were mixed at different times. This implies that the fluid should travel along the reaction tube as if it were a solid plug, a condition which is called plug or bulk flow. In reality, it is found that in tubes, the flow velocity is always higher at the center of the tubes than at the periphery. Therefore

Reproduced with permission of the copyright owner. Further reproduction prohibited without permission.

the fluid travelling along the walls of the tube will arrive at the observation point later than the fluid which travelled in the center of the tubes. The net effect of the nonuniform velocities is longitudinal dispersion of the solution and a blurring of the time scale of the reaction (also referred to by chemical engineers as backmixing).

If the reaction proceeded at a constant rate for the entire period of the reaction (a zero order reaction), there would be no observed effect, since the elements which remained in the reaction tube longer than the average time would be counteracted by elements which remained less than the average time. However, for most reactions, the rate is not constant and therefore the effects of longitudinal dispersion do not cancel. A number of investigators have calculated the error in determining rate constants due to deviations from plug flow (7, 21, 40), and have concluded that with laminar flow the error approached ten percent, and with turbulent flow the error was less than two percent. It was also found that the error is larger for first order reactions than for second order reactions.

However, a simple experiment performed in order to obtain some feeling how large an effect longitudinal dispersion is in the reaction tubes employed in the rapid freezing apparatus, cast some doubt on the validity of the calculations of earlier workers. The experiment was to fill a reaction tube with water, place a narrow

Reproduced with permission of the copyright owner. Further reproduction prohibited without permission.

band of highly colored phenol red behind it, and then force this band to flow through the reaction tube by flowing water behind it while observing how the colored band was dispersed in the tube. This experiment was patterned after the classical studies by Taylor on both laminar (48) and turbulent (50) flow, but used tubing of approximately 1 mm bore which had considerable curvature, rather than the 1 cm (and larger) bore straight tubing employed by Taylor; therefore his results could not be applied directly to rapid freezing in this work. The result was that the narrow band was dispersed over a disturbingly large distance as it flowed down the tube. The band, which was equivalent to about 0.01 ml before flowing, was dispersed into a band approximately Gaussian in shape (as judged by eye) with a width at half-height which appeared linearly related to the volume the center of the band had flowed in the tube. Table 3 shows this relationship.

Table 3

Dispersion of Material During Flow in Reaction Tube

Distance Travelled (ml)	Half-width (ml)*
0	0.01
0.15	0.08
0.25	0.12
0.50	0.20
0.75	0.30

* Estimated visually.

Reproduced with permission of the copyright owner. Further reproduction prohibited without permission.

It was found that the spreading phenomenon was essentially the same for the entire range of velocities used in the rapid freezing technique and was therefore mainly dependent on the distance the narrow band flowed down the tube.

Taylor (48) has shown in the above type of experiment under the conditions of laminar flow, that when the total flow time is short compared with the time in which by the process of diffusion an appreciable amount of material passes over a distance equal to the radius of the tube (which is 2-20 seconds for a 1 mm tube), a band which was initially narrow will be spread nearly evenly over a distance extending from the point of initiation of flow to twice the average flow distance (as calculated from the mean flow rate). If the time of flow is long (i.e., a low flow rate), however, radial diffusion tends to counteract this longitudinal dispersion by exchanging the faster moving fluid at the center of the tube with the slower moving fluid at the periphery and the band passes down the tube while spreading only slowly. In later work Taylor (50) showed that in turbulent flow the turbulence could be treated essentially as a very rapid diffusion process which counteracted the longitudinal dispersion qualitatively in the same way as diffusion. It is possible that the result obtained with the rapid freezing apparatus can be explained by assuming a condition which lies between the conditions of laminar flow with no diffusion and of turbulent flow as described by Taylor.

Reproduced with permission of the copyright owner. Further reproduction prohibited without permission.

Having obtained this qualitative result of a large longitudinal dispersion, it became necessary to analyze the quantitative implications of the longitudinal dispersion on the determination of kinetic rate constants. The model was to consider the cross-section of a tube as consisting of ten separate annuli of equal thickness. Each annulus would thus consist of fluid moving at a velocity which could be determined from the velocity distribution function for the type of flow to be considered. In order to consider the worst cases as well as to keep the analysis simple, it was assumed that no axial dispersion of fluid occurred (i.e., once fluid was in a given annulus it did not leave it for the entire period of flow). The velocity distribution for laminar flow is obtained from Poisseuille's equation (20a.) while that for turbulent flow is obtained from Prandtl's equation (20b.) (13).

20a. $U = 2\overline{U}(1-r_i^2/a^2)$

20b. $U = 1.225\ \overline{U}(1-r_i/a)^{1/7}$

where U = flow velocity, a = radius of tube, r_i = distance from center of tube to i^{th} annulus, $\overline{U}$ = average flow velocity. The velocity can be related to the time very simply as shown in equations 21.

21. (a) (laminar) $t_i = \dfrac{\overline{t}}{2(1-r_i^2/a^2)}$

(b) (turbulent) $t_i = \dfrac{\overline{t}}{1.225(1-r_i/a)^{1/7}}$

where $r_i = \dfrac{(2i-1)a}{20}$, i.e., a/20, 3a/20, 52/20, ..., 19a/20

= mean radius of ith annulus.

Reproduced with permission of the copyright owner. Further reproduction prohibited without permission.

let us consider a first order decay reaction as before.

6. $$\frac{C}{C_o} = \exp(-kt)$$

We wish to calculate the mean conversion of the reaction at a given cross-section which ideally would correspond to the conversion at $\bar{t}$. The weighting factor for the reaction fluid in a given annulus will be the area of the annulus, $A_i = 2\ r_i a/10$. Combining equations 21. and 6. and including the appropriate weighting factor, we can calculate the observed extent of the reaction in order to compare it with the theoretical extent of the reaction for each $\bar{t}$.

22. $$\frac{C_{observed}}{C_o} = \frac{\sum_{i=1}^{10} A_i \exp(-kt_i)}{\sum_{i=1}^{10} A_i} = \frac{\sum_{i=1}^{10} \frac{2\pi r_i a}{10} \exp(-kt_i)}{\pi a^2}$$

for laminar flow this is:

22a. $$\frac{C_{observed}}{C_o} = \sum_{i=1}^{10} \frac{2\pi r_i a}{10} \exp\left[-k\frac{\bar{t}}{2(1-r_i^2/a^2)}\right]$$

while for turbulent flow this is

22b. $$\frac{C_{observed}}{C_o} = \sum_{i=1}^{10} \frac{2\pi r_i a}{10} \exp\left[-k\frac{\bar{t}}{1.225(1-r_i/a_i)^{1/7}}\right]$$

By calculating these sums for several values of $\bar{t}$ and comparing the curves so obtained for both laminar and turbulent flow with the curve from equation 6., an estimate is obtained of the error which is introduced to the study of kinetics by nonideal flow. This has been done arbitrarily using the rate constant, $k = 0.693\ sec^{-1}$,

Reproduced with permission of the copyright owner. Further reproduction prohibited without permission.

and is shown in Figure 44 both in direct and in logarithmic forms. The insert shows the velocity distribution in a pipe for laminar and turbulent flow and demonstrates how much more nearly plug flow is approximated by turbulent flow than by laminar flow.

It is seen from these results that even under the worst conditions (i.e., laminar flow with no diffusion), the errors resulting from non-plug flow are not very large. Allowing for diffusion and turbulent mixing of the annuli (which must occur to some extent), these calculated curves show upper limits for the deviations due to nonideal flow. Again, as was the case for mixing, the apparent rate constant can be calculated fairly well even under nonideal circumstances. However, the reaction progress curve is affected considerably, a result which could lead to misinterpretation of the apparent order of the reaction.

To verify these theoretical results, it was decided to perform a rapid freezing study on a system which could also be investigated by the stopped-flow technique. The latter method makes observations on a non-flowing system as a function of time, and thus the problem of nonideal flow is not important. The system chosen was the well characterized reaction of metmyoglobin with azide (see discussion later in the section on quenching time). The reaction was investigated under conditions in which its half-life was 250 msec. The details of the experimental conditions are in the legend and in the section on the quenching time. The stopped-flow data were obtained

Reproduced with permission of the copyright owner. Further reproduction prohibited without permission.

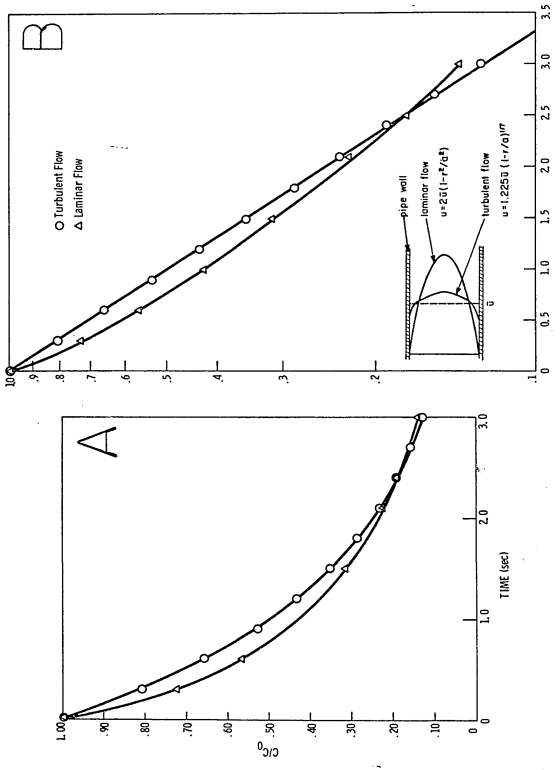

Figure 44. Effect of Flow Dispersion on Apparent Reaction Progress (Theoretical)

Reproduced with permission of the copyright owner. Further reproduction prohibited without permission.

with a Gibson-Milnes stopped-flow instrument with spectrometric observation at 670 nm (the myoglobin being too concentrated to permit transmission of sufficient light at shorter wavelengths) with a 3.5 nm bandwidth. The results are presented in Figure 45 where it is seen that within experimental error of the quenching technique the two methods agree. The numerous similar experiments performed in the investigation of the quenching times (see later) which were for shorter flow times always gave results comparable with those shown in Figure 45.

Note also that with the push-push technique, the problem of longitudinal dispersion is reduced, since the same volume is flowed for each experiment; the time is varied by changing the delay time between injection and ejection. Figure 45 contains data points from both the push-push and the single push techniques and no significant difference is seen between them. Although this limited experiment is admittedly not a very critical test for the push-push vs. single push effect, an experiment designed to test this phenomenon more carefully is described later (Chapter 5). This was an experiment on the decay of the superoxide anion radical at pH 9.6 produced by the oxidation of reduced flavin by oxygen.

Thus the conclusion is that longitudinal dispersion is not a significant factor in the use of the rapid freezing technique. The reason the apparently large longitudinal dispersion as observed in the dye experiment does not affect the reaction as much as might

Reproduced with permission of the copyright owner. Further reproduction prohibited without permission.

Legend for Figure 45

Metmyoglobin, 0.4 mM, was reacted with sodium azide, 5.0 mM, in 0.1 M KNO_3, 0.02 M Tris, pH 7.8 at 2°C. The solid line is obtained from stopped-flow experiments as described in the text and the points are from rapid freezing experiments.

Reproduced with permission of the copyright owner. Further reproduction prohibited without permission.

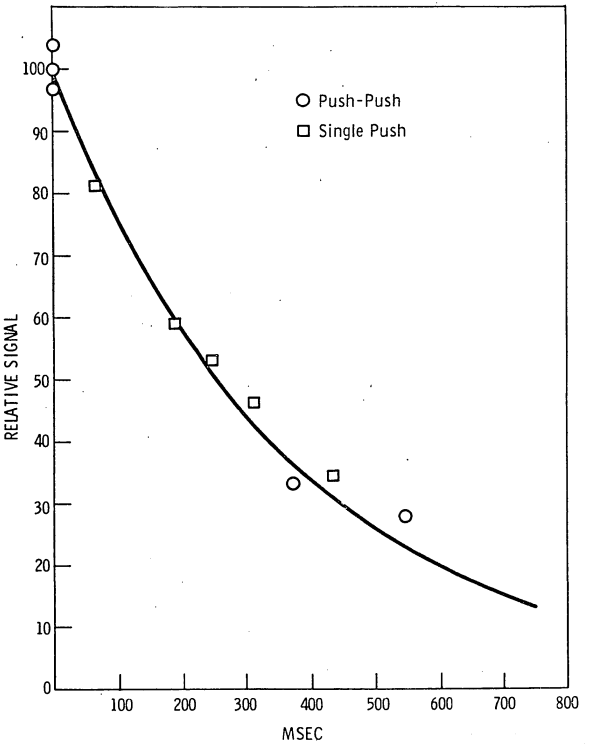

Figure 45. Effect of Flow Dispersion on Apparent Reaction Progress (Experimental)

Reproduced with permission of the copyright owner. Further reproduction prohibited without permission.

be expected, is that the reacting solution at any given cross-section is intermixed mostly with solution which is of an age very similar to itself, and thus only a short segment of the exponential curve is being intermixed. Any short segment of an exponential can be approximated by a straight line so that the intermixing with components which are both slightly older and slightly younger than itself tends to cancel the effect.

F. Quenching Studies

Previous studies on two biochemical reactions (23-25) have indicated that the quenching time for the rapid freezing technique is about 10 msec. Since analysis of the other time-related parameters (see above) have revealed that this quenching time was certainly the limiting factor in studying rapid reactions by this method, it was desired both to determine more accurately the quenching time for typical biochemical reactions, and to find how the quenching time could be minimized. These studies required that there be available a reaction which had the following properties: (a) So that the results would be directly applicable to the EPR technique, at least one of the reactants or products should have an EPR signal which, for the sake of convenience, could be measured at temperatures greater than -196°C (77°K). (b) The results obtained by the rapid freezing technique should be verifiable by an independent method; thus at least one of the reactants or products should be measurable by a second rapid kinetic method. Since the technique

Reproduced with permission of the copyright owner. Further reproduction prohibited without permission.

readily available to me was the stopped-flow method, it was desired that one of the components of the reactions have spectral properties which could be analyzed optically. (c) The kinetics of the reaction should be simple so that the analysis could be straightforward. Since an independent measuring technique was being used, more complex kinetic behavior could be accommodated, but a pseudo first order reaction would simplify interpretation of the results. (d) The reaction should be fast enough to resolve anticipated quenching times of 2-15 msec which implied that, for first order reactions, the half-life should be about 15-20 msec. For measurement of the packed, frozen crystals by the EPR technique, it is often found that the concentrations of the species to be analyzed should be 10^{-3} to 10^{-4} M, and for pseudo first order kinetics, the second reactant should be at least ten-fold in excess. Taken together, these three requirements indicate that the second order rate constant should be about 10^{3} to 10^{4} M^{-1} sec^{-1}. (e) Because the quenching process is a temperature related phenomenon and because the method was to be used primarily for biochemical studies, the reaction should have a kinetic temperature dependence which is typical of biochemical reactions. (f) The reactants should be readily available.

The requirement that the signals be EPR-detectable limits the possible reaction types of systems containing either transition metal ions or organic free radicals. Since there are few cases (if

Reproduced with permission of the copyright owner. Further reproduction prohibited without permission.

any) in which careful kinetic studies have been made on the latter, the most likely reactions for this study were thought to be reactions involving transition metal ions. Of the biological compounds which contain these ions, the hemoproteins are the only ones on which there have been extensive kinetic studies (see 51, 52). The first thought was to employ a reaction in which the heme-bound iron was either oxidized from the ferrous to the ferric form or reduced from the ferric to the ferrous form. The cytochrome c reduction by ascorbate employed by Palmer and Beinert (25) is quite a suitable reaction from all of the above considerations except that it requires measuring temperatures significantly below 77°K (31) and therefore requires specialized equipment, the use of which is too expensive for extensive studies. Stopped-flow work has been done (53) on the oxidation of hemoglobin to methemoglobin by ferricyanide and the second order rate constant which was determined to be about 10^4 M^{-1} sec^{-1} indicated that the reaction might be useful for quenching studies. However, the kinetics showed a dependence on oxygen concentration and were not simple, so the search was extended to find a simpler system. The similar, but simpler reaction involving myoglobin had a rate constant (2×10^6 M^{-1} sec^{-1}) too high to be useful.

It is well known that transition metal compounds which contain unpaired electrons often can exist in different spin states depending upon the nature of the surrounding ligands. Thus it is

Reproduced with permission of the copyright owner. Further reproduction prohibited without permission.

found that ferrimyoglobin and ferrihemoglobin exist in spin states ranging from spin 5/2 to spin 1/2 (27, 28, 54-56) depending upon the sixth ligand in their coordination spheres. High spin configurations of these proteins (spin 5/2) are typified by H_2O or F^- as the sixth ligand and exhibit EPR spectra with $g_{11} = 2$ and $g_{\perp} = 6$, whereas the low spin configurations (spin 1/2) of these proteins are typified by N_3^-, CN^-, imidazole, ammonia, and hydroxide as the sixth ligand and exhibit EPR spectra with $1 \leq g_x \leq 2$, $g_y \approx 2.2$, and $2.4 \leq g_z \leq 3.1$. At X-band frequencies (9.2 gHz) the high spin forms yield an absorption with a derivative maximum at about 1100 gauss, whereas the low spin forms yield derivative lines corresponding to about 2500 gauss, 3100 gauss, and 4000 gauss; therefore, the spectra of the two spin states are easily distinguishable. The optical spectra of the high and low spin derivatives of the ferric hemoproteins are also easily distinguishable, and there are studies which have correlated the spin states and optical properties (54).

Of these systems, extensive kinetic studies have only been reported for the reactions of metmyoglobin hydrate with azide (29, 30, 57) and imidazole (58, 59). The rate constant for the reaction of $[Mb(Fe^{+3}) \cdot H_2O]$ with azide at 25°C is 2.8×10^5 M^{-1} sec^{-1} at pH 5.1 and 2.5×10^3 M^{-1} sec^{-1} at pH 7.5 (29, 30), while for imidazole the rate constant is 45 M^{-1} sec^{-1} at pH 5.0 and 3.5×10^2 M^{-1} sec^{-1} at pH 8.0 (59). The imidazole system has the disadvantage that the

Reproduced with permission of the copyright owner. Further reproduction prohibited without permission.

dissociation constant is about 10^{-2} M so that when the hydrate is initially 10^{-3} M, at least 0.1 M imidazole is required for greater than 90% conversion to the complex. Considering the magnitude of the rate constant, for many studies this is quite acceptable, but the range of rates amenable to study is somewhat limited by the fact that the imidazole concentration has to be so high. However, the azide ion is bound more tightly (dissociation constant is about 5.0×10^{-5} M at pH 7.8 (30)) and thus even 5×10^{-3} M assures 99% binding when the hydrate is initially 10^{-3} M.

Thus it appears that of the kinetically well characterized reactions of the hemoproteins, the reaction of metmyoglobin hydrate with azide is the most suitable for the quenching studies. The ready availability and stability of the reactants makes this reaction particularly desirable for this study. Over the range 0.5°C to 35°C the rate constant (as determined by the stopped-flow technique) shows strictly linear Arrhenius behavior with an activation energy of 12.5 kcal-$^{\circ}$K-mole. Figure 46 shows data collected from numerous experiments (both by the stopped-flow and the rapid freezing methods). With this activation energy it can be calculated that the rate will almost exactly double on raising the temperature from 25 to 35°C. An examination of the temperature dependence of several biological reactions (60) indicates that this is typical. Detailed stopped-flow studies showed that when azide was more than ten-fold in excess the reaction was rigorously pseudo

Reproduced with permission of the copyright owner. Further reproduction prohibited without permission.

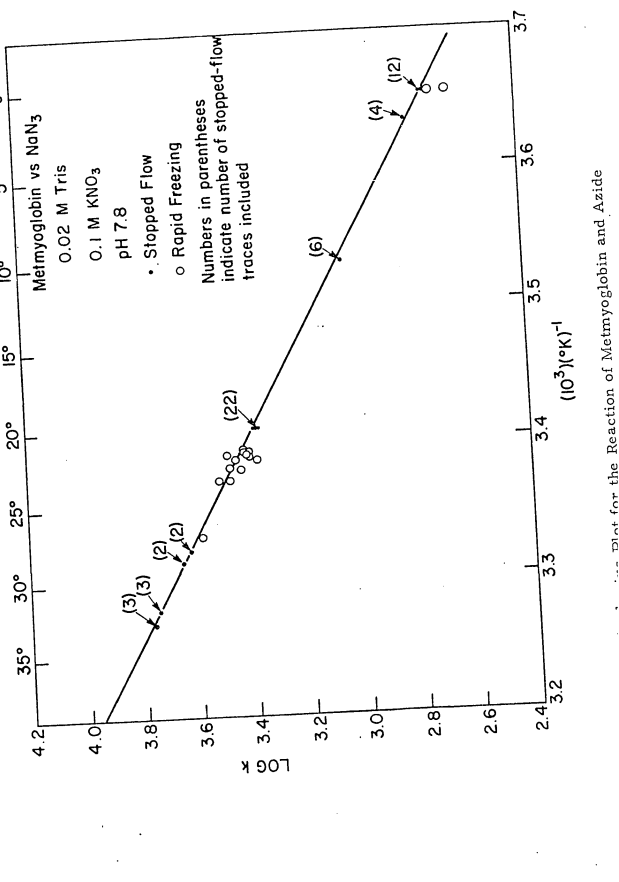

Plot for the Reaction of Metmyoglobin and Azide

Reproduced with permission of the copyright owner. Further reproduction prohibited without permission.

first order for more than three half-lives, and that the pseudo first order rate constant was linearly dependent upon the azide concentration over the range 5 to 80 mM with metmyoglobin concentrations ranging from 0.05 to 0.45 mM. The kinetic results obtained at a number of different wavelengths (440, 503, 550, 575, 635, 670 nm) were identical, indicating there were no complexities which would interfere with the quenching studies.

It is generally accepted that there is a thermal equilibrium between the high spin and the low spin forms of most ferric hemoproteins and their derivatives (54). From data of Beetlestone and George (61), Smith and Williams (56) have estimated that at 20°C metmyoglobin hydrate is about 90% in the high spin form and 10% in the low spin form and the azide complex is about 80% in the low spin form and 20% in the high spin form. The question arises as to whether the high spin form and the low spin forms of the hydrate have different reactivities toward azide. Iizuka and Kotani (27, 28) have shown that at temperatures below -150°C, the hydrate can be considered pure high spin while the azide complex can be considered pure low spin. In the quenching studies EPR measurements are made at about -193°C and therefore at low magnetic fields the remaining hydrate will be measured with no interference from any high spin azide complex. If the two spin forms of the hydrate had very different reactivities toward azide, it might be expected that since a change in temperature would change the spin

Reproduced with permission of the copyright owner. Further reproduction prohibited without permission.

equilibrium, there would be anomalies in the temperature dependence of the rate constant and in kinetic order. However, the observation (Figure 46) that there is strict Arrhenius behavior suggests that this does not occur. Smith and Williams (54) have concluded that in the ferric form of the hemoproteins the spin equilibrium is very finely balanced and is highly sensitive to pH, temperature, change of ligand, and change in conformation. Being so sensitive, it might be expected that the spin transition would have a very low activation energy and thus be very rapid so that an equilibrium would be maintained during the course of the reaction even though one spin state were more reactive than the other. This explanation could not be distinguished from the obvious possibility that the two spin states of the hydrate are equally reactive toward azide.

The basic conclusion, however, is that the presence of two spin states in metmyoglobin hydrate does not effect the interpretation of the quenching data.

A second problem similar in character to the one just discussed is due to the equilibrium which exists between the hydrate and the hydroxide complexes. The pK of this equilibrium is about 9.0 (58) and therefore at pH 7.8 where the reactions occur, nearly 10% of the metmyoglobin will be complexed by hydroxide rather than by water, yielding the reaction scheme:

Reproduced with permission of the copyright owner. Further reproduction prohibited without permission.

$$\underline{23a.}\quad [Mb(Fe^{+3})\cdot H_2O] + N_3^- \xrightarrow{k_a} [Mb(Fe^{+3})\cdot N_3^-] + H_2O$$

$$\Big\downarrow\Big\uparrow\ K = 10^{-9}$$

$$\underline{23b.}\quad [Mb(Fe^{+3})\cdot OH^-] + N_3^- \xrightarrow{k_b} [Mb(Fe^{+3})\cdot N_3^-] + OH^-$$

The protonic exchange reaction is probably very fast so that the equilibrium between the hydrate and the hydroxyl complexes is maintained during reaction. Therefore the rate equation for the reaction is:

$$\underline{24.}\quad \frac{d[Mb(Fe^{+3})\cdot N_3^-]}{dt} = k_a[N_3^-][Mb(Fe^{+3})\cdot H_2O] + k_b[N_3^-][Mb(Fe^{+3})\cdot OH^-]$$

$$= [k_a + k_b(\frac{K}{[H^+]})][Mb(Fe^{+3})\cdot H_2O][N_3^-]$$

When azide is in large excess this has the form of a pseudo first order process, the rate of which is linearly dependent upon the azide concentration. If the two processes have different temperature dependencies and $k_b(\frac{K}{[H^+]})$ is appreciable compared to k_a, non-linear Arrhenius behavior would be predicted. Since this is not found, the extent to which this reaction does proceed by the two paths is of no concern in the quenching studies.

In all studies bearing on the determination of quenching times, the conditions were essentially identical. Equine heart metmyoglobin (2 x crystallized) was obtained from Calbiochem.

Reproduced with permission of the copyright owner. Further reproduction prohibited without permission.

Without further purification about 400 mg were dissolved into 15-20 ml of buffer at room temperature (0.1 M KNO_3, 0.02 Tris base, pH adjusted to 7.8 with HNO_3). The metmyoglobin solution was dialyzed against the same buffer and filtered through 5-micron Millipore filters just prior to use. The concentration, which was usually about 0.9 mM before mixing, was determined spectrophotometrically using millimolar absorptivities of 9.7 $mM^{-1}cm^{-1}$ at 503 nm or 182 $mM^{-1}cm^{-1}$ at 409 nm. The values used for the absorptivities are probably not accurate to more than $\pm$ 5%, but since the reactions are always run under pseudo first order conditions with azide in excess, the exact concentration of metmyoglobin is not critical. Sodium azide (Matheson, Coleman and Bell) solutions were made up in the same buffer by weight with no correction for absorbed water since in these experiments only the relative concentration is important.

The quenching times were determined in the following manner. Approximately 12.5 mM sodium azide was reacted with about 0.44 mM metmyoglobin at about 22°C, and several samples which were rapidly frozen at appropriate times were collected. Under these conditions the reaction half-time is about 20 msec so that the reaction times of the samples collected ranged from about 5 to 50 msec. These samples were analyzed for the high spin signal by EPR. A pseudo first order least squares line was calculated for the data according to a computer program which is

Reproduced with permission of the copyright owner. Further reproduction prohibited without permission.

described in an appendix. This program is designed to correct for the bias which is ordinarily manifested by least squares fitting of nonlinear data (see discussion in the Appendix). The best fit line is then extrapolated back to intersect with the amplitude of its "zero-time shots" (shots collected by mixing buffer with the metmyoglobin and rapid freezing in the usual manner) and this is taken to be the true zero time. The quenching time is the difference between the true zero time and the apparent zero time as calculated by equation 1. A typical experiment is shown in Figure 47, which also demonstrates a second method of determining the quenching time. In this alternative procedure the reaction is run at two (or more) different concentrations of azide. The two sets of data are plotted on the same graph and the intersection of the two curves is interpreted as the true zero time. This technique was not used routinely since it is more laborious than the first and the intersection of the two curves is very sensitive to small changes in slope and vertical positions of the rate curve. However, this method was used for determining the dead time of the stopped-flow instrument described in Chapter 4. Under favorable conditions, the stopped flow procedure does not have the scatter inherent in the rapid freezing technique and thus the dead time can be calculated by the second extrapolation method.

The quenching studies were performed on only 0.008 inch nozzles since this was found to be the smallest size with which

Reproduced with permission of the copyright owner. Further reproduction prohibited without permission.

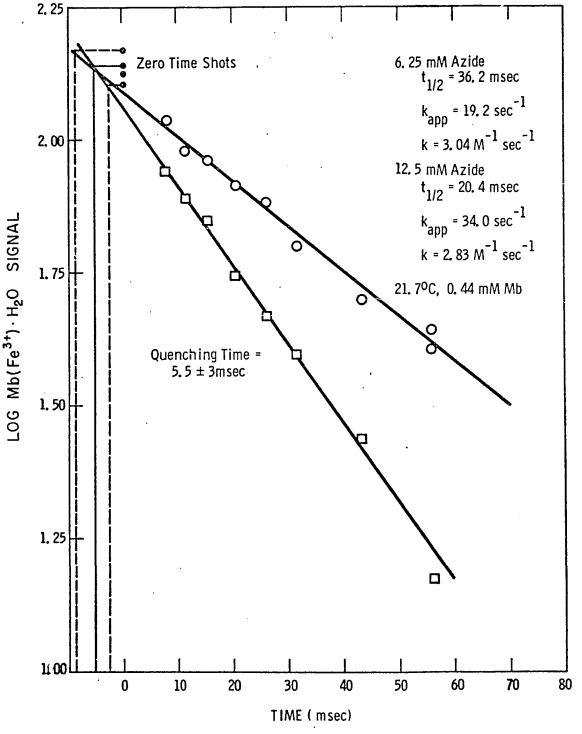

Figure 47. Quenching Time Determination - Method

Reproduced with permission of the copyright owner. Further reproduction prohibited without permission.

samples could be easily packed. Earlier experiments by Bray (20) had indicated, as might be anticipated, that the smaller nozzle sizes were more efficient for quenching than the larger nozzle sizes, and since the object of the study was to find the most efficient quenching conditions, larger nozzles were not studied. Beinert and his collaborators (62) independently have also found that 0.008 inch nozzles are the most effective. Since these findings were observed only at flow velocities of about 1 $ml \cdot sec^{-1} \cdot (2\ nozzles)^{-1}$, it is conceivable that at lower flow velocities smaller nozzles could be used effectively. This has not been investigated.

The first parameter investigated was the effect of nozzle velocity on the quenching time. The nozzle velocities investigated were limited to the range 0.3 to 0.7 $ml \cdot sec^{-1} \cdot (2\ nozzles)^{-1}$ due to the constraints of packing. When the velocity is higher than this the frozen crystals obtained tend to be very fine and float in the isopentane instead of settling into the neck of the EPR tube where they can be packed. When the velocity is below this range, the apparently larger granular crystals obtained coalesce into a hard plug in the neck of the EPR tube and cannot be packed.

A summary of the results obtained on how the nozzle velocity affects the quenching time is shown in Figure 48. It is seen that the quenching time is especially sensitive to the nozzle velocity in the range 11-14 m/sec (0.4 to 0.45 $ml \cdot sec^{-1} \cdot (2\ nozzles)^{-1}$) suggesting that an abrupt change in the physical properties of the jets occurs in

Reproduced with permission of the copyright owner. Further reproduction prohibited without permission.

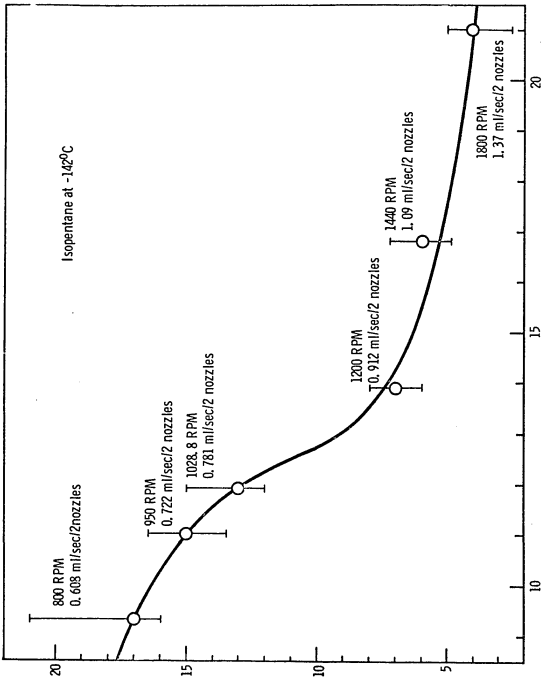

Figure 48. Quenching Time versus Nozzle Velocity (0.008 in Jets)

Reproduced with permission of the copyright owner. Further reproduction prohibited without permission.

this range. This is supported by the fact that the critical velocity for an 0.008 inch diameter stream in which one centipoise solution flows, is about 10 m/sec. One possible model is that at low nozzle velocities the jets maintain an essentially cylindrical shape until frozen, whereas at velocities exceeding the critical velocity, the jets break up into spheres which due to viscous stresses, are then flattened into deformed disc shapes; this physical transformation results in more efficient heat transfer and a reduced quenching time due to an increase in the surface area to volume ratio. It is known (63) that in viscous fluids bubbles deform in this manner and thus it is reasonable to suppose that droplets of immiscible liquids would also deform similarly. This model is probably not very accurate, however, since observations on basic phenol red solution ejected from the nozzles into acid showed that under most conditions the streams were dispersed almost instantaneously and did not have cylindrical shapes. The one exception to this occurred when both acid and base were in 60% glycerol (10 centipoise) and the nozzle was submerged (this is not the case for rapid freezing); in this instance the cylindrical stream of the basic phenol red remained stable until it reached the bottom of the vessel which contained the acid. Even under these extreme conditions the solution appeared to disperse instantaneously (within 1-2 mm of the acid surface) when the nozzle was not submerged. In view of this observation, a modified model in which at the critical velocity the aqueous particles

Reproduced with permission of the copyright owner. Further reproduction prohibited without permission.

are dispersed into smaller particles which have a larger surface to volume ratio, is probably more reasonable.

Another consideration which may help to explain how the nozzle velocity affects the quenching rate is the mixing action by the jet turbulence of the isopentane with the aqueous reaction fluid. Momentum from the jet is transferred to the adjacent layers of the isopentane by the shear stress between the fast moving aqueous fluid and the nearly stagnant isopentane, as well as by the turbulent eddies of the jet into the surrounding medium (64). This causes the cone-shaped dispersion of jets, a typical diagramed example of which is shown in Figure 49. The rate of mixing and thus the efficiency of the cooling process will depend on the velocity of the jet. The problem of quenching by rapid freezing is probably impossible to interpret quantitatively, but it is hoped that this discussion points out some of the salient fluid dynamical aspects of this problem.

The basic conclusion to be reached from the above study is that at least for many biological reactions, a 0.008 inch nozzle will permit a quenching time of 4-7 msec, depending upon the fluid velocity. The velocity most commonly employed is 1.1 $ml \cdot sec^{-1} \cdot (2\ nozzles)^{-1}$ and from Figure 48 it can be determined that the quenching time is 6 ± 1 msec. This value has been confirmed by Orme-Johnson and Hansen (65).

In general the quenching was done at $-142 \pm 2^{\circ}C$. However, in order to find out how fluctuations in the isopentane bath temperature

Reproduced with permission of the copyright owner. Further reproduction prohibited without permission.

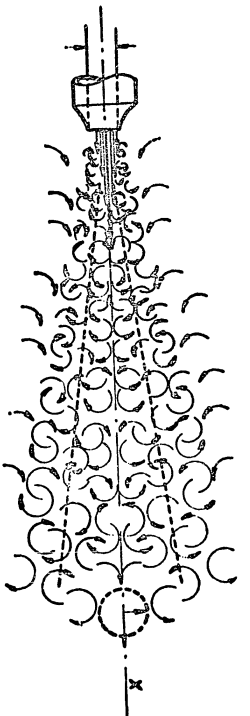

Figure 49. Schematic of Jet Dispersion

Reproduced with permission of the copyright owner. Further reproduction prohibited without permission.

affect the quenching time, two tests were performed at warmer quenching temperatures. In the first the isopentane bath was maintained at -100°C and the flow velocity was 1.1 ml·sec^{-1}·(2 nozzles)$^{-1}$, and it was found that the quenching time was 11 ± 2 msec. When compared to the 6 ± 1 msec obtained for -142°C, this result appears quite reasonable. The second test was performed at -60°C and the quenching time obtained was 8.5 ± 5 msec. The rather large uncertainty in this measurement derives from the fact that the frozen particles tended to be very granular and difficult to pack. This quenching time is considerably shorter than expected, although the uncertainty probably can account for the result.

It thus appears that although the quenching time is somewhat dependent upon the quenching temperature, changes of a few degrees in the isopentane bath temperature will not cause a serious error in the kinetic experiments. In the range -140 to -100°C it can be estimated that a 10°C change in the bath temperature will produce slightly more than a 1 msec change in the quenching time. A consideration which is much more difficult to quantitate is how the bath temperature affects the packing factor, a parameter which will be discussed later. To avoid possible problems in this regard, it is probably a good idea to regulate the temperature to better than ± 5°C.

According to Bray (20) the quenching process can be considered to occur in four stages: (a) the reactants are cooled from

Reproduced with permission of the copyright owner. Further reproduction prohibited without permission.

the reaction temperature to approximately 0°C, (b) the solution at about 0°C is frozen, (c) the frozen particles are cooled to the temperature of the quenching bath (approximately -140°C, and (d) the frozen, packed particles are cooled to liquid nitrogen temperature (-196°C). In addition, a fifth stage should be considered: (e) the samples are stored at -196°C until ready for measurement. If the first stage were a major part of the quenching process it would be expected that if the reaction were run at 0.5°C, the quenching time would be appreciably shortened. In one experiment the reaction temperature was 0.5°C and the azide concentration was 62.5 mM (so that the half-life of the reaction would be short enough to resolve the quenching time - 25 msec or less). The results showed that within experimental uncertainty (which was about ± 3 msec), the quenching time was 7 msec, i.e., it is about the same as when the reaction took place at 20°C. From this experiment it can be estimated that the time required to cool the reactants from 20°C to 0°C is probably not more than 2 msec.

One possible method for estimating the amount of reaction which occurs in stage (c) is the following. A sample which has been quenched in the usual manner is measured, then warmed to a known temperature, cooled to liquid nitrogen temperature, and measured again. If the signal has not changed, one of two conclusions can be made: (a) since the present experiment is done quite slowly compared with the rapid quenching process, very

Reproduced with permission of the copyright owner. Further reproduction prohibited without permission.

little reaction could have occurred during the quenching process, or (b) all of the change that could take place was completed during the quenching process and thus no further change was observed. This warming process can be repeated, each time warming to a higher temperature, until a suitable estimate of this parameter is obtained. To estimate this third stage for the metmyoglobin azide reaction, the sample was warmed to -60°C and maintained for 90 minutes at -60°C. In this experiment the warming had no effect on the signal and thus it is concluded that once the sample is frozen, this reaction is, for most practical purposes, quenched.

It is not surprising that for bimolecular reactions the freezing process, by preventing diffusion, essentially completes the quenching of the reaction. However, more complicated reaction systems such as xanthine oxidase, possibly could continue intramolecular reaction, even in the frozen state. However, the fact that the kinetics of different centers in these more complicated proteins are different, is testimony that intramolecular transfer does not occur to any appreciable extent during the slower phases of the quenching process. If there were an appreciable amount of intramolecular reaction during either quenching or while in the frozen state, although frozen at different times after mixing, all of the samples would adjust to their equilibrium concentrations, which would be the measured signals. To a good approximation, the kinetics of the various species would be identical. Results

Reproduced with permission of the copyright owner. Further reproduction prohibited without permission.

obtained by the rapid freezing method on several enzymes which have multicentered oxidation-reduction sites, have shown that the signals corresponding to the different sites do indeed have different kinetic profiles. A partial list is: milk xanthine oxidase (23, 66), liver aldehyde oxidase (67), DPNH-dehydrogenase (68), and cytochrome oxidase (69). Rapid freezing studies on dihydroorotate dehydrogenase (70), however, show no kinetic distinction between the iron and flavin semiquinone signals. This finding has two possible explanations: (a) intramolecular transfer does occur in the frozen state, or (b) the intramolecular reaction is too fast to resolve by this method.

Stage (d) is very difficult to measure, although it probably can be assumed if no reaction occurred at warmer temperatures, no reaction occurs in this stage.

It appears that for most reactions no appreciable reaction occurs in stage (e). Bray (20) has found that for xanthine oxidase, no change in the signals was observed even when stored for several days at -196°C. In work done in this laboratory the O_2^- radical and the metmyoglobin hydrate (in the presence of azide) as well as xanthine oxidase have all proven to be stable for at least several days at -196°C. However, Bray (71) has found that O_2^- becomes unstable when warmed to -65°C, demonstrating that each system must be treated individually.

Reproduced with permission of the copyright owner. Further reproduction prohibited without permission.

For most reactions it is probably safe to assume that the quenching time will be about the same as that reported in this work for the metmyoglobin azide system. An area in which considerable caution should be exercised, however, is that of free radical chain reactions which in some cases are known to react readily in the frozen state.

In conclusion, one can deduce that in most cases the quenching time is not a severe limitation in the study of fast reactions by the rapid freezing method. It is probable that with a quenching time of 6 msec kinetic constants for reactions with half-lives of about the same size can be determined. The fastest reaction determined in this work had a half-life of 15 msec, but this did not appear to be a limiting case. It is not so much a question of how long the quenching time is, but of how accurately it can be determined. Thus, if the quenching time is known to be 12 msec, a reaction with a half-life of 6 msec would still have 25% reaction which could be measured. However, if the quenching time were 6 $\pm$ 6 msec, it would be difficult to obtain accurate data for the same reaction.

Part II. Variables Associated with Measurement of EPR Signals

In the rapid freezing method the two experimental parameters which have the most effect on the ability to accurately determine the concentration of reactants, products and intermediates of

Reproduced with permission of the copyright owner. Further reproduction prohibited without permission.

reactions are (a) the packing factor and (b) the sensitivity, specificity, and reproducibility of the EPR method. These will now be discussed.

A. Packing Factor

Subsequent to being sprayed into the cold isopentane and settling into the neck of the EPR tube, the frozen suspension of sample must be packed into the narrow portion of the tube (Figures 26 and 27) so that the measurement can be made. Since the suspension consists of irregular shapes and sizes, there are spaces between the packed particles filled with isopentane. In order to quantitate the signals observed, the relative amounts of isopentane and aqueous frozen sample must be known. The relationship between these quantities, which is called the packing factor, makes it possible to relate the concentration of samples which have been prepared by the rapid freezing method, with laboratory standards (see section on EPR sensitivity).

In the measuring of the kinetics of first-order reactions it is only necessary to know the relative concentrations of species since the rate constant can be determined from the reaction half-time, but with second and higher order reactions it is necessary to determine the absolute concentrations of the reactants and products in order to obtain the rate constants. When comparing experimental with computer simulated results, it is also important to know the absolute concentrations of the reactants and intermediates.

Reproduced with permission of the copyright owner. Further reproduction prohibited without permission.

The packing factor is also a measure of the reproducibility of packing, which is obviously important, since any variation of the packing factor will directly affect the apparent concentration of measured species. The packing factor is defined as the multiplier which converts the signal obtained by the rapid freezing method to the hypothetical value it would have if prepared by standard techniques. The packing fraction is the reciprocal of the packing factor.

There are two basic methods which were used to determine the packing factor. The first, called the signal method, involves rapid freezing a nonreacting solution (e.g. metmyoglobin hydrate or $CuSO_4$-EDTA) in the usual manner and comparing its EPR signal with an identical sample which has been frozen slowly in the absence of isopentane. The ratio, (signal of slowly frozen sample)/(signal of rapidly frozen sample), is the packing factor. The second, called the height method, simply involves measuring the height of the frozen portion just before thawing and the height of the aqueous portion subsequent to thawing (the isopentane is immiscible and less dense than water and therefore the two layers are easily distinguished). The ratio, (height before thawing)/(height after thawing), is the packing factor. The disadvantage of the first method is that it is only applicable for measuring reactants or products of reactions which are stable and amenable to quantitation. Therefore this method can only be used with standard samples; the packing factor for the transient intermediates which are of interest cannot be

Reproduced with permission of the copyright owner. Further reproduction prohibited without permission.

determined directly. Although the second method does not have this disadvantage, it is imprecise. The average values obtained from several samples tend to be quite reproducible, but the accuracy of individual measurements is not very good. It is not certain whether this is a manifestation of the packing procedure or of the measuring technique. Furthermore, it is not clear that the values obtained by the height method are really packing factors: (a) the presence of isopentane may cause signal enhancement or attenuation and this is not taken into account (it is, however, in the signal method); (b) the sample's expansion upon thawing, may lead to incorrect results. The values obtained in several experiments by both methods are listed in Table 4.

From these studies it can be calculated that the packing factor obtained by the signal method is 1.63 ± 0.09 while that obtained by the height method is 1.79 ± 0.04. The studies of the $CuSO_4$-EDTA solutions were not included in these estimates since they seem to pack differently than the protein solutions (packing factor for $CuSO_4$-EDTA is 1.41 ± 0.06). There is no significant difference between the samples frozen at different temperatures, nor between those samples ejected at different nozzle velocities. In view of the difference in packing ease under these various conditions, this finding is quite surprising and suggests that to a first approximation, samples are packed as tightly as possible under all of the conditions investigated. The smaller result obtained for the $CuSO_4$-EDTA

Reproduced with permission of the copyright owner. Further reproduction prohibited without permission.

Reproduced with permission of the copyright owner. Further reproduction prohibited without permission.

Table 4

Experimental Packing Factors[a]

Method	Volume velocity (ml/sec)	Nozzle velocity (m/sec)	Material	Packing Factor	Packing Fraction	Comments[b]
Signal	0.608	9.3	$CuSO_4$-EDTA[c]	1.56	0.60	
Signal	0.608	9.3	$CuSO_4$-EDTA[c]	1.35	0.74	
Signal	0.608	9.3	$CuSO_4$-EDTA[c]	1.33	0.75	
Signal	0.608	9.3	$CuSO_4$-EDTA[c]			
Signal	0.722	11.0	Mb(H_2O)	1.64	0.61	
Height	0.722	11.0	Mb(H_2O)	1.74 ± 0.07	0.57 ± 0.03	
Signal	0.781	11.9	Mb(H_2O)	1.58	0.63	
Height	0.781	11.9	Mb(H_2O)	1.80 ± 0.08	0.55 ± 0.03	
Height	1.11	16.9	Mb(H_2O)	1.81 ± 0.06	0.55 ± 0.02	0 to -142°C
Height	1.11	16.9	Mb(H_2O)	1.88 ± 0.08	0.53 ± 0.02	0 to -142°C
Signal	1.09	16.8	$CuSO_4$-EDTA[c]	1.53	0.66	
Signal	1.09	16.8	$CuSO_4$-EDTA[c]	1.36	0.74	

Reproduced with permission of the copyright owner. Further reproduction prohibited without permission.

Table 4 (Cont.)

Method	Volume velocity (ml/sec)	Nozzle velocity (m/sec)	Material	Packing Factor	Packing Fraction	Comments[b]
Signal	1.09	16.8	$CuSO_4$-EDTA[c]	1.35	0.74	
Signal	1.09	16.8	$Mb(H_2O)$	1.42	0.71	
Signal	1.09	16.8	$Mb(H_2O)$	1.77	0.57	0 to -142°C
Height	1.11	16.9	$Mb(H_2O)$	1.73 ± 0.1	0.58 ± 0.04	-20° to -60°C
Signal	1.37	21.0	$Mb(H_2O)$	1.79	0.56	
Height	1.37	21.0	$Mb(H_2O)$	1.82 ± 0.07	0.55 ± 0.02	
Height	1.11	16.9	O_2^-	1.77 ± 0.04	0.56 ± 0.01	
Signal	1.82	27.9	$CuSO_4$-EDTA[c]	1.42	0.71	
Signal	1.82	27.9	$CuSO_4$-EDTA[c]	1.39	0.72	
Signal	1.82	27.9	$CuSO_4$-EDTA[c]	1.42	0.71	
Signal	1.82	27.9	$Mb(H_2O)$	1.54 ± 0.15	0.65 ± 0.07	
Height	1.11	16.9	$Mb(H_2O)$	1.81 ± 0.06	0.55 ± 0.02	

Reproduced with permission of the copyright owner. Further reproduction prohibited without permission.

Table 4 (Cont.)

Method	Volume velocity (ml/sec)	Nozzle velocity (m/sec)	Material	Packing Factor	Packing Fraction	Comments[b]
Signal	1.11	16.9	$Mb(H_2O)$	1.66 ± 0.09	0.60 ± 0.03	20° to $-100^{\circ}C$
Height	1.11	16.9	$Mb(H_2O)$	1.72 ± 0.06	0.58 ± 0.02	20° to $-100^{\circ}C$

[a] Double 0.008 inch nozzles were used in these studies.

[b] Unless otherwise noted isopentane bath was at $-142^{\circ}C$.

[c] These values were obtained by integration since the signal shapes for the rapid frozen $CuSO_4$-EDTA solutions are different than for those frozen slowly.

solutions (i.e., the samples pack more tightly) than for the protein (and O_2^-) solutions, has no obvious explanation.

Under favorable conditions the variation of the packing factor between samples causes a measurement uncertainty of the order of 5%, and is therefore the major limitation to obtaining accurate kinetic results. Although it is frustrating that in most cases the seemingly trivial problem of putting the sample into the observation tube is the major limitation of the rapid freezing method, there seems to be no obvious means of correcting it. The best one can do is to try and minimize the deviations and artifacts which arise from packing, and to this end, the following suggestions are offered. Since it has been found that packing varies when different persons perform the operation (evidence for this is that Bray et al. (24) have obtained a larger packing factor), only one person should do the packing for a given kinetic run, and he should try to maintain all conditions constant. The packing factor does not appear to be the same for all chemical systems, and therefore each system should be checked at least by the height method. (This can easily be done at the end of each experiment.) Although there are no apparent temperature effects on the packing, it is probably wise to maintain the isopentane bath constant to within 5.0°C during the packing operation.

Reproduced with permission of the copyright owner. Further reproduction prohibited without permission.

B. Measuring the Signal

The specificity, sensitivity and reproducibility of detection are of obvious importance in any analytical tecnique. However, in the EPR method these parameters are very difficult to define since they depend upon a large number of factors. Each chemical species to be measured by EPR must be evaluated individually with respect to these parameters and moreover, the criteria applied will be different depending upon what information is needed to be obtained from the measurements. For example, the definition of the order of appearance of intermediates in a multicomponent enzyme such as xanthine oxidase, requires minimal information about the absolute concentrations of the intermediates, whereas the determination of the second order rate constant for the dismutation of the O_2^- radical (see Chapter 5) is directly dependent upon knowing the absolute concentrations.

A detailed discussion about how to use the EPR technique in conjunction with rapid freezing is far beyond the aims of this thesis. There are, however, several good references which provide practical information about the theory and technology of EPR (72, 73). Since the EPR method is sensitive only to unpaired electrons, the observation of any signal potentially can provide information about reactants, products, and intermediates of reactions which is extremely useful. In addition, by the careful choice of magnetic field positions and scanning widths, microwave power, modulation bandwidth, and

Reproduced with permission of the copyright owner. Further reproduction prohibited without permission.

temperature, it is possible to distinguish rather fine chemical differences and obtain detailed information on the nature of the species (74).

Although it is not possible to set down hard and fast rules about how large concentrations must be to do effective rapid freezing EPR studies, it has been found in many instances that quantitative kinetic data can be obtained if at any time during observation the concentration of the observed species is $\geq$ the values given in Table 5. The values given are the concentrations before freezing (i.e., in the reaction tubes). It is possible that smaller concentrations could be effectively used if specialized noise averaging techniques are employed.

A factor of great importance in performing quantitative EPR studies is good temperature control. Within certain ranges, the intensity of signals is linearly proportional to T^{-1} and it is found, for example, that in the temperature range -196 to -160°C (77 to 107°K) metmyoglobin hydrate shows this linear type of behavior. If the signal is normalized to be 100 at -196°C (77°K), the equation fitting this behavior is:

25. Signal = $(1.53 \times 10^4 \cdot K)(T)^{-1} - 101$

This means that if the signals are measured nominally at -193°C (80°K), an uncertainty of 5°C in temperature will introduce an uncertainty in the observed intensity of 13%. To avoid these problems, a temperature controlling device (35) with 0.5°C regulation was

Reproduced with permission of the copyright owner. Further reproduction prohibited without permission.

Table 5

Minimum Concentrations Necessary for Effective

Rapid Freezing Studies

Species	Concentration	Comments
Flavin and flavoprotein semiquinones	10^{-5} M	
O_2^-	10^{-5} M	
High spin Fe^{+3} (myoglobin hydrate)	2×10^{-4} M	
Low spin Fe^{+3} (myoglobin azide)	2×10^{-4} M	May require helium temperatures
Molybdenum (xanthine oxidase)	10^{-4} M	
Non-heme iron (ferredoxin, xanthine oxidase)	2×10^{-4} M	May require helium temperatures
Ti^{+3}	2×10^{-4} M	
Cu^{+2}	2×10^{-4} M	

Reproduced with permission of the copyright owner. Further reproduction prohibited without permission.

constructed (see Appendix). With this regulation, the uncertainty in the signal will be less than 1% for metmyoglobin hydrate. This device also enables easy and rapid adjustment of the cavity temperature within the range -196 to 0°C, which is particularly convenient for optimizing sensitivity and selectivity in the measurement of certain species.

Absolute quantitation of paramagnetic species can in principle be derived from the spectra since the area under the absorption curve is proportional to the number of unpaired electrons. The method is to compare laboratory standards with the samples to be quantified. It is advisable, however, to use standards which have signals of similar g values and line-widths and which are measured at the same temperature, instrumental conditions and solvent as the signals being measured (74). Although differences in g values can be crudely corrected by the factor $g_{\perp}^{-2}$ (74), in general it is best to use as standards, substances which have similar spectra to the samples. In most of this work we have used $CuSO_4$-EDTA solutions (about 10^{-3} M in copper) as a secondary standard. Its concentration is determined by weighing. In measuring flavin radicals an alternate standard can be employed. Since the light activated reduction of flavodoxin by EDTA leads to quantitative production of the stable flavodoxin semiquinone (75), this free radical can be used as a standard. The optical absorptivity of the semiquinone is known to

Reproduced with permission of the copyright owner. Further reproduction prohibited without permission.

within 2% (75) to be 4.5 $mM^{-1}cm^{-1}$ at 580 nm so that its concentration can be readily determined.

Derivative EPR spectra of the standards and the samples can be doubly integrated (73) to obtain the integrated intensities of the absorptions which are compared in order to calculate the sample concentration. Under favorable conditions the integrations are reproducible to within 5%, which is the limit of the method's accuracy. With modern EPR spectrometers provided with good temperature regulation and a sample which permits a signal-to-noise ratio greater than about fifty, intensities are reproducible to within one or two percent. The EPR tubes (Figures 26 and 27) are carefully selected to be well-matched and are calibrated to within 2% by measuring the EPR signals of standard solutions. Alternatively, it has occasionally been convenient to measure the optical absorption of standard solutions in the tubes in order to calibrate them. This has been done with the aid of specially designed EPR tube holders which have the outer dimensions of standard 10 mm cuvets. These holders have a 4.5 mm bore to accomodate the EPR tubes and they mask the light beam to a rectangle 1 mm in width and 5 mm in height, so that only the central portion of the EPR tube is illuminated. This minimizes lens effects from the round sample tubes and allows the determination of optical spectra which are reproducible to within about 2% with a Zeiss DMR 21 split beam spectrophotometer. It should be noted that this procedure is

Reproduced with permission of the copyright owner. Further reproduction prohibited without permission.

only applicable to solution spectra and is not directly useful for obtaining spectra of frozen samples.

Part III. Discussion

There are three general aspects about the rapid freezing apparatus I would like to discuss. The first is concerned with improvements in the apparatus and some possible alternative components which could be useful. The second aspect deals with certain parameters and precautions for the rapid freezing technique for which no direct experimental evidence has been obtained. Finally, I would like to mention a few areas to which the flow system of the rapid freezing apparatus could be applied and discuss certain operational features of using various syringe combinations.

A. Instrumental Improvements

The major recommendation for improvement of this apparatus is to use a speed reducer which has a sturdier output shaft than the gearbox presently employed. Although there are many manufacturers of suitable speed reducers for this application (including the Boston Gear Co. which manufactured the reducer employed in this apparatus), I would like to mention the Gear Systems Division of United Shoe Machinery Corp., since this company uses a different principle of speed reduction (harmonic drive) having certain advantages over other methods; namely, harmonic drive units are lightweight, exceptionally strong, efficient, and have essentially zero backlash. A suitable reducing unit is Model HDUC 32 with a 100:1

Reproduced with permission of the copyright owner. Further reproduction prohibited without permission.

reduction ratio. The output shaft is 1-1/16 inch in diameter and is rated for an overhung load of more than 1000 lb which is surely more than sufficient for the flow applications. The standard model mounts in a horizontal attitude, but verticle mounting is also available. In either case a slightly different physical layout than for this apparatus would be required.

The motor used on this apparatus is no longer available from Sears and Roebuck Co. Some recommended substitutions are: Dayton models 6K011, 6K064, and 5K994. The first is a half-wave SCR-controlled 1/2 hp series wound motor with a continuously adjustable speed range of 500 to 5000 rpm and it appears to be identical to the Sears and Roebuck motor used in this apparatus. The cost is about $100. The second is a 1/2 hp shunt wound DC motor with full-wave SCR-controlled speed which is adjustable from 0 to 2500 rpm and costs about $200. The third type is an adjustable speed (700-4000 rpm) encased belt-drive unit employing a 1/2 hp capacitor-start motor and costs about $110. This unit maintains full torque throughout most of its speed range since the motor runs at a constant speed. These motors are all sold by W. W. Grainger, Inc. A fourth motor is model 504-08-019 3/4 hp DC motor with the TA-100P speed control produced by the Minarik Electric Co. This motor ($150) has been used on two flow units which were constructed according to plans in this thesis, by the University of Michigan Physics Instrument Shop (about $1500 ea.).

Reproduced with permission of the copyright owner. Further reproduction prohibited without permission.

It is our philosophy that the use of a flywheel driven by relatively inexpensive motors such as those above is the most economical solution to the problem of producing power sufficient to impart the linear motion for driving the syringes. The use of stepping motors is an obvious alternative, but a stepping motor which could achieve the driving power of the flywheel mechanism would be far more costly than the latter. It should be realized that this is only true for situations such as in the rapid flow system where the power does not need to be applied for long periods of time so that the total energy requirement is small compared with the energy "stored" in the flywheel. If the power has to be applied for a long period of time a stepping motor drive might be necessary.

I would like to discuss two features of the cam construction which may not be obvious to readers unfamiliar with cam design. Linear motion of the cam follower depends upon there being a constant pressure angle between the cam follower and the cam. The pressure angle is the obtuse angle subtended by the direction of linear motion and the perpendicular of the intersection of the cam and follower surfaces. For maximum efficiency this would ideally be 180°, but in practice it is always between 90° and 180°. Since the radius of curvature of the cam changes during rotation, the pressure angle between the cam follower and the cam surface does not remain constant. This results in a changing cam efficiency and a possibly nonlinear motion, even though the cam is rotating uniformly.

Reproduced with permission of the copyright owner. Further reproduction prohibited without permission.

Clearly, for a given amount of linear motion, the larger the cam, the smaller is the change in curvature and therefore in pressure angle. Since the cam must be of finite size, this problem is not totally resolvable, although it is found that a cam of the size described in this thesis is a convenient compromise. The problem of maintaining a linear motion with a changing pressure angle is solved by machining the cam with a milling tool of the same diameter as the cam follower. Since the cutter moves linearly with rotation of the cam regardless of the changing pressure angle, a cam follower of the same size must also move linearly.

The present syringe ram (Figure 10) is far more complex than necessary and its complexity derives from the fact that it was designed before the linear motion device was conceived and was later adapted to it. An alternative which is more substantial and easier to construct is shown in Figure 50. The parts A and B are mounted on the lathe bed and a 1-1/4 by 1 inch aluminum bar about 22 inches long is fastened to these parts A and B. The ball bearing cam follower is fastened to one end of the bar as shown. The other end of the bar and part B are flush and come into direct contact with the syringe plungers so as to form the syringe ram. If the sturdier speed reducer recommended above were used, this would replace both the syringe ram and the cam follower and its simpler construction would probably more than compensate for the difference in costs between the speed reducers.

Reproduced with permission of the copyright owner. Further reproduction prohibited without permission.

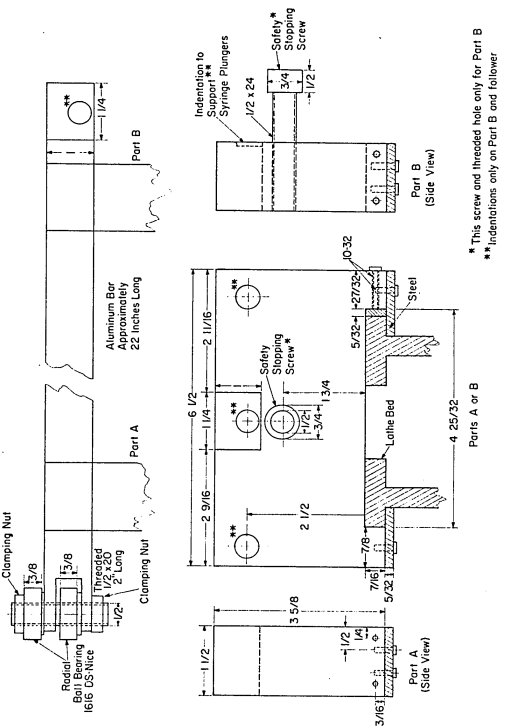

Figure 50. Alternative for Syringe Ram and Cam Follower

Reproduced with permission of the copyright owner. Further reproduction prohibited without permission.

The heavy walled polyethylene tubing employed in this apparatus (and the stopped-flow apparatus to be described in Chapter 4) could be replaced by the commercially available teflon tubing, Cheminert Tubing (Chromatronix Inc.). This tubing and its fittings are somewhat more expensive and require a special oven (Chromatronix Inc.) for making the tips. To use it for anaerobic purposes, a similar arrangement to that described in Chapter 2 (Figure 17D) would be possible. In applications where metal-to-solution contact is not detrimental to studies, stainless steel tubing could be used and connected with suitable connectors. This would make it possible to achieve very good anaerobiosis. It would be extremely desirable if there were available stainless steel tubing which was coated on the inside with a thin film of teflon; this for most purposes would have both the benefits of being inert as well as being anaerobic and durable.

It was mentioned in Chapter 2 that an improvement in the Palmer-Beinert mixer would be discussed. The jets of the mixer described (Figure 18B) are arranged so that reactants A and B meet each other at right angles. It is proposed that if the jets were arranged so that the two reactant streams were tangentially opposed, the mixers would function better. This could be accomplished by placing the two entrance screw holes opposite to each other (rather than at right angles) and milling quarter-circles which are centered at these holes instead of semi-circles as in the Palmer-Beinert

Reproduced with permission of the copyright owner. Further reproduction prohibited without permission.

mixer. Then the verticle channels are milled and the holes which form the mixer are drilled as described in Chapter 2. This would be no more difficult to construct than the usual Palmer-Beinert mixer. I feel, however, that since the Ballou mixer is simpler to construct, works at least as well, and because it can be taken apart, is easier to clean in the event that protein becomes dried in the channels, this mixer is to be recommended.

B. Precautions and Unmeasured Parameters

Although the dead space of the flow system is considered to be the sum of the volumes of the mixing chamber and the reaction tube, there is a finite delay between the time the fluid leaves the nozzles and when it enters the isopentane which is not considered, but which is minimized by placing the nozzles very close to the isopentane (typically less than 5 mm from the surface of the isopentane).

Referring to Table 3 in the Appendix, it is seen that at the usual flow velocity (1.1 ml/sec), the jet velocity is 17.1 m/sec. Considering that the fluid travels 5 mm or less before entering the isopentane, it can be calculated that this delay corresponds to less than 0.3 msec and therefore is unimportant in the time resolution of the apparatus. However, in studies on cytochrome oxidase, a protein which in its reduced form reacts very rapidly with oxygen, Beinert and Hansen (76) have found that some reaction with oxygen occurs after the solution leaves the nozzles. They believe that some oxygen may become trapped in the fine aqueous streams during

Reproduced with permission of the copyright owner. Further reproduction prohibited without permission.

travel to the isopentane (perhaps because of jet turbulence) and some oxygen is undoubtedly picked up by the aqueous stream while in the cold isopentane (oxygen is at least ten-fold more soluble in cold isopentane than it is in water (77)). Therefore these investigators have undertaken the development of an anaerobic quenching bath (76).

Another parameter which should be considered is the amount of heating which occurs in capillary flow. Grundfest et al. (78) and Gerrard et al. (79) have found that even under extreme conditions (Gerrard et al. flowed 100 centipoise solutions at 200 psi through a 0.4 mm capillary 10.4 cm long) the temperature rise was less than $0.2^{\circ}C$. Since this is the usual limit of temperature control used for rapid kinetic studies (excluding thermal studies), capillary heating effects apparently can be ignored.

Although there are undoubtedly numerous factors which have not been explicitly considered, the present evaluation covers all of the parameters which I believe most important. Many of the studies are of complex phenomena (especially mixing, flow, and quenching) so that several parameters not explicitly considered are included in these studies. The basic result of all of these investigations is that the rapid freezing method enables the study by EPR of features of many fast chemical reactions which is not possible by other methods. The time resolution of the method is sufficient that the method is in many studies complementary to the optical stopped-flow technique.

Reproduced with permission of the copyright owner. Further reproduction prohibited without permission.

For example, if we consider that 10^{-4} M solution is necessary for determining rate constants of a particular species, and if a reaction with a half-time of 10 msec is the fastest reaction we can measure accurately, the maximum second order rate constant which can be determined is thus about 10^{5} M^{-1} sec^{-1}. This is 10^{2}-10^{3}-fold less than the limit for stopped-flow spectrophotometry, but is nevertheless within the range in which most stopped-flow studies are performed. The time consuming observations of complexities in saturation behavior, signal shapes, and number of spins of reaction intermediates which are made possible by the fact that the reaction is quenched by rapid freezing, would go unnoticed with other techniques (80) in which observation must be made simultaneously as the reaction progresses. However, it should be emphasized that, especially due to the complexities of the freezing process which may in some cases produce artefacts, the interpretation of results obtained by the rapid freezing method must be made with care, and whenever possible correlated with parallel fast kinetic studies by optical or other means.

C. Possible Applications of the Flow System

The flow system of this rapid freezing apparatus is adaptable to nearly all of the measuring techniques which can be used in continuous flow methods; for example: (a) optical observations, (b) calorimetric measurements, (c) electrode measurements, (d) chemical quenching and sampling, and (e) cryogenic quenching

Reproduced with permission of the copyright owner. Further reproduction prohibited without permission.

(rapid freezing). The first four are described quite fully by Gutfreund (16) and Roughton (13) and the fifth is the main subject of this thesis so that I will not discuss the principles of these techniques further. In the past the continuous flow method has been used for reasons of simplicity and because observation techniques had inherently long time constants and/or poor signal-to-noise characteristics. The period of time required for measurement was much longer than the reaction time which was to be observed. In recent years, however, many of the standard measuring techniques which are mentioned above have been improved to the extent that good signal-to-noise characteristics are possible with time constants of considerably less than one second. Because of its requirement for only small volumes of reactants for each kinetic curve, the stopped-flow method is usually preferred. However, except where highly specialized (and expensive) equipment is employed (for example, Berger and Stoddart (81) have reported such a thermal stopped-flow), its use has been limited to optical measuring techniques (both absorption and fluorescence). Although in principle thermal and polarographic instruments can have a time response of less than 5 msec (81, 82), in practice these measurements remain difficult in the stopped-flow mode, probably due to the transitory nature of the boundary layers in the vicinity of the detector. An alternative is to employ the pulsed-flow technique (8, 9) which is essentially a short period of continuous flow which is started

Reproduced with permission of the copyright owner. Further reproduction prohibited without permission.

and stopped very abruptly. With this method the quantities of reactant required will depend upon (a) the sensitivity of the measuring technique, (b) the response time of the detection system, (c) the dead volume necessary for the measuring probe, (d) the reaction time to be measured, and (e) the shape of the velocity profile (if the profile is ideal, i.e. the pulse is a step function, no reactants need to be wasted in attaining and terminating a constant velocity). With this apparatus the flow velocity is very nearly a step function - due to the unique requirements of the rapid freezing method. If the dead volume of the probe is about 5 microliters, 0.5 second is required for the measurement, a holdup (reaction) time of 20 msec is desired, and if the flow rate is one ml/sec, then only about 0.26 ml of each reactant needs to be used to obtain the measurement. If ten points are sufficient for obtaining a rate constant, then a total of only about 2-5 ml of reactants needs to be consumed. Thus measurements can be made with the pulsed-flow technique which have the time resolution and nearly the fluid economy of the stopped-flow method, and moreover, these measurements are possible with a number of techniques unsuitable to the stopped-flow mode of operation.

With this flow machine a small block could be constructed which contained an observation cell designed for the specific type of measurement desired (optical, thermal, or electrode) and which could be connected to various delay tubes in order to obtain

Reproduced with permission of the copyright owner. Further reproduction prohibited without permission.

measurements at different times after mixing in much the same manner that rapid freezing studies are performed. Since this method maintains constant conditions at the observation point, in contrast to other methods where the probe has to be physically moved or else the flow rate must be varied, it is likely that better stability and accuracy can be achieved. (Changing the flow rate can have quite an effect on thermal and electrode measurements.) This method also simplifies the calibration procedure since calibration needs to be done only once for each specific type of measurement. Another advantage is that the entire flow system can easily be submerged in a water bath, thereby making possible excellent temperature control.

I would like to mention two possibly less obvious applications in which pulsed flow would be considerably more suitable than stopped-flow. The first is for differential measurements in which one detector is placed at the point to be measured and the other is placed a suitable distance downstream. Since the same conditions exist for both detectors during measurement, the differential measurement obtained will be due only to the chemical reaction and thus the difficulties of measuring small changes on top of large signals, is avoided. This technique was originally employed by Roughton (83) for thermal studies where heat from mixing, viscous shear, and other flow parameters were compensated by placing a second thermocouple downstream. Gutfreund (16) has proposed the

Reproduced with permission of the copyright owner. Further reproduction prohibited without permission.

interesting idea that if the pair of thermocouples are suitably spaced and moved together, keeping the distance between them constant, data can be directly obtained for first order reactions that are suitable for Guggenheim plots (49). This would be particularly straightforward if both detectors were placed in the same block and the time for the measurement was varied by employing reaction tubes of suitable volumes.

The second application would use a rapid scanning monochromator and photodetection unit which is capable of scanning rather broad regions of the spectrum in times as short as 2 msec (such devices are available from Warner/Swasey). This could be used to scan the spectral region of interest many times during flow and the information could be stored and noise-averaged (for example, by a CAT) in order to improve signal-to-noise. With such a device the entire spectrum could be scanned 50 to 200 times in a period of about one second and the entire spectrum of the mixture could be measured during flow at various reaction times of interest while only consuming about 5 ml total of each reactant. Light pipes could be employed to transmit the light from the lamp to the observation cell and from the observation cell to the monochromator. A stopped-flow device using this monochromator system has been described (84), but I believe that the pulsed-flow method makes it possible to obtain higher resolution and more sensitivity.

Reproduced with permission of the copyright owner. Further reproduction prohibited without permission.

Chemical quenching and sampling is an important application in which this flow system can be directly applied. The analysis of components "trapped" by this technique can be done at one's leisure, which has the advantage of permitting very sensitive and specific assay techniques, as well as for assaying more than one component. The Lowry microassay (recycling) method (85) used in conjunction with chemical quenching offers the intriguing possibility of studying rapid reactions with reactants (or products) in concentrations as small as 10^{-12} molar.

The chemical quenching method has been discussed quite extensively by Gutfreund (16), but I would like to mention a few points which may be particularly appropriate to this apparatus. There are two basic methods of initiating the quenching process: (1) The quenching reagent is introduced from a third syringe by coupling the output of the reaction tube with the quenching reagent via a second mixing chamber. (2) The reaction mixture is squirted as a fine stream into a beaker which contains an excess of quenching reagent (just as in the rapid freezing method). Method (1) is to be preferred since quenching can be done without as much dilution of the reaction mixture and because it is likely to be more reproducible than the second method owing to the fact that mixing is probably more efficient, and in part to the fact that in method (2) spattering can occur when the reaction mixture enters the quenching solution thereby

Reproduced with permission of the copyright owner. Further reproduction prohibited without permission.

ruining the quantitation; this is not true for the two mixer method since all of the collected mixture is of the same composition.

In using the three syringe method in conjunction with any technique, certain precautions must be taken. In reference to Figure 51 the following relationship must be satisfied.

$$\underline{26}. \quad \frac{\text{Volume}_{DE}}{\text{Volume}_{CE}} = \frac{\text{Volume Syringe C}}{\text{Volume Syringe A} + \text{Volume Syringe B}}$$

This can be accomplished in at least four different ways: (a) The volumes of the tubes can be judiciously chosen to meet this requirement (which is not always convenient). (b) The tube, CE, is filled, but syringe C is depressed just enough that the ram does not begin driving it until the volume, DE, which is initially empty, is filled. (c) A volume, CE, satisfying equation 26. can be withdrawn into syringe C, and then the three syringes are pushed simultaneously. (d) The first bit of ejected solution can be discarded so that all of the solution which is collected is of the same composition. The latter two methods are the easiest to use. Method (d) is done automatically by means of a solenoid valve in a recent apparatus constructed for chemical quenching (86).

The use of three syringe methods, in principle can be quite useful, but it should be realized that all of the complications which are discussed in the earlier sections of this chapter are multiplied and thus the resolution of times by this method is bound to be less precise than in the two syringe method.

Reproduced with permission of the copyright owner. Further reproduction prohibited without permission.

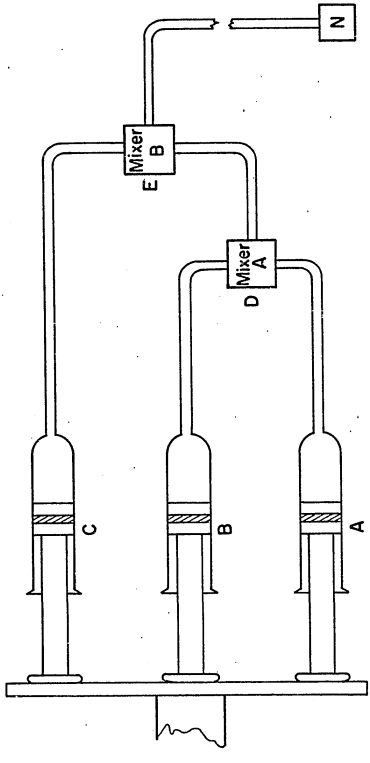

Figure 51. Three Syringe Continuous Flow Method

Reproduced with permission of the copyright owner. Further reproduction prohibited without permission.

CHAPTER 4

AN ABSOLUTE ABSORBANCE STOPPED-FLOW SPECTROPHOTOMETER

As described in the introduction, almost all optical stopped-flow instruments employ only a single beam for analysis and because of this one obtains from these instruments the absorbance of the sample with respect to the absorbance at "infinite" time. This chapter describes an optical stopped-flow apparatus which directly records the absolute absorbance of the reactants and products as a function of time at a given wavelength. This is made possible by incorporating into the observation block a reference cell adjacent to the reaction cell. Observation of either reference or reaction solution is conveniently selected by means of a sliding shutter and the optical density is recorded directly from the output of a Gilford optical density converter. This new feature in stopped-flow spectrometry not only gives a direct measure of the concentration changes during the progress of the reaction, but also enables one to plot directly from kinetic progress curves obtained at various wavelengths, the absolute optical spectra of nascent intermediates at selected times during the reaction. The instrument uses only small volumes of reactants (about 0.1 ml of each reactant per shot) and as shown in the present study, has sensitivity and response comparable to most previously described stopped-flow spectrophotometers (for example, 13, 14, 87, 88).

Reproduced with permission of the copyright owner. Further reproduction prohibited without permission.

The remainder of this chapter is divided into two parts. Part I describes the construction and Part II is an evaluation of the performance of the apparatus.

Part I. Details of Construction

A. General Layout and Principle of Operation

The general arrangement of the apparatus is shown in the photographs in Figure 52. The reagents are placed in storage vessels from which they are transferred to the driving syringes located in the driving module by means of three-way Hamilton valves. The syringes are driven by the hydraulic ram forcing the reactants to flow through the flexible plastic tubing to the mixing and observation module and thence to the stopping syringe assembly where the mixed reactants rapidly drive the plunger of the stopping syringe upwards until it strikes the stopping block. When this happens the flow is suddenly stopped and a record is obtained from the output of the Gilford spectrophotometer as a trace on the storage oscilloscope. To repeat observation the contents of the stopping syringe are exhausted by means of a three-way Hamilton valve on the stopping module and the hydraulic ram is reactivated to drive the syringes. The Gilford spectrophotometer is operated in the usual manner with observation of the reference solution alternating with observation of the sample solution by means of the sliding shutter.

Reproduced with permission of the copyright owner. Further reproduction prohibited without permission.

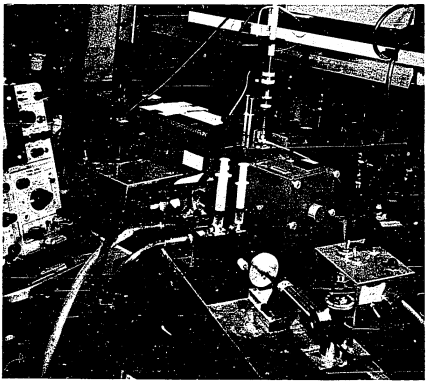

Figure 52 A

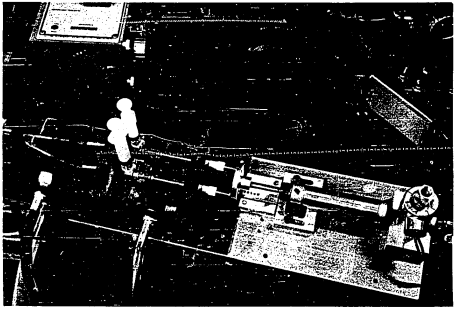

Figure 52 B

Reproduced with permission of the copyright owner. Further reproduction prohibited without permission.

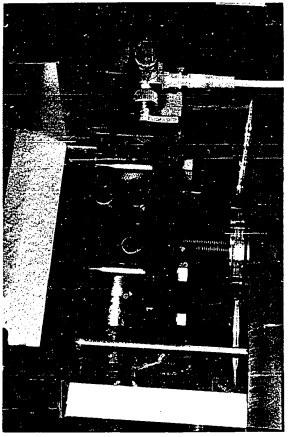

Figure 52 C

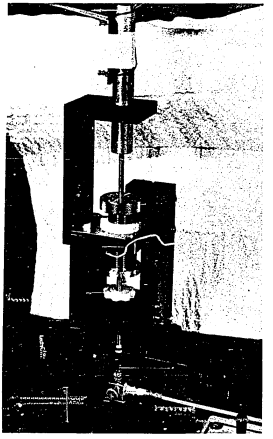

Figure 52 D

Figure 52. Absolute Absorbance Stopped-Flow Spectrophotometer

A. Overall View
B. Fluid Driving Block
C. Observation Assembly
D. Stopping Module

Reproduced with permission of the copyright owner. Further reproduction prohibited without permission.

B. Driving Unit - Details

The driving unit (Figures 53 and 54) consists of an aluminum water bath which holds three Hamilton 1001 gastight syringe barrels with plungers modified as in Figure 15, and three Hamilton 3 MFF 3 three-way valves, a Bimba model 092-D hydraulic cylinder and a Skinner VG-6 solenoid valve. The RC discharge circuit shown in Figure 55 activates the solenoid so as to hold the valve open for about 30 msec thus allowing gas at about 40-55 psi from a compressed air cylinder to be delivered to the hydraulic piston, which then drives the syringes. The total flow time is 15-20 msec depending upon the amount of solution flowed, and thus the pressure on the fluid system is only present slightly longer than the actual flow period. The syringes are mounted into the water bath in the same way and are interchangeable with those in the rapid freezing apparatus (Figures 15 and 16). During usual operation only two syringes are used, but in instances where three syringe capability is needed (e.g. when one reactant is somewhat labile under the conditions of observation), a second mixer can be employed for tandom mixing. Since all Hamilton gastight barrels up to 2.5 ml are easily interchanged, variable ratio mixing is also possible. The plastic tubing connecting the driving module to the mixing and observation unit are the same as used in the rapid freezing apparatus and are described in Figure 18. They are encased by a short length

Reproduced with permission of the copyright owner. Further reproduction prohibited without permission.

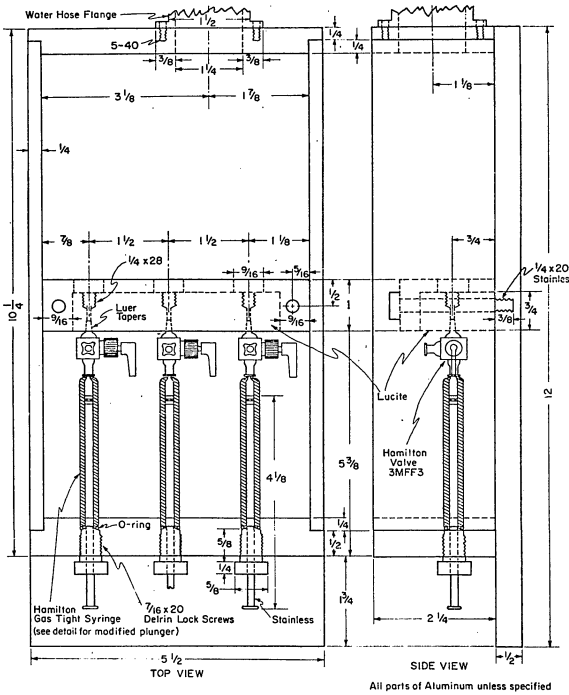

Figure 53. Driving Module - Water Bath

Reproduced with permission of the copyright owner. Further reproduction prohibited without permission.

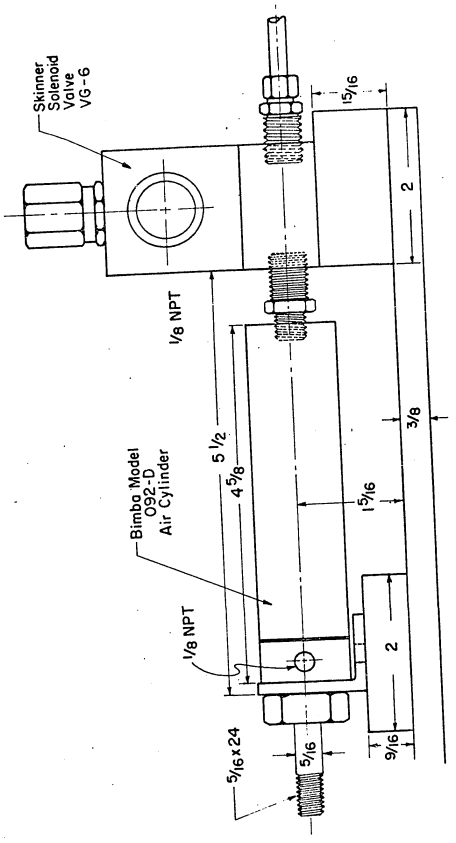

Figure 54. Driving Module - Solenoid Valve and Hydraulic Cylinder

Reproduced with permission of the copyright owner. Further reproduction prohibited without permission.

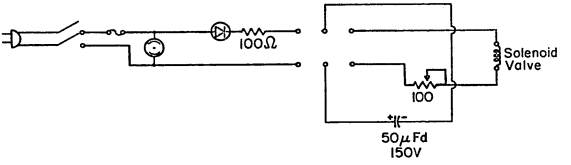

Figure 55. Solenoid Valve Activator

Reproduced with permission of the copyright owner. Further reproduction prohibited without permission.

of expanded vacuum cleaner hose through which constant temperature water is circulated from the driving unit to the observation assembly.

C. Mixing and Observation Module - Details

The observation and mixing module (Figure 56) has the same outside dimensions and is precisely positioned in the optical path with locating pins in the same way as the normal thermostated cell compartment of Gilford and Beckman equipment. The design of the Kel-F observation block is shown in Figure 57. The mixer is machined as channels on the front face and the 2 cm long observation and reference paths are formed from 1.5 mm diameter holes drilled clear through. These holes are sealed by pressure fitting two 1 inch circular quartz flats (Esco Products) against the ends of the block. These flats also serve as the windows for the light path. The V-shaped bottom of the mixing block facilitates quick and accurate alignment in the observation module and allows easy interchanging of mixing blocks which have different path lengths (although this has never been done). Water is excluded from the optical path by the use of a threaded aluminum tube fitted with O-rings which are screwed against the pressure block (part B of Figure 56). Since even with the O-rings this type of fitting can have small leaks, a recommended substitute is a metal bellows which can be obtained from Mini-Flex Corp. or Cajon Co.

Reproduced with permission of the copyright owner. Further reproduction prohibited without permission.

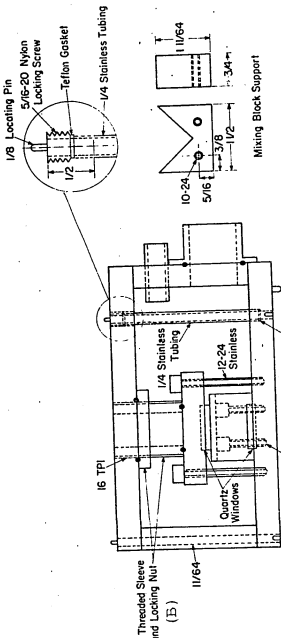

Figure 56

Reproduced with permission of the copyright owner. Further reproduction prohibited without permission.

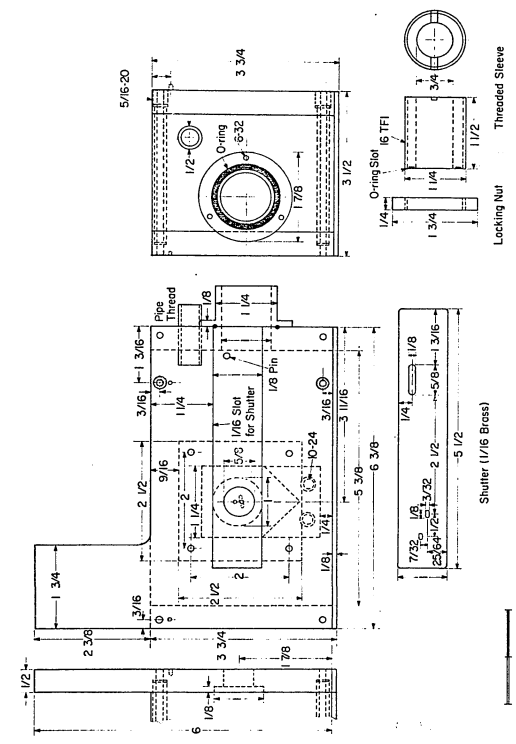

Figure 56. STOPPED-FLOW OBSERVATION ASSEMBLY
All Parts of Anodized Aluminum Unless Specified

Reproduced with permission of the copyright owner. Further reproduction prohibited without permission.

Legend for Figure 57

The insert in the upper right corner is not to scale, but is to indicate the flow channels.

a = 0.788 inch (2 cm)
b = 1-1/2 inches
c = 1/8 inch
d = 3/4 inch
e = 2 inches
f = 1-15/64 inches
g = 3/8 inch
h = 3/16 inch
i = 5/16 inch
j = 1/4 inch
k = 5/16 inch
l = 5/8 inch
m = 11/32 inch
n = 37/64 inch
o = 49/64 inch
p = 0.118 inch
q = 11/16 inch
r = 1/8 inch
s = 53/64 inch

Reproduced with permission of the copyright owner. Further reproduction prohibited without permission.

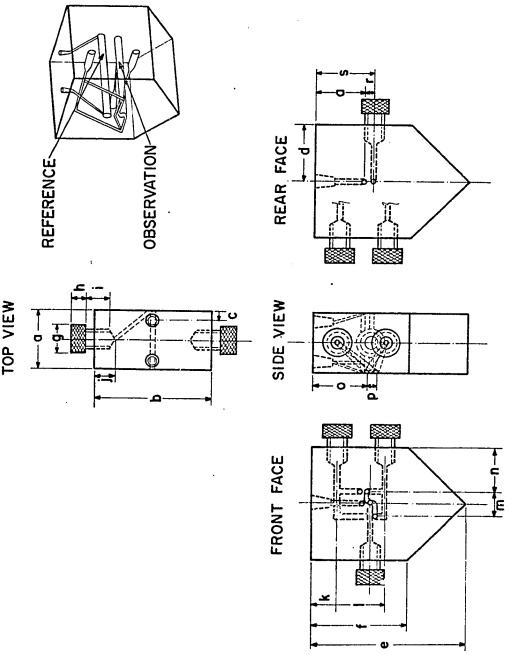

Figure 57. Kel-F Observation and Mixing Block

Reproduced with permission of the copyright owner. Further reproduction prohibited without permission.

The absorbance is obtained from the analog output of a Gilford Model 220 optical density converter. (This output is usually recognized as a tri-lead microphone jack on the rear of the converter.) The normal recorder output is attenuated by a factor of about five to meet the requirements of the recorder used in the Gilford converter; this attenuated voltage is too small to expand sufficiently on the oscilloscope. The absorbance function, which is only a fraction of a volt, is the difference between two carrier voltages, each of which varies between 0 and 10 volts. Therefore to measure the actual absorbance function, this carrier or common mode voltage must be removed. Ordinarily recorders have differential or floating inputs and thus perform this function directly so that the effect is not noticed. However, the 3A72 input amplifier of the Tektronix Model 564 oscilloscope is single-ended and therefore measures the voltage between a single input and ground. Therefore a common mode rejection unit was constructed (Figure 58a) which subtracts the large voltage common to both inputs and references the difference voltage thus obtained to ground. The output of the common mode rejection unit can be connected directly to the oscilloscope which measures the absorbance. This rejection unit has a high input impedance so that only a negligible amount of current is drawn from the Gilford. The characteristics allow one to make differential measurements with millivolt sensitivity on signals as much as 10 volts above or below ground. Many of the newer

Reproduced with permission of the copyright owner. Further reproduction prohibited without permission.

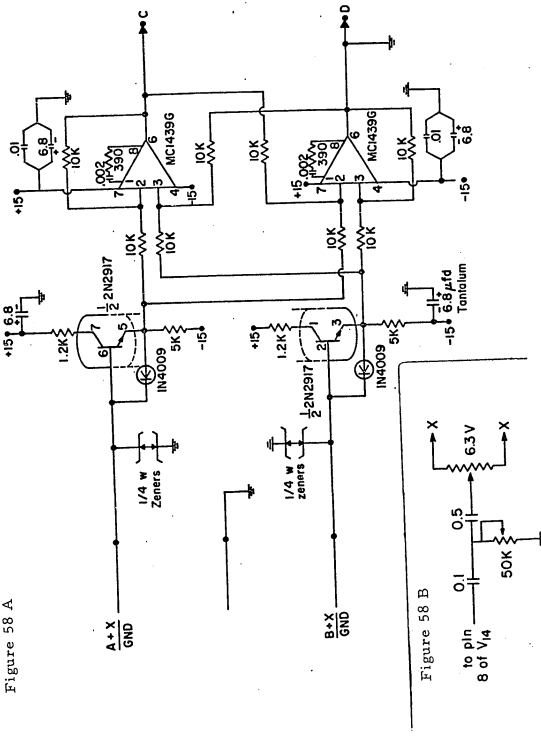

Figure 58. Circuits for Conditioning Optical Density Signal for Stopped-Flow
A. Common Mode Rejection Unit
B. 60 CPS Noise Correction Unit

Reproduced with permission of the copyright owner. Further reproduction prohibited without permission.

oscilloscopes have differential input as a standard feature so that the common mode rejection unit would be unnecessary.

The 60 cps ripple common to Gilford instruments was substantially reduced by biasing the signal with a small portion of the 60 cps filament voltage which was adjusted to be 180° out-of-phase and of the optimum magnitude to minimize the noise ripple. This device (Figure 58b) was tied to the cathode (pin 8) of V_{14}, which in the Gilford Model 220, functions as the reference arm of a differential amplifier. (It may be recognized that this type of dynamic signal correction is commonly used in color television raster correction.)

D. Stopping Syringe Assembly - Details

The stopping syringe assembly (Figure 59) consists of the stopping syringe, a three-way Hamilton valve for emptying the syringe, an oscilloscope trigger which can be adjusted to activate the oscilloscope trace either during flow or at the end of flow, and a Sanborn LV SYN 6LVA8 transducer whose output is a function directly related to the solution flow velocity. The stopping syringe is a Hamilton gastight barrel cut to the appropriate length and having a specially constructed plunger tip (Figure 15) and a plunger which is directly coupled to the magnet of the velocity transducer. Thus the record of the flow can be recorded simultaneously with the record of the absorbance on the dual trace oscilloscope enabling determination of the stopping time to within one millisecond. This

Reproduced with permission of the copyright owner. Further reproduction prohibited without permission.

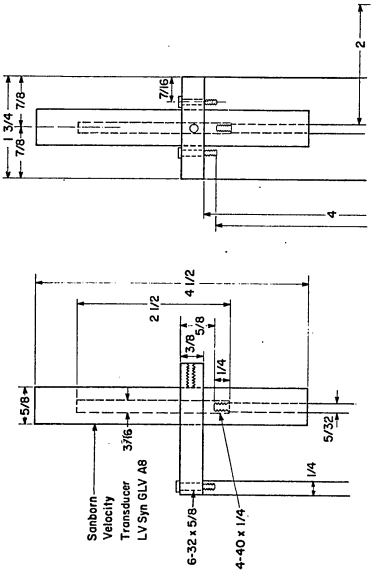

Figure 59 STOPPING SYRINGE ASSEMBLY

Reproduced with permission of the copyright owner. Further reproduction prohibited without permission.

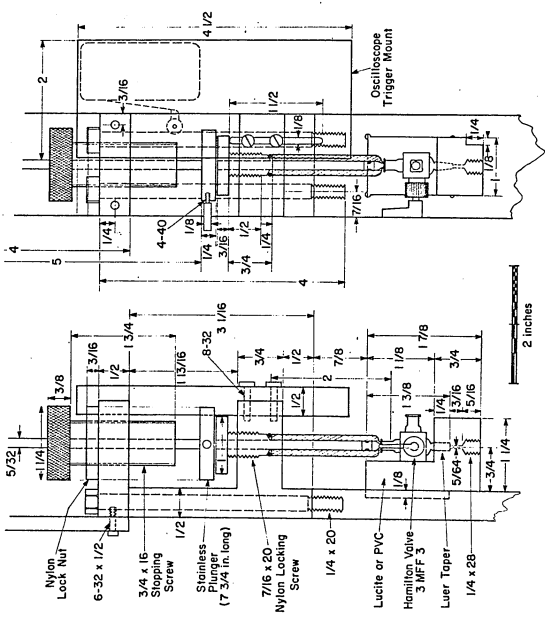

Figure 59. Stopping Syringe Assembly (Also see Figure 52)

Reproduced with permission of the copyright owner. Further reproduction prohibited without permission.

may be particularly valuable in analyzing traces in which the optical traces do not show an abrupt change at the cessation of flow. The amount of solution used per shot is controlled by adjustment of the stopping bolt. The oscilloscope trigger is a Robertshaw BZ 2RS microswitch which can be variably positioned. The entire stopping syringe assembly detaches from the mixing unit and is frequently used with the driving unit in a very sensitive fluorescence stopped-flow instrument (43).

Part II. Performance and Evaluation

For our purposes the criteria most important in stopped-flow spectrophotometry are: (1) Good reproducibility and signal-to-noise characteristics, (2) A short dead time (The dead time is a complex function determined from the dead volume, the flow rate, and the mixing efficiency, but its operational definition will be that time during which reaction occurs before observation is possible. Experimentally this can be estimated in the same way that the quenching time was determined in the preceding chapter.), (3) Sensitivity to small changes in optical density, (4) A requirement for only small volumes of reagents, and (5) The ability to maintain anaerobic conditions.

(1) Reproducibility and signal-to-noise characteristics are demonstrated in Figure 60. This shows superimposed duplicate traces recorded at four different oscilloscope sweep rates (eight shots altogether) monitored at 570 nm for the reaction of $Fe(NO_3)_3$

Reproduced with permission of the copyright owner. Further reproduction prohibited without permission.

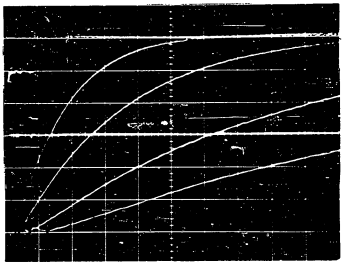

Figure 60. Reproducibility and Signal-to-Noise of Stopped-Flow

10^{-3} M $K_3Fe(NO_3)_3$ was reacted with 10^{-2} M KCNS in 0.1 N HNO_3 at room temperature (22°C). The Gilford spectrophotometer was used to monitor the absorbance at 570 nm. The total absorbance change was 0.407 (0.67 per division). There are eight traces displayed; two each at 100, 50, 20, and 10 msec per division.

Reproduced with permission of the copyright owner. Further reproduction prohibited without permission.

with KCNS. The total absorbance change is 0.407 (0.067 per division) with the two cm path. The noise is not detectable and the duplicates are indistinguishable.

(2) The dead time is determined by the cell dimensions, the flow velocity, and the efficiency of mixing. The transport time is the time required to flush the space from the first point of mixing to the middle of the observation cell (the dead volume) and can be calculated from the cell dimensions and information in the flow trace. Ideally, the transport time is identical to the dead time. In this stopped-flow instrument the dead volume is 0.037 ml so that when the flow velocity is 23 ml/sec (which is the case when 50 psi of air pressure is used to drive the syringes) the transport time is 1.6 msec. Since the cell volume is 0.036 ml there will be an uncertainty in the age of the material being observed which is equal to the time required to flow 0.018 ml or 0.8 msec at 23 ml/sec.

To determine the dead time, metmyoglobin was reacted with various concentrations of azide under pseudo first order conditions and the intersection of the curves was taken to be the true zero time of the reaction. The difference between this zero time and the time when flow stopped is a good estimate of the dead time. It can be noted that this is the same as method (b) for determining the quenching time in the rapid freezing process. The slewing rate of the Gilford optical density converter was thought to be about 1-2 msec per absorbance unit and therefore would not allow the precise determination

Reproduced with permission of the copyright owner. Further reproduction prohibited without permission.

of the dead time, which was anticipated to be 1-3 msec. Therefore a photomultiplier detector (EMI 9592) equipped with a current to voltage converter which is integral with the PMT housing (42) and having an overall time constant of 2×10^{-5} sec was substituted for the Gilford detection unit.

The results of these tests are summarized in Figures 61 and 62 where it can be seen that although both detection units are sufficient for accurately determining pseudo first order rate constants in excess of 100 sec^{-1}, only the PMT system allows the accurate determination of the dead time. From Figure 61 it can be calculated that the dead time is between one and two msec which within the time resolution of the stopped-flow instrument, is the same as the transport time and implies that mixing is not a limiting factor. The initial curvature seen in the very rapid first order plots of Figure 62 is due to the Gilford response rather than to mixing inefficiencies; the effect is similar to that caused by small inefficiencies in mixing as demonstrated in Figures 42 and 43 (Chapter 3). From Figure 62 when the change in 25% of the reaction (corresponding to 0.1 absorbance) takes 5 msec or longer, no curvature in the traces is noticeable. This implies that the response characteristics of the Gilford optical density converter is not distorting the trace. To avoid distortions in the kinetic records, a good "rule of thumb" is that the rate of optical change should be less than 0.1 OD/5 msec. Each of the curves in Figures 61 and 62 consists of at least three separate shots using

Reproduced with permission of the copyright owner. Further reproduction prohibited without permission.

Legend for Figure 61

$[Mb(Fe^{3+})\cdot H_2O]$ at 4.1×10^{-5} M was reacted with NaN_3 at the concentrations indicated in 0.1 N KNO_3, 0.02 N Tris, pH 7.8 at room temperature (22°C). The optical transmission at 550 nm (2 nm bandwidth) was measured with a photomultiplier and follower (43) using a time constant of 2×10^{-5} sec. The total absorbance change was 0.407.

N_3^- (mM)	$t_{1/2}$ (msec)	k' (sec^{-1})	$k \times 10^{-3}$ (M^{-1} sec^{-1})
5	39.7	17.45	3.49
12.5	16.3	42.5	3.40
25	8.4	82.5	3.30
50	4.65	149	3.0

Legend for Figure 62

$[Mb(Fe^{3+})\cdot H_2O]$ was reacted with NaN_3 as above, but the Gilford electronics were used to record the absorbance directly.

N_3^- (mM)	$t_{1/2}$ (msec)	k' (sec^{-1})	$k \times 10^{-3}$ (M^{-1} sec^{-1})
5	37.5	18.5	3.7
12.5	15.3	45.3	3.62
25	8.4	82.5	3.30
50	4.3	161	3.22

Reproduced with permission of the copyright owner. Further reproduction prohibited without permission.

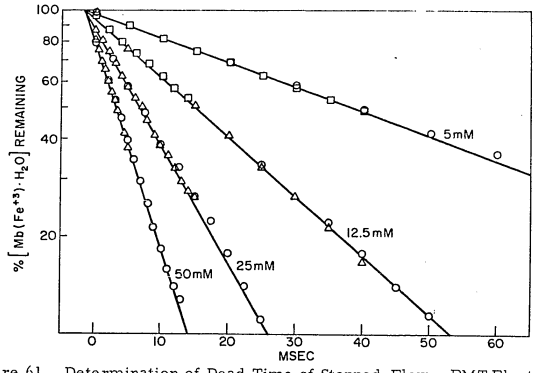

Figure 61. Determination of Dead Time of Stopped-Flow - PMT Electronics

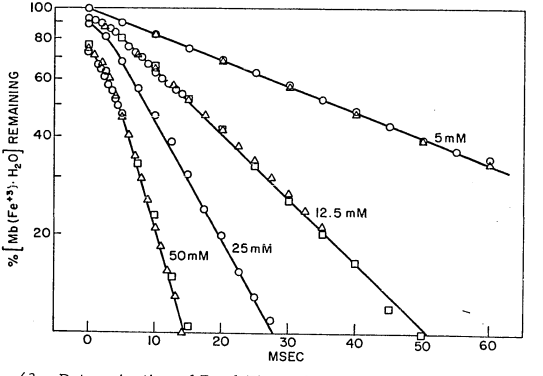

Figure 62. Determination of Dead Time of Stopped-Flow - Gilford Electronics

Reproduced with permission of the copyright owner. Further reproduction prohibited without permission.

different sweep rates to optimize the measurement of the various portions of the curves; the fact that the different traces overlap so well further demonstrates the reproducibility of the apparatus.

A further demonstration of the quality of mixing and flow is shown in Figure 63 in which the entire flow trace and the absorbance during flow are shown together. The important features to notice are that once the cell has been flushed from the old material the absorbance remains very constant during flow (which from the flow trace is also very stable) and that the trace has an abrupt change at cessation of flow. If the flow and mixing were of poor quality (i.e. imperfect mixing and/or flow which does not approximate plug flow), the absorbance during flow would not remain constant. The total volume of reagent used in this experiment was 0.13 ml per syringe and it can be seen that this could be reduced considerably since it is only necessary to shoot enough solution to reach the plateau as indicated by the arrow.

(3) The sensitivity limitations are mainly due to the residual 60 cps noise and to instability of the Gilford spectrophotometer. The 60 cps noise and the instability each amount to 0.0037 absorbance units which is quite constant from about 0-1.3 OD. Although the stability can be improved with the use of a line voltage stabilizer, the residual 60 cps noise may still be bothersome. For reactions with rate constants smaller than 20 sec^{-1}, the 60 cps noise can be averaged out by eye, but when the reaction rates are comparable

Reproduced with permission of the copyright owner. Further reproduction prohibited without permission.

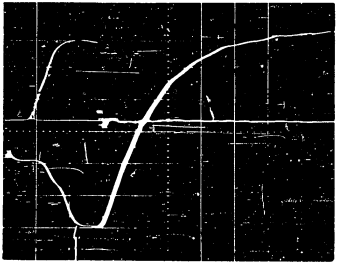

Figure 63. Demonstration of Mixing and Flow Characteristics of Stopped-Flow

2.5×10^{-4} M potassium dichromate was reacted with 0.1 M H_2O_2 in 0.05 M HNO_3 at room temperature (22°C). The reference cell had 2.5×10^{-4} M potassium dichromate. The absorbance is measured with the Gilford spectrophotometer at 580 nm with a spectral bandwidth of 4 nm. The horizontal axis is 10 msec/division and the vertical axis is 0.067 absorbance units/division. The upper trace is the flow trace measured from the motion of the stopping syringe (see text). The arrow indicates when all of the solution from the previous shot has been flushed from the cell.

Reproduced with permission of the copyright owner. Further reproduction prohibited without permission.

with the 60 cps noise (i.e. greater than 20 sec^{-1}), averaging is not possible. If the total absorbance change in the reaction (for a 2 cm path) is 0.1 or greater, good quality kinetic traces can be obtained since the noise is only about 4% of the total change.

A better idea of how the sensitivity and stability limit the determination of rate constants may be gained with the aid of examples. It can be seen from Figures 61 and 62 that pseudo first order rate constants as large as 150 sec^{-1} can be quantified. Considering that during reactions the molar absorptivity of Soret absorptions of hemoproteins often changes as much as 10^5 M^{-1} cm^{-1} (88), an absorbance change of 0.1 would correspond to 5×10^{-7} M reacted hemoprotein in the 2 cm path. If one were observing the pseudo first order change of the hemoprotein, the second reactant would have to be at least ten-fold in excess, or 5×10^{-6} M. Thus the derived second order rate constant would be 3×10^7 M^{-1} sec^{-1}. With flavoproteins there is a change in absorptivity of about 10^4 M^{-1} cm^{-1} at 450 nm in passing from the reduced to the oxidized forms so that an absorbance of 0.1 would correspond to 5×10^{-6} M of reacted material. Following the same argument as above, a second order rate of 3×10^6 M^{-1} sec^{-1} could be quantified. If one were observing reactions under second order conditions it would be possible to measure rate constants as high as 3×10^8 M^{-1} sec^{-1}. From this it is seen that the performance of this instrument is comparable to other stopped-flow instruments (15). Although given

Reproduced with permission of the copyright owner. Further reproduction prohibited without permission.

a very stable and powerful light source and a low noise electronic detection unit, it is conceivable that the sensitivity and time response of this apparatus could be improved, it is evident that the majority of stopped-flow studies would not be limited by the performance of this instrument. Certainly for the intended use - namely to provide optical studies as complementation for the rapid freezing work - further enhancement of the performance is not warranted.

(4) The requirement for using only small volumes of reagents is met since only about 0.1 ml of each reactant is necessary for each shot. It should be pointed out, however, that the minimum volume of sample for performing an experiment is considerably greater than 0.2 ml since to assure that all of the previous solution has been removed, the entire flow system must be thoroughly flushed with reagents. For many studies it has been found that about 2-3 ml must be "wasted" in order to do this operation and when anaerobiosis is required, the conditions being more stringent, 5-10 ml may be necessary depending upon what previous solutions were present. Therefore in planning experiments it is probably advisable to be prepared to use 10 to 20 ml of each reactant.

When changing wavelengths and obtaining spectra, the reference cell can be of aid in conserving reactants. With most other stopped-flow instruments the observation chamber must be flushed

Reproduced with permission of the copyright owner. Further reproduction prohibited without permission.

with buffer in order to establish a baseline. This means that the reaction solution must be completely flushed from the cell with buffer, and after establishing the baseline, the buffer must be completely flushed from the cell with reactant, thus consuming a considerable quantity of sample (and time). However, with this stopped-flow instrument it is possible to establish the baseline using the reference solution contained in the reference cell, selectively observing it by means of the shutter; thus no solution is wasted. In addition, since the operation is easy, the baseline can be checked as frequently as is necessary to correct for instrumental instabilities.

(5) The ability to maintain anaerobic conditions is documented in Chapter 5 where the studies of reduced flavin with oxygen are described. Studies were performed on samples of about 10^{-5} M which require the oxygen to be less than 10^{-6} M in order to obtain meaningful results.

Reproduced with permission of the copyright owner. Further reproduction prohibited without permission.

CHAPTER 5

THE USE OF COMBINED STOPPED-FLOW AND RAPID FREEZING INSTRUMENTATION IN THE STUDY OF THE MECHANISM OF THE OXIDATION OF FLAVINS AND FLAVOPROTEINS BY OXYGEN

One of the outstanding problems in the study of flavoprotein catalysis is the reactivity of reduced flavins and flavoproteins with molecular oxygen. Gibson and Hastings (89) have shown that the reaction of oxygen with free flavins proceeds moderately fast, but the kinetics are quite complicated, showing autocatalytic behavior. In the reduced forms of the flavoprotein dehydrogenases the reactivity with oxygen is usually less and never much more than that of the free flavins while the oxidases have a very high reactivity with oxygen. In both of these classes the products of the reactions are the oxidized flavins and peroxide. With yet another class of flavoproteins (the hydroxylases) one atom of oxygen is converted to H_2O and the other is used to hydroxylate specific substrates.

Massey et al. (90) suggested (with reference to Figure 64) that the reduced flavin moiety, I, was attacked by oxygen to produce one of the two oxygen adducts, II or III. Reactions at carbons 1a and 4a are documented (91, 92) and the proposal of a reduced flavin-oxygen compound (II) is also consistent with the kinetic data of the oxidation of $FMNH_2$ and $FADH_2$ obtained by Gutfreund (93) and Gibson and Hastings (89). Hydrogen peroxide could be eliminated from this oxygen adduct (Figure 65) directly as in pathway 1 to yield

Reproduced with permission of the copyright owner. Further reproduction prohibited without permission.

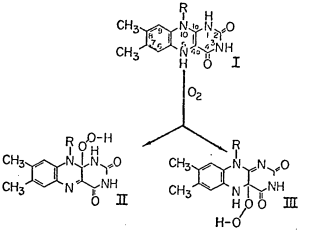

Figure 64. Reaction Scheme for Reduced Flavin with Oxygen

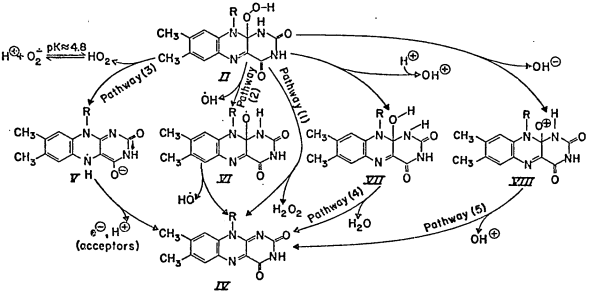

Figure 65. Reaction Scheme for Breakdown of Reduced Flavin-Oxygen Complex

Reproduced with permission of the copyright owner. Further reproduction prohibited without permission.

the flavoquinone IV, or in two steps in the form of two hydroxyl radicals as shown in pathway 2. Alternatively the perhydroxyl radical HO_2 could be eliminated to yield the semiquinone, V, which could either undergo dismutation or reaction with a second electron acceptor as shown in pathway 3. The equivalent of a single oxygen atom (perhaps as the oxonium ion, HO^+) could be eliminated followed by a dehydration as in pathway 4, or dehydration and then elimination of the equivalent of an oxygen atom could occur as in pathway 5. An analogous series could possibly result from reactions of the adduct, III. The pathway by which oxidation occurred was thought to be determined according to the influence of the specific proteins. For example, the oxidases may react preferentially by pathway 1 to yield H_2O_2 and flavoquinone directly. Support for this comes from the fact that in rapid spectroscopic studies no semiquinone intermediates are seen in the reoxidation from the fully reduced state. The hydroxylases may react via pathway 2, 3, or 4, the hydroxylation occurring by reaction with $\dot{O}H$, the oxygen containing flavin compound VI, HO_2, or OH^+. The flavoprotein dehydrogenases may react preferentially by pathway 3 to yield HO_2 which in the pH range generally employed, quickly loses its proton to yield O_2^-, known as superoxide.

A diagnostic test for the superoxide intermediate which was postulated (Figure 65) to occur with the reduced flavoprotein dehydrogenases became feasible with the discovery by McCord and Fridovich

Reproduced with permission of the copyright owner. Further reproduction prohibited without permission.

(94, 95) that erythrocuprein is an efficient superoxide dismutase (SD). These workers found that oxidized cytochrome c was readily reduced by O_2^- but that this reaction was completely inhibited by low concentrations of erythrocuprein (SD). Thus, for example, they observed that SD inhibited the aerobic reduction of cytochrome c which is effected by xanthine oxidase during its turnover. They reasoned from this result that the actual reduction of cytochrome c was by the superoxide species generated in the oxygen reaction with xanthine oxidase. Proof for this was the direct demonstration of Knowles et al. (71), by means of the rapid freezing EPR technique, that O_2^- is indeed a product of the oxidation of substrate reduced xanthine oxidase by oxygen. Both of these groups postulated that the superoxide generation occurred at one of the non-heme iron sites of xanthine oxidase.

In an effort to obtain evidence that it is the flavin moiety of xanthine oxidase which evolves the O_2^- as proposed in Figure 65 (90) rather than the non-heme iron sites, Massey et al. (96) applied the SD diagnostic test for O_2^- to a large number of flavoproteins and to free flavin. They found that free flavin, flavoprotein dehydrogenases, and xanthine oxidase all catalyze the aerobic reduction of cytochrome c, and that this reduction was inhibited by SD. The aerobic reduction of cytochrome c by a deflavo-xanthine oxidase, however, was not inhibited by SD, nor was the reduction by any of the oxidases or hydroxylases. This is a strong argument

Reproduced with permission of the copyright owner. Further reproduction prohibited without permission.

that it is the flavin moiety in xanthine oxidase which evolves the O_2^- and that the flavoprotein dehydrogenases and free flavins do react with oxygen to yield O_2^- as proposed earlier (90).

Therefore we decided to investigate the oxidation of reduced free flavins to determine: (1) if superoxide was produced in appreciable quantities, and (2) if the superoxide evolved could account for the reaction's autocatalytic behavior. The combined useage of rapid freezing and stopped-flow methods is ideally suited to this type of study.

Using the rapid freezing technique, we found (97) that substantial quantities of O_2^- (Figures 66 and 67) were produced in the reaction of oxygen with reduced tetraacetyl riboflavin ($TARFH_2$) and reduced flavin mononucleotide ($FMNH_2$). In order to show that the observed radicals were O_2^-, we reacted KIO_4 with H_2O_2 (Fig. 66) and dithionite with oxygen under the same conditions and obtained similar spectra to those obtained from the reaction of $TARFH_2$ and oxygen. Knowles et al. (71) have also shown that these reactions produced the same radical as xanthine oxidase. The g values of the radical we observed agreed with those found for the O_2^- radical by Bennet et al. (98) and Ichikawa et al. (99) who report the values: $g_{11} = 2.088$ and $g_{\perp} = 2.008$. In an elegant experiment Bray, Pick, and Samuel (100) showed by the hyperfine splitting patterns observed when the isotope, O_2^{17}, was employed in the xanthine oxidase reaction, that the observed radical is unquestionably O_2^-. We also

Reproduced with permission of the copyright owner. Further reproduction prohibited without permission.

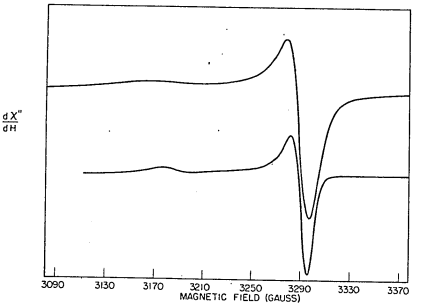

Figure 66. EPR Spectrum of O_2^-

(Top) Radical produced by the reaction of 0.075 M KIO_4 with 0.15 M H_2O_2 in 0.1 M glycine buffer pH 9.9 at 20°C for 545 msec. EPR spectrum recorded at 87°K. (Bottom) Radical produced by reaction of 1.25×10^{-4} M $TARFH_2$ with 6.25×10^{-4} M oxygen in 0.095 M glycine pH 10.6 at 20°C for 444 msec. EPR spectrum recorded at 92°K. Microwave power, 3 mwatts; modulation amplitude, 3 gauss at 100 kHz. Microwave frequency 9.235 GHz.

Reproduced with permission of the copyright owner. Further reproduction prohibited without permission.

Legend to Figure 67

Buffers used were 0.1 M glycine at pH 10.6 and 9.6 and 0.1 M glycylglycine at pH 8.4. TARF was made anaerobic in a tonometer, reduced by irradiation with visible light (by the reaction of the triplet flavin with EDTA), and this solution was transferred anaerobically to the rapid freezing apparatus. The $TARFH_2$ solution was mixed with oxygen equilibrated buffer at $20^{\circ}C$ to produce a reaction mixture 1.25×10^{-4} M in flavin and 6.3×10^{-4} M in O_2. The reacting solutions were quenched by rapid freezing at the indicated times and then analyzed by EPR for the O_2^- signal. The derivative signals were quantitated by double integration and comparison with $CuSO_4$-EDTA solutions which were measured under the same condition. Modulation amplitude was 10 gauss at 10 kHz. Microwave power = 12 mwatts. Microwave frequency = 9.2 GHz. Temperature = $83^{\circ}K$.

Reproduced with permission of the copyright owner. Further reproduction prohibited without permission.

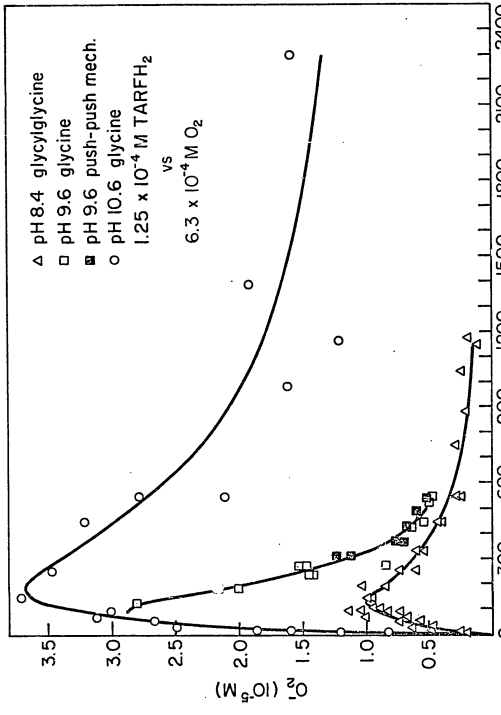

Figure 67. Production of Superoxide in the Reaction of $TARFH_2$ with Molecular Oxygen

Reproduced with permission of the copyright owner. Further reproduction prohibited without permission.

found (Figure 67) in the reactions of $TARFH_2$ and $FMNH_2$ with oxygen that superoxide was continually being formed during the oxidation reaction and then decayed in a second order reaction and that the yields were greater at higher pH, showing a yield of 30% of the reduced flavin employed in the experiment at pH 10.6. This is consistent with the fact that the dismutation of O_2^- is pH dependent (101, 102), being considerably faster at pH 8.3 than at 10.6 (Fig. 67).

The experiment at pH 9.6 was performed using both the regular and the push-push arrangement and it can be noticed that the results from the two methods overlap. This provides further verification that plug flow is nearly accomplished (see Chapter 3).

The third observation (Figure 68) was the direct demonstration that O_2^- is very reactive towards cytochrome c and that O_2^- is rapidly destroyed by very small amounts of erythrocuprein (SD). These experiments were performed using the three syringe technique (Chapter 3 - Discussion) which produced the radical by the reaction at pH 8.4 of $TARFH_2$ and O_2 contained in the first two syringes, and after a delay of 181 msec, introduced SD or cytochrome c via the third syringe. By varying the dead volume from the second mixing chamber to the exit nozzles, a kinetic curve of the reaction catalyzed by SD or with cytochrome c could be obtained. Stopped-flow studies (Figure 69) showed that more than 98% of the flavin had been oxidized at 181 msec when the third reagent was introduced and thus further reaction with reduced flavin could be neglected. The decay

Reproduced with permission of the copyright owner. Further reproduction prohibited without permission.

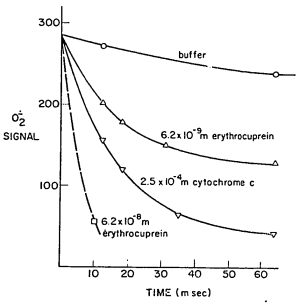

Figure 68. Reaction of O_2^- with Erythrocuprein and Cytochrome c

O_2^- was produced by the reaction of 1.25×10^{-4} M $TARFH_2$ with 6.5×10^{-4} M O_2 in 0.1 M glycylglycine pH 8.4 at 20°C for 181 msec, before reaction from a third syringe with erythrocuprein, cytochrome c, or buffer as shown. The reaction times shown are those from 181 msec and include the 5 msec quenching time. Modulation amplitude 10 gauss at 100 kHz. Microwave power = 12 mwatts. Microwave frequency 9.2 GHz. Temperature = 84°K.

Reproduced with permission of the copyright owner. Further reproduction prohibited without permission.

Legend to Figure 69

TARF, at a concentration of 1.25×10^{-4} M in 0.1 M pyrophosphate pH 8.4 and 10^{-3} M EDTA, was made anaerobic in the dark in a tonometer, placed under a slight positive pressure of N_2 and then reduced by irradiation with visible light. This solution was transferred to the stopped-flow apparatus: The experiment marked (·) is the reaction of the above with air equilibrated buffer. The experiment marked (⊕) is the reaction of the above with air equilibrated buffer containing 2×10^{-7} M SD. The experiment marked (o) is the reaction of the above with air equilibrated buffer containing 1.25×10^{-4} M TARF and 2×10^{-7} M SD.

Reproduced with permission of the copyright owner. Further reproduction prohibited without permission.

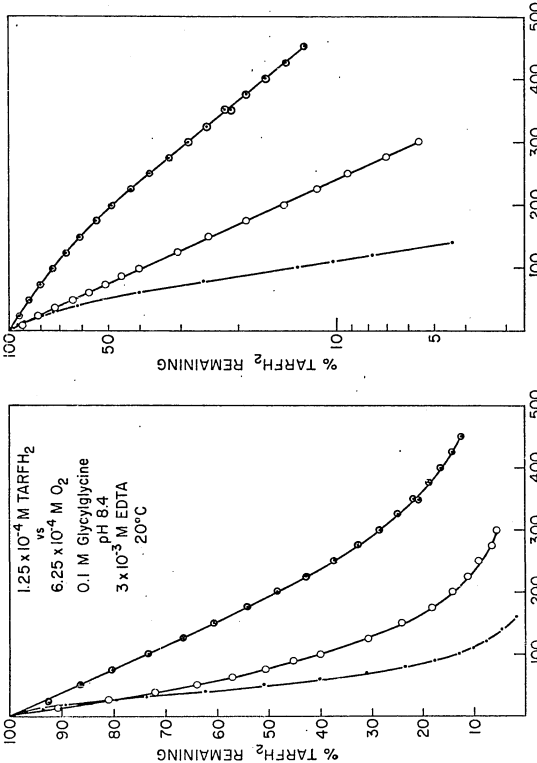

Figure 69. Stopped-Flow Studies of the Reaction of $TARFH_2$ with O_2

Reproduced with permission of the copyright owner. Further reproduction prohibited without permission.

of the superoxide signal in the presence of SD followed second order kinetics which implied that at this concentration of O_2^- the SD is not saturated with substrate; therefore maximum turnover numbers could not be obtained. A lower limit of the turnover number for the superoxide dismutase activity can be estimated to be at least 10^6 moles O_2^- min^{-1} mole SD^{-1}. The fact that at concentrations greater than 6.2×10^{-7} M SD, no O_2^- could be detected after 12 msec (this includes the quenching time) gives some idea of the extreme efficiency of this enzyme.

From the limited studies of the reaction of cytochrome c with O_2^- (Figure 68), a pseudo first order rate constant of 40 sec^{-1} was obtained. Since the cytochrome c was 2.5×10^{-4} M, this corresponds to a second order rate constant of $1.6 \pm 0.5 \times 10^5$ M^{-1} sec^{-1}. If the reaction is simple, it should have strict pseudo first order kinetics, but the data seem to fit second order better than first order plots. Although this limited investigation (Figure 68) does not permit absolute distinction between first and second order behavior, this point deserves further study.

The fact that O_2^- was observed as a product of this reaction of reduced flavin and oxygen in such yields was quite surprizing in view of the literature values for the redox potentials (E'_o) of the $O_2:O_2^-$ couple of approximately -0.59 volts (103) and of the relatively positive values of the midpoint potentials for reduced flavins which Draper (104) has determined to be -0.365 and -0.29 volts for

Reproduced with permission of the copyright owner. Further reproduction prohibited without permission.

FMN $\longrightarrow$ FMNH· and FMNH· $\longrightarrow$ $FMNH_2$ respectively at pH 10.6. Thus either there is some unknown mechanism for the stabilization of the O_2^- radical produced or as suggested by Mason (105), the value E'_o may be higher than -0.3 volts, which would be more consistent with the above experiments.

To test whether the superoxide produced in the reaction could account for the autocatalytic nature of the reaction of reduced flavins with oxygen, stopped-flow studies comparing the reaction rates in the presence and in the absence of SD were done. This is shown in Fig. 69 for the oxygen reaction with $TARFH_2$ at pH 8.4. The effect is quite dramatic, but it can be seen that the reaction still has autocatalytic character. Gibson and Hastings (89) found that the presence of oxidized flavin increased the rate of the reaction suggesting that the flavin semiquinone formed by reaction 27. was very reactive with oxygen and thus accounted for part of the behavior.

27. FMN + $FMNH_2 \rightleftharpoons$ 2 FMNH·

Testing this hypothesis it is seen (Figure 69) that in the presence of both SD and TARF nearly all of the autocatalytic behavior is abolished. Recently Vaish and Tollin (106) using flash photolysis have shown that the rate constant for reaction 28. is about $3 \times 10^8\ M^{-1}\ sec^{-1}$ under the conditions we employed.

28. FH· + $O_2 \longrightarrow O_2^-$ + F

Reproduced with permission of the copyright owner. Further reproduction prohibited without permission.

This only applied for the anionic flavin radical since they have calculated that an upper limit for the reaction of oxygen with the neutral radical is 4×10^4 M^{-1} sec^{-1}. Since the rate constant is so high for the anionic flavin radical, even a small amount of flavin semiquinone would contribute considerably to the rate of the reaction. Thus in the experiment in which oxygen and $TARFH_2$ were reacted, the product, TARF, could combine with $TARFH_2$ to produce 2 molecules of FH· which could then react with O_2 (and O_2^-) to contribute to the rate and thus account for the autocatalysis. Since O_2^- is a very likely product of the reaction as shown in equation 28., it is conceivable that it could react with the semiquinone. If this reaction were very fast it could account for as much as half of the total rate and thus the rate constant reported by Vaish and Tollin (106) could, in the extreme case, be overestimated by a factor of two. To account for the above observations the following scheme of reactions has been proposed.

29. $$FH_2 + O_2 \underset{k_{-1}}{\overset{k_1}{\rightleftarrows}} FH_2O_2$$

30. $$FH_2O_2 \xrightarrow{k_2} FH\cdot + O_2^- + H^+$$

31. $$2\ FH\cdot \underset{k'_{-3}}{\overset{k'_3}{\rightleftarrows}} FH_2 \leftrightarrow F \underset{k''_{-3}}{\overset{k''_3}{\rightleftarrows}} F + FH_2$$

32. $$FH\cdot + O_2 \xrightarrow{k_4} F + O_2^- + H^+$$

Reproduced with permission of the copyright owner. Further reproduction prohibited without permission.

33. $FH\cdot + O_2^- + H^+ \xrightarrow{k_5} F + H_2O_2$

34. $FH_2 + O_2^- + H^+ \xrightarrow{k_6} FH\cdot + H_2O_2$

35. $2\ O_2^- + 2\ H^+ \xrightarrow{k_7} O_2 + H_2O_2$

The evidence for reaction 29. is that: (a) a spectral intermediate can be detected which is formed rapidly and (b) plots of k_{app}^{-1} versus $[O_2]^{-1}$ intersect the ordinate at a point greater than zero (107). The evidence for reaction 30. is the rapid freezing result that substantial amounts of superoxide are formed. The rapid equilibrium of 31. is well known (106, 108, 109) with $k'_3k''_3 \approx 10^9\ M^{-1}\ sec^{-1}$ and $k'_{-3}k''_{-3} \approx\approx 5 \times 10^5\ M^{-1}\ sec^{-1}$. Evidence for 32. (106) has already been mentioned. The fact that SD decreases the rate so markedly (Figure 69) implies that at least one reaction involving O_2^- is involved and there is a distinct possibility that more complicated behavior is present. For example, the coupling of reactions 32. and 34. or other similar combinations of reactions, allows FH· and O_2^- to act catalytically converting FH_2 and O_2 to F and peroxide. This may well explain how the rate can be diminished as much as four-fold in the presence of SD (Figure 69). Without such an hypothesis the reaction as explained by steps 29., 30., 31., and 34. would have a rate only two-fold less than in the presence of SD. Thus it appears that the major route of oxidation by oxygen is through reactions involving superoxide.

Reproduced with permission of the copyright owner. Further reproduction prohibited without permission.

Work on this system is far from complete and computer simulations which are in progress can not yet be applied. However, these studies are testimony as to how rapid freezing-EPR and stopped-flow optical studies can be extremely complimentary in the elucidation of pathways of complex reactions.

I would like to mention a further connected study in which apparently anomalous results which were obtained by the rapid freezing method were qualitatively resolved by correlative studies by the stopped-flow method (work is not yet complete so that quantitation is not realized).

The studies above were undertaken with the hope of resolving some of the complexities in the oxygen reactions of reduced flavins. However, reactions such as 31. as well as the occurrence of three possible ionization states for each of the flavin species, leads to a myriad of possible reactions which are difficult to analyze. In an attempt to simplify this situation we thought that the flavoprotein dehydrogenase, flavodoxin (75), would react simply with O_2 yielding semiquinone and O_2^- quantitatively, since the reactions of flavodoxin semiquinone with O_2 is very slow, taking several minutes to reach completion, and the reaction which is equivalent to reaction 31. above is essentially nonexistent. Rapid freezing studies were performed with the surprising result that very little O_2^- was observed and only about 75% of the semiquinone was evident. Studies of the frozen samples varying modulation amplitude and microwave power

Reproduced with permission of the copyright owner. Further reproduction prohibited without permission.

showed that the flavin radical formed behaved somewhat differently than the radical produced in the presence of SD or by stoichiometric titration with dithionite, and thus the samples may have had some O_2^- hidden under the flavin radical signal or else some kind of radical-radical interaction was taking place.

Stopped-flow studies were then performed which greatly clarified the above results. Figures 70 and 71 show the results obtained without and with SD while monitoring the reaction at 580 nm which allows direct determination of the semiquinone. The points to notice are: (a) the rate of the reaction in the absence of SD is considerably faster than in the presence of SD and is apparently autocatalytic, (b) in the absence there is a second phase of the reaction in which semiquinone is consumed and which is abolished by SD. A spectrum computed from the stopped-flow traces at 100 msec after initiation of the reaction, indicated that there were no species other than the reduced and semiquinone forms of flavodoxin.

Although these are merely preliminary studies, they do give evidence for the following mechanism which qualitatively accounts for the results seen by rapid freezing and by stopped-flow.

36. $FH_2 + O_2 \xrightarrow{\text{fast}} FH\cdot + O_2^-$

37. $FH_2 + O_2^- \xrightarrow{\text{fast}} FH\cdot + \text{peroxide}$

Reproduced with permission of the copyright owner. Further reproduction prohibited without permission.

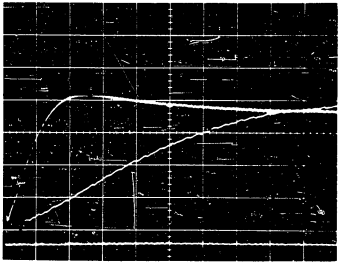

Figure 70. Reaction of Reduced Flavodoxin with Oxygen.

1.25×10^{-4} M reduced flavodoxin was reacted with air equilibrated buffer in the stopped-flow instrument. Time scales are 100 and 20 msec per division. The vertical scale is 0.043 absorbance per division.

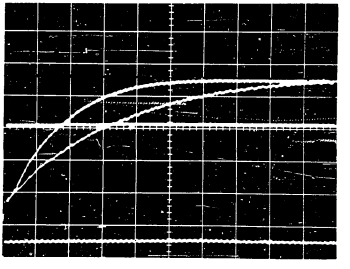

Figure 71. Reaction of Reduced Flavodoxin with Oxygen in the Presence of Superoxide Dismutase.

Conditions are the same as above, but 7.4×10^{-7} M SD is included in the buffer syringe. Time scales are 100 and 50 msec per division.

Reproduced with permission of the copyright owner. Further reproduction prohibited without permission.

38. $FH\cdot + O_2^- \xrightarrow{\text{moderate}} F + \text{peroxide}$

39. $FH\cdot + O_2 \xrightarrow{\text{slow}} F + O_2^-$

There is additional evidence for reactions 38. and 39. since Mayhew (110) has found that the slow reoxidation of the flavodoxin semiquinone by oxygen is inhibited by the presence of SD. Reactions 36. and 37. could account for the initial autocatalytic oxidation as shown in Figure 70 while the disappearance of semiquinone could be a result of reaction 38. In the presence of SD reactions 37. and 38. do not occur so that the formation of semiquinone proceeds by 36. alone. It can be noted from Figure 70 that the reaction is autocatalytic whereas in Figure 71 the reaction is apparently pseudo first order and slower, which is predicted by the proposed mechanism.

It should be pointed out that although these are only preliminary studies, nevertheless, the combination of these two techniques has provided a powerful means of investigating many features of these rather complex reactions. More detailed and quantitative work using these as well as other techniques will undoubtedly be useful in the eventual understanding of these reactions.

Reproduced with permission of the copyright owner. Further reproduction prohibited without permission.

REFERENCES

1. Hartridge, H. and Roughton, F. J. W., Proc. Roy. Soc. (London), A104, 376 (1923).
2. Hartridge, H., Proc. Roy. Soc. (London), A102, 575 (1923).
3. Hartridge, H. and Roughton, F. J. W., Proc. Roy. Soc. (London), A104, 395 (1923).
4. Hartridge, H. and Roughton, F. J. W., Proc. Cambridge Phil. Soc., 23, 450 (1926).
5. Brinkman, R., Margaria, R., and Roughton, F. J. W., Trans. Roy. Soc. London, A232, 65 (1933).
6. Roughton, F. J. W., Proc. Roy. Soc. (London), B115, 473 (1934).
7. Roughton, F. J. W. and Millikan, G. A., Proc. Roy. Soc. (London), A155, 258 (1936).
8. Millikan, G. A., Proc. Roy. Soc. (London), A155, 277 (1936).
9. Chance, B., J. Franklin Inst., 229, 455, 613, 737 (1940).
10. Gibson, Q. H., Disc. Faraday Soc., 17, 137 (1954).
11. Gibson, Q. H. and Milnes, L., Biochem. J., 91, 161 (1964).
12. Caldin, E. F., Fast Reactions in Solution, John Wiley & Sons, Inc., New York, 1964.
13. Roughton, F. J. W. and Chance, B., in A. Weissberger, E. S. Lewis, and S. L. Friess (Editors), Techniques in Organic Chemistry, Vol. 8, Part II, Wiley (Interscience), New York, 1963, p. 704.

Reproduced with permission of the copyright owner. Further reproduction prohibited without permission.

14. Gibson, Q. H., Ann. Rev. Biochem., 35, 435 (1966).

15. Gibson, Q. H., in K. Kustin (Editor), Methods in Enzymology, Vol. XVI, Academic Press, New York, 1969, p. 187.

16. Gutfreund, H., in K. Kustin (Editor), Methods in Enzymology, Vol. XVI, Academic Press, New York, 1969, p. 229.

17. Chance, B., Eisenhardt, R. H., Gibson, Q. H., and Lonberg-Holm, K. K. (Editors), Rapid Mixing and Sampling Techniques in Biochemistry, Academic Press, New York, 1964.

18. Bray, R. C., Biochem. J., 81, 189 (1961).

19. Bray, R. C. and Pettersson, R., Biochem. J., 81, 194 (1961).

20. Bray, R. C., in B. Chance, R. H. Eisenhardt, Gibson, Q. H., and Lonberg-Holm, K. K. (Editors), Rapid Mixing and Sampling Techniques in Biochemistry, Academic Press, New York, 1964, p. 195.

21. Dalziel, K., Biochem. J., 55, 79 (1953).

22. Bray, R. C., Biochem. J., 81, 196 (1961).

23. Bray, R. C., Palmer, G., and Beinert, H., J. Biol. Chem., 239, 2667 (1964).

24. Palmer, G., Bray, R. C., and Beinert H., J. Biol. Chem., 239, 2657 (1964).

25. Palmer, G. and Beinert, H., in B. Chance, R. H. Eisenhardt, Q. H. Gibson, and K. K. Lonberg-Holm (Editors), Rapid Mixing and Sampling Techniques in Biochemistry, Academic Press, New York, 1964, p.

Reproduced with permission of the copyright owner. Further reproduction prohibited without permission.

26. Palmer, G. and Beinert, H., Anal. Biochem., 8, 95 (1964).

27. Iizuka, T. and Kotani, M., Biochim. Biophys. Acta, 181, 275 (1969).

28. Iizuka, T. and Kotani, M., Biochim. Biophys. Acta, 194, 351 (1969).

29. Goldsack, D. E., Eberlein, W. S., and Alberty, R. A., J. Biol. Chem., 240, 4312 (1965).

30. Duffey, D., Chance, B., and Czerlinski, G., Biochem., 5, 3514 (1966).

31. Salmeen, I. T. and Palmer, G., J. Chem. Phys., 48, 2049 (1968).

32. Hansen, R. E. and Beinert, H., Anal. Chem., 38, 484 (1966).

33. Silicon Controlled Rectifier Manual, 4th Edition, General Electric Co., Syracuse, New York, 1967, p. 213.

34. Mayhew, S. G., personal communication.

35. Hansen, R., Kalal, J., and Beinert, H., Anal. Biochem., 20, 10 (1967).

36. Olson, R. M., Essentials of Engineering Fluid Mechanics, 2nd Edition, International Textbook Co., Scranton, Pa., 1966, p. 222.

37. Tanford, C., Physical Chemistry of Macromolecules, J. Wiley & Sons, Inc., New York, 1961, p. 390.

38. Lange, N. A. (Editor), Handbook of Chemistry, 9th Edition, Handbook Publishers, Inc., Sandusky, Ohio, 1956, p. 1669.

Reproduced with permission of the copyright owner. Further reproduction prohibited without permission.

39. Berger, R. L., Balko, B., and Chapman, H., Rev. Sci. Inst., 39, 493 (1968).

40. Trowse, F. W., Ph. D. Dissertation, Leeds, 1952.

41. Dubois, D., J. Biol. Chem., 137, 123 (1941).

42. Holmes, L. P., Silzars, A., Cole, D. L., Rich, L. D., and Eyring, E. M., J. Phys. Chem., 73, 737 (1969).

43. Becvar, J., Ballou, D., and Palmer, G. (in preparation).

44. Vassilatos, G. and Toor, H. L., A. I. Ch. E. J., 11, 666 (1965).

45. Chance, B., in B. Chance, R. H. Eisenhardt, Q. H. Gibson, and K. K. Lonberg-Holm, Rapid Mixing and Sampling Techniques in Biochemistry, Academic Press, New York, 1964, p. 125.

46. Li, Wen-Hsuing and Lam, Sau-Hai, Principles of Fluid Mechanics, Addison-Wesley Publishing Co., Inc., Reading, Mass., 1964.

47. Horn, F. J. M. and Parish, J. D., Chem. Eng. Sci., 22, 1549 (1967).

48. Taylor, G., Proc. Roy. Soc. (London), A219, 186 (1953).

49. Frost, A. A. and Pearson, R. G., Kinetics and Mechanism, 2nd Edition, John Wiley & Sons, Inc., New York, 1961, p. 161.

50. Taylor, G., Proc. Roy. Soc. (London), A223, 446 (1954).

51. Gibson, Q., in J. A. Butler and B. Katz (Editors), Progress in Biophysics and Biophysical Chemistry, Vol. 9, Permagon Press Book, Macmillan Co., New York, 1959, p. 2.

Reproduced with permission of the copyright owner. Further reproduction prohibited without permission.

52. Antonini, E., Physiol. Rev., 45, 120 (1965).

53. Antonini, E., Brunori, M., and Wyman, J., Biochem., 4, 545 (1965).

54. Smith, D. W. and Williams, R. J. P., in C. K. Jorgensen, J. B. Neilands, R. S. Nyholm, D. Reiner, and R. J. P. Williams (Editors), Structure and Bonding, Vol. 5, Springer - Verlag, New York, 1969, p. 2.

55. Yonetani, T. and Schleyler, H., J. Biol. Chem., 242, 3926 (1967).

56. Smith, D. W. and Williams, R. J. P., Biochem. J., 110, 297 (1968).

57. Czerlinski, G., in B. Chance, R. W. Estabrook, T. Yonetani (Editors), Hemes and Hemoproteins, Academic Press, New York, 1966, p. 195.

58. Diven, W. F., Goldsack, D. E., and Alberty, R. A., J. Biol. Chem., 240, 2437 (1965).

59. Goldsack, D. E., Eberlein, W. S., and Alberty, R. A., J. Biol. Chem., 241, 2653 (1966).

60. Temperature Conversion Tables, Boehringer Mannheim Corp., New York.

61. Beetlestone, J. and George, P., Biochem., 3, 707 (1964).

62. Beinert, H., Hansen, R., and Orme-Johnson, W. H., personal communication.

Reproduced with permission of the copyright owner. Further reproduction prohibited without permission.

63. Berkhoff, G. and Zarantonello, E. H., Jets, Wakes, and Cavaties, Academic Press, Inc., New York, 1957, p. 257.

64. Sterbacek, Z. and Tausk, P., Mixing in the Chemical Industry, translated by K. Mayer, Permagon Press, Oxford, 1965.

65. Orme-Johnson, W. H. and Hansen, R., personal communication.

66. Bray, R. C., Knowles, P. F., and Meriwether, L. S., in A. Ehrenberg, B. G. Malstrom, and T. Vanngard (Editors), Magnetic Resonance in Biological Systems, Permagon Press, 1967, p. 249.

67. Rajagopolan, K. V., Handler, P., Palmer, G., and Beinert, H., J. Biol. Chem., 243, 3797 (1968).

68. Beinert, H., Palmer, G., Cremona, T., and Singer, T. P., J. Biol. Chem., 240, 675 (1965).

69. Beinert, H. and Palmer, G., J. Biol. Chem., 239, 1221 (1964).

70. Aleman, V., Handler, P., Palmer, G., and Beinert, H., J. Biol. Chem., 243, 2569 (1968).

71. Knowles, P. F., Gibson, J. F. ···k, F. M., and Bray, R. C., Biochem. J., 111, 53

72. Poole, C. P., Electron Spin R··· ···e, A Comprehensive Treatise on Experimental Techniques, Interscience Publishers, New York, 1967.

Reproduced with permission of the copyright owner. Further reproduction prohibited without permission.

73. Alger, R. S., Electron Paramagnetic Resonance: Techniques and Applications, Interscience Publishers, New York, 1968.

74. Beinert, H. and Palmer, G., in F. F. Nord (Editor), Advances in Enzymology, Vol. 27, Interscience Publishers, New York, 1965, p. 105.

75. Mayhew, S. G. and Massey, V., J. Biol. Chem., 244, 794 (1969).

76. Beinert, H. and Hansen, R., personal communication.

77. Glasstone, S., Textbook of Physical Chemistry, D. Van Nostrand Co., Inc., New York, 1940, p. 695.

78. Grundfest, H., Young, J. P., and Johnson, N. L., J. Applied Phys., 35, 18 (1964).

79. Gerrard, J. E., Steidler, F. E., and Appeldrom, J. K., Ind. Eng. Ch. Fund., 5, 260 (1966).

80. Beinert, H., in E. C. Slater (Editor), Flavins and Flavoproteins, Elsevier Publishing Co., Amsterdam, 1966, p. 49.

81. Berger, R. L. and Stoddart, L. C., Rev. Sci. Inst., 36, 78 (1965).

82. Davies, P. W., in W. L. Nostuk (Editor), Physical Techniques in Biological Research, Vol. IV, Academic Press, New York, 1962, p. 137.

83. Roughton, F. J. W., Proc. Roy. Soc. (London), A126, 439, 470 (1930).

84. Bulletin PB-1, Warner & Swasey Co., Flushing, New York.

Reproduced with permission of the copyright owner. Further reproduction prohibited without permission.

85. Lowry, O. H., J. Biol. Chem., 236, 2746 (1961).

86. Lynn, R. W., Gibson, Q. H., and Hanacek, J., Rev. Sci. Inst., 42, 356 (1971).

87. Strittmatter, P., in B. Chance, R. H. Eisenhardt, Q. H. Gibson, and K. K. Lonberg-Holm (Editors), Rapid Mixing and Sampling Techniques in Biochemistry, Academic Press, New York, 1964, p. 71

88. Gibson, Q. H. and Antonini, F., Biochem. J., 77, 328 (1960).

89. Gibson, Q. H. and Hastings, J. W., Biochem. J., 83, 346 (1962).

90. Massey, V., Müller, F., Feldberg, R., Schuman, M., Sullivan, P. A., Howell, L. G., Mayhew, S. G., Matthews, R., and Foust, G., J. Biol. Chem., 244, 3999 (1969).

91. Muller, F., in H. Kamin (Editor), Third International Symposium on Flavins and Flavoproteins, (in press).

92. Mager, H. I. X. and Berends, W., Biochim. Biophys. Acta, 118, 440 (1966).

93. Gutfreund, H., Biochem. J., 74, 17P (1960).

94. McCord, J. M. and Fridovich, I., Federation Proc., 28, 346 (1969).

95. McCord, J. M. and Fridovich, I., J. Biol. Chem., 244, 6049 (1969).

Reproduced with permission of the copyright owner. Further reproduction prohibited without permission.

96. Massey, V., Strickland, S., Mayhew, S. G., Howell, L. G., Engel, P. C., Matthews, R. G., Schuman, M., and Sullivan, P. A., Biochem. Biophys. Res. Comm., 36, 891 (1969).

97. Ballou, D., Palmer, G., and Massey, V., Biochem. Biophys. Res. Comm., 36, 898 (1969).

98. Bennet, J. E., Mile, B., and Thomas, A., Trans. Faraday Soc., 64, 3200 (1968).

99. Ichikawa, T., Iwasaki, M., and Kuwata, K., J. Chem. Phys., 44, 2979 (1966).

100. Bray, R. C., Pick, F. M., and Samuel, D., Eur. J. Biochem., 15, 352 (1970).

101. Rabani, J. and Nielsen, S. O., J. Phys. Chem., 73, 3736 (1969).

102. Bechar, D., Czapski, G., Rabani, J., Dorfman, L. M., and Schwarz, H. A., J. Phys. Chem., 74, 3209 (1970).

103. Sutin, N., in J. E. King, H. S. Mason, and M. Morrison (Editors), Oxidases and Related Redox Systems, John Wiley and Sons, New York, 1965, p. 34.

104. Draper, R. D., Ph. D. Thesis, University of California, Davis, 1964. №65-2917, Univ. Microfilms, Ann Arbor, Mich.

105. Mason, H. S., Ann. Rev. Biochem., 34, 595 (1965).

106. Vaish, S. P. and Tollin, G., Bioenergetics, 2, 33 (1971).

Reproduced with permission of the copyright owner. Further reproduction prohibited without permission.

107. Massey, V., Palmer, G., and Ballou, D., in H. Kamin (Editor), Third International Symposium on Flavins and Flavoproteins, (in press).

108. Gibson, Q. H., Massey, V., and Atherton, N. M., Biochem. J., 85, 369 (1962).

109. Holmström, B., Acta Physica Polonica, 26, 419 (1964).

110. Mayhew, S. G., personal communication.

Reproduced with permission of the copyright owner. Further reproduction prohibited without permission.

Appendix 1

Treatment of Kinetic Data

To determine the most reliable values when calculating rate constants from kinetic data which are not very precise, such as those obtained by the rapid freezing method, it is customary to use the least squares analysis. For first and second order reactions the following equations can be used (49):

First Order

$A \xrightarrow{k}$ Product $\qquad \ln A = -kt + \ln A_o$

Type I Second Order

$A + A \xrightarrow{k}$ Product $\qquad \frac{1}{A} = kt + \frac{1}{A_o}$

Type II Second Order

$A + B \xrightarrow{k}$ Product $\qquad \left(\frac{1}{A_o - B_o}\right) \ln\left(\frac{A_o - x}{B_o - x}\right) = kt + \ln\frac{A_o}{B_o}$

Therefore plots of the quantities $\ln A$, A^{-1}, and $(A_o - B_o)^{-1} \ln[(A_o - x)/(B_o - x)]$ versus t have slopes which are equal to the rate constants for first, type I second, and type II second order reactions respectively.

If the experimental uncertainty is of constant size regardless of sample size, then the standard least squares analysis will give results which are distorted by an amount which depends upon the particular function being applied. Consider first order data: If two experimental points are equidistant from the "true result", when plotted logarithmically, the point with the smaller value will be

Reproduced with permission of the copyright owner. Further reproduction prohibited without permission.

farther from the true result than the point with the larger value. Because of this, simple least squares analysis will yield a rate constant which is too large. To compensate for this type of distortion a weighted least squares analysis is performed[1].

Since in least squares analysis the squares of the residuals are minimized we want to use weighting functions, W_i, which will make the terms $W_i\triangle_i'^2 = \triangle_i^2$ where $\triangle_i' = f(y + \triangle_i) - f(y)$ and where $\triangle_i$ = the uncertainty in the actual measurement. Thus the purpose of using W_i is to correct the residuals of f(y) (e.g. log(y)) to reflect the true uncertainty of y. If we expand the function $f(y + \triangle)$ by a Taylor series we obtain

$$f(y + \triangle) = f(y) + f'(y)\triangle + \frac{f''(y)\triangle^2}{2!} + \ldots$$

From the above we see that $\triangle'$ equals the second and successive terms of the Taylor series so that to a first approximation the term $[f'(y)]^{-2}\triangle'^2 = \triangle^2$. Therefore we use the terms $[f'(y)]^{-2}$ as the weights W_i. The procedure followed consists of the following steps:

1. A straight line is fit to the data without weights or with predetermined weights reflected by the measurements.
2. From this line residuals and hence a set of weights are obtained.
3. A second straight line is fit with the weights from (2).
4. Steps (2) and (3) are repeated until the change from one iteration to another is smaller than a predefined value.

[1] Cooper, B. E., Statistics for Experimentalists, Permagon Press, Oxford, 1966, p. 214.

Reproduced with permission of the copyright owner. Further reproduction prohibited without permission.

To have an estimate of the variance of the rate constant (slope) obtained by the above analysis, one evaluates[1] $\hat{\sigma}^2 / \sum_i (x_i - \bar{x})^2$ where $\hat{\sigma}^2$ is the estimate of the true variance $W_i \Delta_i^2$. From this estimate of the variance one can calculate a confidence interval (95%) based on the student's t-distribution.

Program Algorithm

The program first reads in the data points until an end-of-file is reached [140-200].[2] A standard, unweighted least squares analysis is done [140-200] to obtain a first approximation of the slope and intercept.

$$S = \sum_i z_i^2 = \sum_i (f_i - b - mx_i)^2$$

$$\hat{m} = \frac{n \sum_i x_i y_i - \sum_i x_i \sum_i y_i}{n \sum_i x_i^2 - (\sum_i x_i)^2}$$

$$\hat{b} = \overline{f(y)} - \hat{m}\bar{x}$$

$$\bar{f} = \frac{1}{n} \sum_i f_i \; ; \; \bar{x} = \frac{1}{n} \sum_i x_i$$

where f_i is the appropriate linear function for the kinetic data. A successive iteration technique is used [400-620] as described above.

$$S = \sum_i W_i z_i^2 = \sum_i W_i (f_i - b - mx_i)^2$$

$$\hat{m} = \frac{\sum_i W_i x_i y_i \sum_i W_i - \sum_i W_i x_i \sum_i W_i y_i}{\sum_i W_i \sum_i W_i x_i^2 - (\sum_i W_i x_i)^2}$$

$$\hat{b} = \bar{y} - \hat{m}\bar{x}$$

[1] Ibid.

[2] Numbers in brackets refer to statement numbers.

Reproduced with permission of the copyright owner. Further reproduction prohibited without permission.

The slope variance is calculated by $\frac{\hat{\sigma}^2}{\sum_i W_i (x_i - \bar{x})^2}$ [630-640], and BTAB is used to generate a confidence limit (95%). The results are printed and the process is repeated iteratively until in batch a convergence criterion [660] is satisfied, or, in conversational mode (terminal), user prompting specifies termination [700-720]. The calculated values are printed and the program returns for a new data set, until a null set is encountered [190].

Program Usage

The general structure of an MTS* run input is:

```
$RUN INVERSE    [S = *SOURCE*  6 =*SINK*]

1st data set    [data lines
                $END FILE

2nd data set    [data lines
                $END FILE

last data set   [data lines
                $END FILE

null data set   $END FILE
```

The user specifies the file for the appropriate program:

INVERSE	calculates $1/y = mx + b$
LOG	calculates $\log y = mx + b$
SECOND	calculates $\left(\frac{1}{a-b}\right)\log\left(\frac{a-x}{b-x}\right) = mx + b$

* MTS = Michigan Time Sharing computing service.

Reproduced with permission of the copyright owner. Further reproduction prohibited without permission.

The program reads from logical unit 5 (default to *SOURCE*) and writes on 6 (default to *SINK*); 5 may be assigned to a previously prepared data file, and 6 to a permanent file to be listed later in batch. The program first echoes the function to be fitted as a check that the correct program has been invoked (if incorrect, push the attention key at this point). The second order program (SECOND) prompts for initial reactant concentrations. All three programs prompt for data lines (time and y values) which are specified by # # # # # headings. The data set is terminated with $END FILE. The program will now print successive slope approximations and the calculated 95% confidence intervals for the slopes. In conversational mode [110-130] the user is asked if he wishes to continue: reply with a "YES" or "NO". Having replied "NO" the values are printed as x, y, residuals, f(x), and calculated f(x). The program again prompts for a new data set. Termination is effected by $END FILE.

Reproduced with permission of the copyright owner. Further reproduction prohibited without permission.

Reproduced with permission of the copyright owner. Further reproduction prohibited without permission.

Kinetic Rate Constant Program Listing
Inverse

```
      DIMENSION V(40),Y(40),X(40),X2(40),XV(40),CALV(40),RES(40)          LS0010
      DIMENSION RTAB(40)                                                 LS0020
      INTEGER IN,YES                                                     LS0030
      LOGICAL CON                                                        LS0040
      REAL M,MXNR,MOLD                                                   LS0050
      DATA     RTAB/12.706,4.303,3.182,2.776,2.571,2.447,2.365,2.306,    LS0060
     $2.262,2.228,2.201,2.179,2.160,2.145,2.131,2.120,2.110,2.101,2.093, LS0070
     $2.086,2.080,2.074,2.069,2.064,2.060,2.056,2.052,2.048,2.045,2.042, LS0080
     $10*2.0/,YES/'Y'/,CON/.FALSE./                                      LS0090
      WRITE(6,99)                                                        LS0100
      CALL CREPLY(&30)                                                   LS0110
      CON=.TRUE.                                                         LS0120
   20 WRITE(6,100)                                                       **LS0130
   30 N=1                                                                LS0140
      IC=1                                                               LS0150
   40 READ(5,200,END=50) X(N),Y(N)                                       ++LS0160
      N=N+1                                                              LS0170
      IF(N.LE.40) GO TO 40                                               LS0180
   50 IF(N.EQ.1) STOP                                                    LS0190
      N=N-1                                                              LS0200
      NM1=N-1                                                            LS0210
      FN=FLOAT(N)                                                        LS0220
      SV=0.                                                              LS0230
      SX=0.                                                              LS0240
      SX2=0.                                                             LS0250
      SXV=0.                                                             LS0260
      DO 60 I=1,N                                                        LS0270
      V(I)=1./Y(I)                                                       **LS0280
      SV=SV+V(I)                                                         LS0290
      SX=SX+X(I)                                                         LS0300
```

```
      X2(I)=X(I)*X(I)                                                  LS0310
      SX2=SX2+X2(I)                                                    LS0320
      XV(I)=X(I)*V(I)                                                  LS0330
   60 SXV=SXV+XV(I)                                                    LS0340
      M=(SX*SV-FN*SXV)/(SX*SX-FN*SX2)                                  LS0350
      B=(SV-M*SX)/FN                                                   LS0360
      WRITE(6,300) M,B                                                 LS0370
   70 IC=IC+1                                                          LS0380
      SWXV=0.                                                          LS0390
      SW=0.                                                            LS0400
      SWX=0.                                                           LS0410
      SWV=0.                                                           LS0420
      SWX2=0.                                                          LS0430
      WZ2=0.                                                           LS0440
      DO 80 I=1,N                                                      LS0450
      MXNB=M*X(I)+B                                                    LS0460
      CALV(I)=MXNB                                                     LS0470
      CALCY=1./MXNB                                                   **LS0480
      RES(I)=Y(I)-CALCY                                                LS0490
      T=V(I)-MXNB                                                      LS0500
      W=CALCY*CALCY*CALCY*CALCY                                       **LS0510
      WZ2=WZ2+W*T*T                                                    LS0520
      SWXV=SWXV+XV(I)*W                                                LS0530
      SW=SW+W                                                          LS0540
      SWX=SWX+W*X(I)                                                   LS0550
      SWV=SWV+W*V(I)                                                   LS0560
   80 SWX2=SWX2+W*X2(I)                                                LS0570
      MOLD=M                                                           LS0580
      FACT=SW*SWX2-SWX*SWX                                             LS0590
      IF(FACT.EQ.0..OR.SW.EQ.0.) GO TO 85                              LS0600
```

Reproduced with permission of the copyright owner. Further reproduction prohibited without permission.

```
      M=(SW*SWXV-SWX*SWV)/FACT                                          LS0610
      B=(SWV-M*SWX)/SW                                                  LS0620
      VARB=(W72*SW)/( FLOAT(N-2)*FACT )                                 LS0630
      CONF=     RTAB(NM1)*SQRT( VARB/FLOAT(NM1) )                       LS0640
      WRITE(6,310) M,B,CONF                                             LS0650
      IF(ABS((MOLD-M)/M).GT.0.005.AND.IC.LT.10) GO TO 70                LS0660
   85 IF(CON) GO TO 90                                                  LS0670
      WRITE(6,400) (X(I),Y(I),RES(I),V(I),CALV(I),I=1,N)                LS0680
      GO TO 30                                                          LS0690
   90 WRITE(6,500)                                                      LS0700
      READ(5,600) IN                                                    LS0710
      IF(IN.EQ.YES) GO TO 70                                            LS0720
      WRITE(6,400) (X(I),Y(I),RES(I),V(I),CALV(I),I=1,N)                LS0730
      GO TO 20                                                          LS0740
   99 FORMAT(' 1/Y=M*X+B')                                              **LS0750
  100 FORMAT('1ENTER X  AND  Y(X)',/,' ########## ##########')          ++LS0760
  200 FORMAT(G10.0,1X,G10.0)                                            ++LS0770
  300 FORMAT('1    SLOPE',7X,'INTERCEPT',/,1P2E13.3)                    LS0780
  310 FORMAT(1P3E13.3)                                                  LS0790
  400 FORMAT('0',/,7X,'X',11X,'Y(X)',6X,'RESIDUAL Y',5X,'1/Y(X)',4X,    **LS0800
     $'CALCULATED 1/Y',/,(1P5E13.3))                                    **LS0810
  500 FORMAT(' CONTINUE ITERATION?')                                    LS0820
  600 FORMAT(A1)                                                        LS0830
      END                                                               LS0840
```


Reproduced with permission of the copyright owner. Further reproduction prohibited without permission.

Reproduced with permission of the copyright owner. Further reproduction prohibited without permission.

Program - "Log" Substitutions

```
 20 WRITE(6,100)                                                    **LS0130
    V(I)=ALOG(Y(I))                                                 **LS0280
    CALCY=EXP(MXNB)                                                 **LS0480
    W=CALCY*CALCY                                                   **LS0510
 99 FORMAT(' LOG(Y)=M*X+B')                                         **LS0750
400 FORMAT('0',/,7X,'X',11X,'Y(X)',6X,'RESIDUAL Y',5X,'LOG(Y)',4X,  **LS0800
   $'CALCULATED LOG',/,(1P5E13.3))                                  **LS0810
```

Program - "Second" Substitutions

```
 20 WRITE(6,101)                                                    **LS0130
    READ(5,200) A0,B0                                               **LS0131
    A0B0=A0-B0                                                      **LS0132
    WRITE(6,100)                                                    **LS0133
    V(I)=ALOG( (A0-Y(I))/(B0-Y(I)) )/A0B0                           **LS0280
    EAB=EXP(A0B0*CALV(I))                                           **LS0480
    CALCY=(A0-B0*EAB)/(1.-EAB)                                      **LS0481
    W=(1./(B0-Y(I)) - 1./(A0-Y(I)))/A0B0                            **LS0510
 99 FORMAT(' LOG( (A-Y)/(B-Y) ) / (A-B)=M*X+B')                     **LS0750
101 FORMAT('0ENTER A0 AND B0',/,' ########## ##########')           **LS0751
400 FORMAT('0',/,7X,'X',11X,'Y(X)',6X,'RESIDUAL Y',5X,'LOG(Y)',4X,  **LS0800
   $'CALCULATED LOG',/,(1P5E13.3))                                  **LS0810
```

Reproduced with permission of the copyright owner. Further reproduction prohibited without permission.

Program Substitutions for Adding Experimental Weights

```
    DIMENSION WW(40)                                                    ++LS0021
 40 READ(5,200,END=50) X(N),Y(N),WW(N)                                  ++LS0160
    W=W**WW(I)                                                          ++LS0511
100 FORMAT('1ENTER X AND Y(X) AND W',/,' ########## ########## ########++LS0760
   S###')                                                               ++LS0761
200 FORMAT(G10.0,1X,G10.0,1X,G10.0)                                     ++LS0770
```

Program Modification

The program listing (above) is the basic program for the inverse function. Listed below the program are the necessary statement changes for converting to the other functions. Only the statements marked with asterisks need be changed. To handle more data points than 40, change the DIMENSION cards [10-20] and [180]. the BTAB table is the student's -t for 95% confidence: the DATA statement [60-90] may be retyped with the appropriate new table to change the confidence limit. The fractional change of 0.5%, or 10 iterations as a maximum, may be reset with [660]. The input format for data lines is given by [770]; the G format allows F or E type constants depending on the number size needed. The column headings are defined by [760]. The slope, intercept, and values are printed with [760] and [790], and the end results in exponential form with [800-810].

The last section listed is used if it is desired to apply experimental weights. These statements are inserted in the positions marked by +.

Reproduced with permission of the copyright owner. Further reproduction prohibited without permission.

Appendix 2

Tables for Operating Rapid Freezing Apparatus

Table 1

Time Resolution for Push-Push Cam

RPM	Flow Velocity (ml/sec)	Minimum Time Resolution (msec)
800	0.617	111
900	0.695	93
1028.6	0.794	81
1200	0.926	69
1400	1.111	58
1800	1.389	46
2400	1.852	35

Reproduced with permission of the copyright owner. Further reproduction prohibited without permission.

Table 2

Dead Times* for Push-Push Cam
(Values in msec)

Hole	RPM						
	800	900	1028.6	1200	1440	1800	2400
1 a	453	403	353	302	252	202	151
b	564	496	434	371	310	248	186
c	675	589	515	440	368	294	221
d	786	682	596	509	426	340	256
2 a	897	775	677	578	484	386	291
b	1008	868	758	647	542	432	326
c	1119	961	839	716	600	478	361
d	1230	1054	920	785	658	524	396
3 a	1341	1147	1001	854	716	570	431
b	1452	1240	1082	923	774	616	466
c	1563	1333	1163	992	832	662	501
d	1674	1426	1244	1061	890	708	536
4 a	1785	1519	1325	1130	948	754	571
b	1896	1612	1406	1199	1006	800	606
c	2007	1705	1487	1268	1064	846	641
d	2118	1798	1568	1337	1122	892	676
5 a	2229	1891	1649	1406	1180	938	711
b	2340	1984	1730	1475	1238	984	746
c	2451	2077	1811	1544	1296	1030	781
d	2562	2170	1892	1613	1354	1076	816
6 a	2673	2263	1973	1682	1412	1122	851
b	2784	2356	2054	1751	1470	1168	886
c	2895	2449	2135	1820	1528	1214	921
d	3006	2542	2216	1889	1586	1260	956

Reproduced with permission of the copyright owner. Further reproduction prohibited without permission.

Table 2 (Cont.)

Hole	RPM						
	800	900	1028.6	1200	1440	1800	2400
7 a	3117	2635	2297	1958	1644	1306	991
b	3228	2728	2378	2027	1702	1352	1026
c	3339	2821	2459	2096	1760	1398	1061
d	3450	2914	2540	2165	1818	1444	1096
8 a	3561	3007	2621	2234	1876	1490	1131
b	3672	3100	2702	2303	1934	1536	1166
c	3783	3193	2783	2372	1992	1582	1201
d	3894	3286	2864	2441	2050	1628	1236
9 a	4005	3379	2945	2510	2108	1674	1271
b	4116	3472	3026	2579	2166	1720	1306
c	4227	3565	3107	2648	2224	1766	1341
d	4338	3658	3188	2717	2282	1812	1376
10a	4449	3751	3269	2786	2340	1858	1411
b	4560	3844	3350	2855	2398	1904	1446
c	4671	3937	3431	2924	2456	1950	1481
d	4782	4030	3512	2993	2514	1996	1516
11a	4893	4123	3593	3061	2572	2042	1551
b	5004	4216	3674	3131	2630	2088	1586
c	5115	4309	3755	3200	2688	2134	1621
d	5226	4402	3836	3269	2746	2180	1656
12a	5337	4495	3917	3338	2804	2226	1691
b	5448	4588	3998	3407	2862	2272	1726
c	5559	4681	4079	3476	2920	2313	1761
d	5670	4774	4160	3545	2978	2364	1796
	5781	4867	4241	3614	3036	2410	1831
	5892	4960	4322	3683	3094	2456	1866

* Delay time plus time to fill reaction tube.

Reproduced with permission of the copyright owner. Further reproduction prohibited without permission.

Table 3

Reynolds Numbers for Various Flow Velocities and Tube Diameters

Tube Diameter		RPM 800	900	1028.6	1200	1440	1800	2400
		Flow Velocity (ml/sec) 0.6174	0.6946	0.7938	0.9262	1.111	1.389	1.852
0.008(1 jet)	cm/sec	1906	2140	2450	2830	3420	4280	5720
	R.N.	3870	4350	4980	5750	6950	8690	11620
0.008(2 jets)	cm/sec	953	1070	1225	1415	1710	2140	2860
	R.N.	1935	2175	2490	2875	3475	4345	5800
0.014	cm/sec	621	696	797	930	1119	1394	1862
	R.N.	2215	2480	2840	3310	3980	4970	6640
0.022	cm/sec	255	286	327	382	458	572	764
	R.N.	1430	1585	1815	2120	2540	3180	4240
0.042	cm/sec	69.2	77.2	88.8	103.8	124.3	155.5	207.7
	R.N.	738	823	946	1106	1321	1659	2207
0.0787	cm/sec	19.6	22.0	25.2	29.5	35.4	44.1	58.9
	R.N.	392	440	504	590	708	882	1178

These values were calculated from the following equations:

$$U = \frac{\text{ml/sec}}{A} \qquad \text{R.N.} = \frac{U\rho d}{\eta}$$

where A = cross-sectional area of tube, U = linear flow velocity (cm/sec), ρ = density (gm/cm^3), d = diameter (cm), η = viscosity (poise), and

Diam.(in)	Diam.(mm)	Drill Size	Area (cm)^2	(Area)$^{-1}$ (cm)$^{-2}$
0.008	0.203	92	0.324×10^{-3}	3085
0.014	0.356	80	0.995×10^{-3}	1005
0.022	0.555	75	2.425×10^{-3}	412
0.042	1.065	58	8.91×10^{-3}	112.2
0.787	2.00	47	31.4×10^{-3}	31.8

Assuming = 1 gm/cm^3 and = 0.01 poise (H_2O).

Reproduced with permission of the copyright owner. Further reproduction prohibited without permission.

Table 4

Stroboscopic Determination of Rotational Velocity

Discrete rotational velocities can be accurately determined using ordinary fluorescent lamps with 60 cps line current, fluorescent lamps will pulse at 120 cps. Rings of equidistant, uniform size black and white spots will "strobe" or appear to be motionless at discrete rotational velocities. These rotational velocities can be calculated according to 4.

4. $$\text{rpm} = \frac{7200}{\text{No. spots on ring}}$$

Listed below are the rpm which will strobe with various numbers of spots on a given ring.

Spots on Ring	RPM
3	2400
4	1800
5	1440
6	1200
7	1028.6
8	900
9	800

Reproduced with permission of the copyright owner. Further reproduction prohibited without permission.

Appendix 3

List of Manufacturers

Spectrophotometers

American Instrument Co., Inc., Silver Spring, Maryland. (Microflow Stopped-Flow (Strittmatter design), Aminco-Morrow Stopped-Flow, Aminco-Berger Stopped Flow, Dual wavelength spectrophotometers and other instruments)

Atom-Mech Machine Co., Patchogue, New York. (Dulz and Sutin Stopped-Flow)

Cary Instruments, 2724 South Peck Rd., Monrovia, California, 91016. (Recording spectrophotometers, spectropolarimeters)

Durrum Instrument Corp., Palo Alto, California. (Gibson-Milnes Stopped Flow)

Gilford Instrument Laboratories, Inc., Oberlin, Ohio. (Spectrophotometers)

Varian Analytical Instrument Division, 611 Hansen Way, Palo Alto, California, 94303. (EPR, NMR instruments)

Warner & Swasey Co., Control Instrument Division, 32-16 Downing Street, Flushing, New York 11354. (Rapid scanning spectrophotometer)

Yanagimoto Manufacturing Co., Ltd., Japan. (Yanaco SPS-1 Stopped Flow, Hiromi, Ono, Itoh and Nagamura design)

Carl Zeiss, Inc., 444 Fifth Avenue, New York, N.Y. 10018. (Spectrophotometers)

Optical Components

Baird-Atomic, System Components Division, 125 Middlesex Turnpike, Bedford, Massachusetts 01730. (Especially good narrow-band and other optical filters)

Bausch and Lomb, Analytical Systems Division, Rochester, N.Y., 14625. (Filters and monochromators)

Ealing Optics Division, 2225 Massachusetts Avenue, Cambridge, Massachusetts 02140. (Fiber optics)

Reproduced with permission of the copyright owner. Further reproduction prohibited without permission.

List of Manufacturers (Cont.)

EMI/Gencom Division, Varian/EMI, 80 Express Street, Plainview, N.Y. 11803. (Photomultipliers, PMT housings, power supplies)

Esco Products, 171 Oak Ridge Rd., Oak Ridge, New Jersey 07438. (Quartz and glass products - lenses, flats, ground joints)

Jarrell Ash, Division of Fisher Scientific Co., 711 Forbes Ave., Pittsburg, Pennsylvania 15219. (Especially good and economical monochromators and associated equipment)

Precision Cells, Inc., 401 Broadway, New York, N.Y. 10013. (Spectrophotometer cells)

Quartz Scientific, Inc., 34602 Lakeland Blvd., Eastlake, Ohio 44095. (Quartz plates, lenses, ground joints, etc.)

Thermal American Fused Quartz Co., Route 202 & Change Bridge Rd., Montville, New Jersey. (High quality quartz products - especially for metal-free requirements)

Motors and Associated Products

Boston Gear Co., Quincy, Massachusetts. (Power transmission products; gearboxes, couplings, V-belt pulleys, pillow blocks, etc.)

Joseph Dixon Crucible Co., Jersey City, New Jersey. (Lock Ease lubricating fluid)

W. W. Grainger, Inc., 1701 E. McNichols Rd., Detroit, Michigan 48203. (Motors and motor controls)

Minarik Electric Co., 232 E. Fourth Street, Los Angeles, California 90013. (Motors and motor controls)

Talboys Instrument Corp., Emerson, New Jersey. (Stirring motor)

Sears & Roebuck Co. (Motor, lathe bed)

United Shoe Machinery Corp., Gear Systems Division, 81 Bay State Rd., Wakefield, Massachusetts 01880. (Speed reducers - harmonic drive, stepping motors)

Reproduced with permission of the copyright owner. Further reproduction prohibited without permission.

List of Manufacturers (Cont.)

Hydraulic Equipment

Bel-Art Products, Pequannock, New Jersey 07440. (Polyethylene tubing, stainless steel stirrer, plastic laboratory ware)

Bimba Manufacturing Co., Monee, Illinois 60449. (Hydraulic air cylinder)

Cajon Co., 32550 Old S. Miles Rd., Cleveland, Ohio 44139. (Flexible metal tubing and metal tubing connectors)

Chromatronix, Inc., 2743 Eighth St., Berkeley, California 94710. (Cheminert tubing, columns)

Hamilton Co., P. O. Box 307, Whittier, California 90608. (Gas tight syringes, chemically inert valves, special syringes)

Hoffman, Division of MVE Cryogenics, New Prague, Minnesota 56071. (Stainless steel dewars)

Linde Division, Union Carbide Corp., 4801 W. 16th St., Indianapolis, Indiana 46224. (Liquid nitrogen handling equipment)

Mini-Flex Corp., 7916 Woodley Ave., Van Nuys, California 91406. (Metal bellows)

Quality Glass Apparatus, State Rd., Ann Arbor, Michigan 48106. (Glassblowing service - especially good for quartz work, cavity dewars, rapid freezing tubes)

Skinner Electric Valve Division, Skinner Precision Industries, Inc., New Britain, Connecticut 06050. (Solenoid valves)

Superior Air Products Co., 132 Malvern St., Newark, New Jersey. (Stainless steel dewar)

Roger Zatkoff Co., 15110 Plymouth Rd., Detroit, Michigan 48227. (Wide assortment of O-rings)

Electronic Devices

Analog Devices, 221 Fifth St., Cambridge, Massachusetts 02142. (Operational amplifiers and power supplies)

Reproduced with permission of the copyright owner. Further reproduction prohibited without permission.

List of Manufacturers (Cont.)

Bayley Instrument Co., Box 538, Danville, California. (Precision temperature controller)

Computer Instruments Corp. (CIC), Hempstead, New York. (Linear potentiometer)

Edmund Scientific, Barrington, New Jersey 08007. (Tachometer and a wide variety of laboratory related devices. Specializes in optical supplies)

Sanborn Co., Cambridge, Massachusetts. (Fast recorder)

Sorenson Operation, Raytheon Co., Richards Ave., Norwalk, Connecticut 06856. (DC power supplies, voltage stabilizers)

Tektronix, Inc., Portland, Oregon. (Oscilloscopes)

Teledyne-Philbrick-Nexus, Allied Drive at Route 128, Dedham, Massachusetts 02026. (Operation amplifiers, including special logarithmic modules)

Miscellaneous

Cleco Pneumatic, Houston, Texas. (Torque wrench TSK-30A)

Reproduced with permission of the copyright owner. Further reproduction prohibited without permission.